

UNIVERSITY OF GENOA

POLYTECHNIC SCHOOL

DICCA

Department of Civil, Chemical and Environmental Engineering



**MASTER OF SCIENCE THESIS IN
ENGINEERING FOR BUILDING RETROFITTING**

**Critical issues in seismic analysis and safety
verification of irregular masonry building**

Supervisor:

Chiar.mo Prof. Ing. Sergio Lagomarsino

Chiar.ma Prof. Ing. Serena Cattari

Co Supervisor:

Dott. Ing. Sofia Giusto

Candidate:

Ilaria Paternoster

Academic Year 2020/2021

“Stay in the wind”

Problemi aperti nell'analisi sismica e verifica di sicurezza degli edifici irregolari in muratura

Sommario

L'analisi sismica degli edifici, ed in particolare di quelli in muratura, richiede modelli non lineari affidabili come strumenti efficaci sia per la progettazione di nuovi edifici che per la valutazione e l'adeguamento di quelli esistenti. Tra le possibili strategie di modellazione proposte nei codici e in letteratura, questo lavoro è incentrato sulla strategia di modellazione del telaio equivalente, poiché consente l'analisi di edifici 3D completi con un ragionevole sforzo computazionale, adatto anche per scopi di ingegneria pratica. Pertanto, in questo contesto, questo lavoro intende fornire un contributo all'analisi sismica di edifici in muratura, proponendo il programma TreMuri per l'analisi sismica non lineare di strutture in muratura, cercando di risolvere il problema della modellazioni di edifici più complessi, caratterizzati da irregolarità. Per una valutazione più accurata è stato utilizzato un altro metodo di analisi, quello dell'analisi dinamica non lineare e i risultati ottenuti sono stati utilizzati come riferimento per le analisi statiche.

Critical issues in seismic analysis and safety verification of irregular masonry building

Abstract

The seismic analysis of buildings, and in particular of masonry ones, requires reliable non-linear models as effective tools for both design of new buildings and assessment and retrofitting of existing ones. Among the possible modelling strategies proposed in literature and codes, this work is focused on the equivalent frame modelling strategy, since it allows the analysis of complete 3D buildings with a reasonable computational effort, suitable also for practice engineering aims. Therefore, within this context, this work intends to provide a contribution to the seismic analysis of masonry buildings, proposing TreMuri program for the nonlinear seismic analysis (NLSA) of masonry structures, trying to solve the problem of modelling quite complex structure, characterized by irregularities. For this purpose, another method of analysis was used, that of nonlinear dynamic analysis (NLDA), for a more accurate evaluation. The results obtained were used as a reference for the static analyses.

Acknowledgments

Thanks to the collaboration with AD Engineering, an engineering services industry located in La Spezia, I encountered the opportunity to employ some activities in the drafting of executive projects for static and seismic improvement of existing masonry and reinforced concrete structures. Getting inside a cooperated work with Giovanni, the godfather of this thesis, I would like to send him a special thanks for his assistance in the study and design phases of this work. During my traineeship with Giovanni, I learned how to get interventions for the static and seismic improvement of existing structures and I acquired the basic skills to the drafting of preliminary and then executive projects. Thanks to the professors Lagomarsino and Cattari I deepened the whole phase of analysis and verification of the present work. Last, but not least, thanks to Sofia for which any solution for the dynamic analysis was not possible.

I owe a special thanks to Francesco, Dido, who gave me the tools to put myself back in the game and feel up to this university course. If I am here today to discuss this thesis, I certainly owe it to my parents, especially my mom, who allowed and helped me to do all this, my sisters, Carola (my personal translator...and writer), Franci and my dad, to be here today. I have to thank my guardian angels Benny and Ge for the most important and least intrusive help.

I can't help but mention Alice, Giulia and Giada, my college adventurers, even though we have taken and followed different path.

I wish Davide, Mattia and Rogen a good luck and that they will always have something to "speaking about".

Contents

Sommario	I
Abstract.....	II
Acknowledgments.....	III
1. Introduction.....	1
1.1. General framework	1
1.2. Reference codes	2
2. Overview on seismic behavior and modelling of masonry buildings	4
2.1. Unreinforced masonry buildings (URM)	4
2.2. Equivalent frame modelling of URM buildings	5
2.2.1. Masonry elements	8
2.2.2. Modeling of the structure	10
2.2.3. Non-linear static analysis (NLSA)	10
2.2.3.1. Masonry macroelement	13
3. Case Study	15
3.1. Choice of case study	15
3.1.1. Masonry towers	15
3.2. Preliminary feasibility study	16
3.2.1. Data collection	16
3.2.2. Acquisition and analysis of archival documentation	18
3.2.3. Building description and data analysis.....	18
3.2.4. Main body	18
3.3. Property inspection done	23
3.3.1. Verification of structural coherence.....	23
3.3.2. Overall state of the structural elements	23
3.3.3. State of non-structural elements.....	24
3.3.4. Investigation of the tower.....	25
3.3.5. Surveys of slabs and floor	26
Step 1: Structure input	27
4. Modelling phase	28
4.1. Mechanical masonry parameters	29
4.2. Mechanical concrete parameters	31
4.3. Mechanical steel parameters.....	33

4.4. Mechanical parameter of the slabs	34
4.5. Reference parameters adopted in the design phase	34
Step 2: The Analysis	36
5. Preliminary seismic vulnerability results	37
5.1. Equivalent frame definition	37
5.1.1. Load analysis.....	39
5.2. Safety assessment	40
5.2.1. From MDOF to equivalent SDOF systems.....	41
5.3. Nonlinear Static Analysis – Pushover	46
5.3.1. Selection of seismic conditions.....	47
5.3.2. Calculation setting and load patterns	49
5.4. Modal Analysis.....	51
5.4.1. Calculation setting.....	55
5.5. Summary analysis.....	57
Step 3: The Verification	59
6. Analysis of results	60
6.1. Results of non-linear static analysis	60
6.1.1. Definition of the limit states.....	60
6.1.2. Influence of the applied load profile on the capacity curve	61
6.2. Nonlinear Dynamic Analysis (NLDA).....	68
6.2.1. Rayleigh’s coefficients adopted	69
6.2.2. Selection of seismic conditions.....	70
6.3. Comparison between the results of static and dynamic analyses.	73
6.3.1. Distinctive features of NLSA and NLDA.....	82
7. Conclusions.....	84
8. Bibliography.....	86
Appendix A.....	88

1. Introduction

1.1. General framework

Existing and historical unreinforced masonry buildings are characterized by their potential high vulnerability to earthquake, which require to improve the knowledge of their seismic behavior, setting up analytical and numerical models for their structural assessment. The mechanical behavior of these buildings is strongly characterized by a non-linearity which makes the procedures inapplicable of linear analysis commonly used for steel frame and reinforced concrete structures. In recent years, in the field of seismic engineering, many studies have led to the creation of multiple non-linear static calculation procedures for assessing the behavior of buildings under earthquake.

The choice of the most appropriate model for carrying out the nonlinear static analyses (pushover analysis) of masonry structures has become a matter of considerable importance. At present there are two widely used approaches. The first makes use of the finite element method (FEM), in which the constituent parts of the masonry (stone blocks and mortar joints) are discretized into a finite number of elements. These elements are characterized by means of suitable constitutive laws which allow to consider very accurately all the non-linearities involved in the problem. The result can perfectly capture the behavior of the panels, highlighting the breaking mechanisms that intervene in the loading process. However, at present, this type of approach is more often applied to single panels than to entire buildings, due to the serious computational burden that the accuracy of this modeling requires, and which may be unacceptable for professional purposes. Furthermore, the FEM models suffer from a series of other problems such as the potential dependence on the refinement of the mesh, the large number of parameters that are required in input (which, however, are not always available in the usual engineering applications) and the need for particularly specialized users. The second approach is based on the adoption of equivalent one-dimensional elements, commonly called Equivalent Frame Modeling (FME - Frame by Macro Element). The structure is idealized by an assembly of vertical and horizontal elements: piers and spandrels. The first (piers), are the elements designed to resist both vertical loads and seismic actions; the horizontal elements (spandrel), on the other hand, provide the coupling of the piers under seismic action. Piers and spandrels are connected by rigid zones and each of them is modeled with the most appropriate constitutive laws. The simplifications introduced by this approach are significant and therefore the accuracy of the results depends on the correspondence of the hypotheses introduced with respect to the real structural problem.

Among the possible modelling strategies proposed in literature and codes, this work is focused on the equivalent frame modelling strategy. Therefore, it intends to provide a contribution to the seismic analysis of masonry buildings, proposing the TreMuri¹ program: The software is used for the seismic calculation of masonry structures according to the Ministerial Decree 17-1-2018 "Technical Standards for Construction" (NTC2018), which schematizes the structure through the equivalent frame, called macro-element.

The macro-element allows to better understand and predict the seismic behaviour of masonry structures and provide all the necessary information to designer for a thorough examination of the structure itself. It allows the analysis of the whole structure, 3D, with

¹ STADATA. 3Muri Program, commercial release 6.2.1; 2012 [www.3muri.com]

a reasonable computational effort. Furthermore, TreMuri program has a graphic module for the introduction of the structure with intuitive commands, a solver for the creation of the calculation model and the relative solution, of a post-processor for the immediate presentation of results and creation of the calculation report.

In the following chapter some basic knowledge concerning the masonry structures are presented (in §2), going in deep with the equivalent frame modelling approach. Next, in §3, a specific case study is presented, through which it was possible to understand in practice the meaning of idealization of the real model and the related problems that can be encountered for a typical masonry structure characterized by irregularities.

Once introduced the case, a preliminary analysis was performed. To follow, to solve the case, some specific idealization was done especially for the tower element. The aforementioned procedure means to be able to minimize the modelling uncertainties of the current structural behaviour; adopt accurate and reliable models to predict the seismic response and adopt reliable criteria for the safety assessment.

Consequently, nonlinear static analyses were carried out and discussed (in §6) in order to better understand the influence of the choice of the lateral force distribution pattern on the results.

Finally, the previous approach was compared with the results derived from the Nonlinear Dynamic Analysis (NLDA) using some accelerograms compatible with the spectrum. Since the NLDA is the most accurate technique, through the discussion about the outcomes from different pushover analyses and NLDA applied to the case study (in §6.2), the research contributes to better understand the reliability and limitations of available seismic analysis methods.

1.2. Reference codes

The analysis of the structure that will be presented later is addressed through the calculation program TreMuri according to the Ministerial Decree of 17 January 2018, replacing those approved by the Ministerial Decree of 14 January 2008. It has been possible to select the calculation mode through the Circular No. 7 of 21 January 2019, which plays a fundamental role for masonry structures, and which replaces the previous circular n. 617 of 2 February 2009. The purpose of this section is to provide operators in the sector, and in particular designers, with the necessary clarifications, indications, and information elements for the smooth and unambiguous application of these rules. Therefore, we can say that this document refers to the Technical Construction Standards of 2008 (NTC2008), but it's an update. This new edition therefore constitutes an effective support and a clear reference for the professional who intends to address the subject of the analysis of masonry buildings. The main innovations introduced by NTC2018 are mainly four: i) the introduction of the Limit State of Collapse (LSC) that before this legislation was not required for masonry buildings; ii) adjustment measures are introduced (NTC2018-§8.4.3.); iii) a load distribution proportional to the form of multiple significant modes is introduced (NTC2018-§7.3.4.2.). iv) The drift values are updated according to the LSC through the constituent bonds of the masonry. With reference to the latter, it should be noted that the masonry construction is characterized by a complex seismic behavior, both for the geometric and constructive complexity of these buildings and for the mechanical behaviour of the masonry material (It has a weakly tensile resistance). The seismic response is therefore strongly non-linear, and the methods of analysis have to deal with this reality. The equivalent frame approach, adopted by the

NTC, allows to model the masonry building in its original conditions, taking into account the flexibility of the floors, the deformability and limited resistance of the spandrel, the redistribution of the compression actions on the individual wall piers (as the seismic action increases). A better understanding of real behavior is an indispensable condition for an effective intervention project, one that favors conservation as much as possible. About the structural safety required in the seismic consolidation of the existing building, the NTCs provide for three types of intervention:

- The adjustment;
- The improvement;
- Local repair or intervention.

This new classification removes some conceptual constraints and misunderstandings that were inherent in the previous legislation with the innovative introduction of the third class of interventions that can be performed without a calculation of the seismic safety of the entire building. The new seismic improvement therefore represents an additional opportunity for existing masonry buildings. However, it is necessary to have reliable calculation tools for masonry constructions, even complex ones, which make it possible to understand the original functioning and estimate the effectiveness of seismic consolidation interventions. These are the key concepts that will be treated later in the following sections, and they will be the pillars for the execution of this thesis, having regard to the difficulties encountered in the preparation of this work.

2. Overview on seismic behavior and modelling of masonry buildings

2.1. Unreinforced masonry buildings (URM)

Most of the historical buildings around the world, especially in Italy, were made with unreinforced masonry (URM). This is due to its availability in nature, low-cost and durability. Some constructions like towers were mainly built to withstand vertical loading induced by self-weight, without take into account the lateral performance under earthquake loads, mainly by the limitations of masonry.

Among these causes, it is worth remembering that masonry has an acceptable compressive strength with respect to its tensile strength (between 10 and 15% of the compressive strength), while that in shear is almost zero. From literature and laboratory evidence the shear strength might be considered with lower values, in the order of 1–5%. Therefore, it can be said that URM building could presents a poor seismic performance mainly due to the low tensile and shear strength of the whole element, lack of structural integrity, heterogeneity of compounds (i.e. brick/stone and mortar joints) and possible interventions or modifications to which the structures may have been subjected, which once again reduced its seismic resistance.

The aforementioned aspects focus on structural vulnerability and seismic performance of which the masonry buildings are affected, and their failure mechanisms correspond to the anisotropy of this heterogeneous material (i.e. a combination of units and mortar joints) and nonlinearity. Observation of existing masonry buildings following seismic events has shown that the damage mechanisms suffered by this structural typology are attributable to two modes, "the mechanisms of first way" and "the mechanisms of second way". The mode of damage mechanism that is activated depends on the construction and typological characteristics, and the structural deficiencies of the building.

The *mechanisms of the first way* identify damage mechanisms that are activated on walls hit by seismic actions directed orthogonally to them, causing stress of die-casting and cut off the plane and phenomena of overturning.

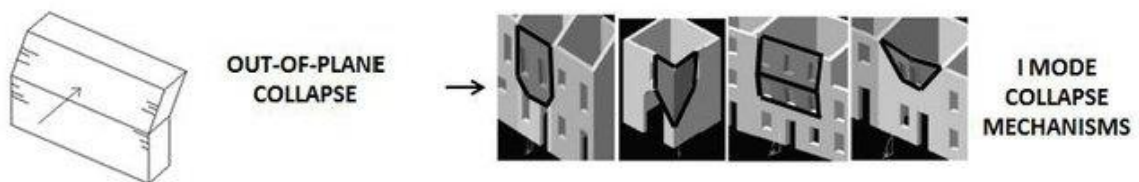


Figure 2.1 - Out of Plane Collapse.

The *mechanisms of second way*, concern walls solicited by seismic actions to them coplanar, with damages typically for cut and die-casting. For them to activate, the construction must be able to produce an overall behaviour, with the different parts called to collaborate ("box behaviour"). Such an overall response requires the softening of the orthogonal walls and an adequate connection between the walls and the floors.

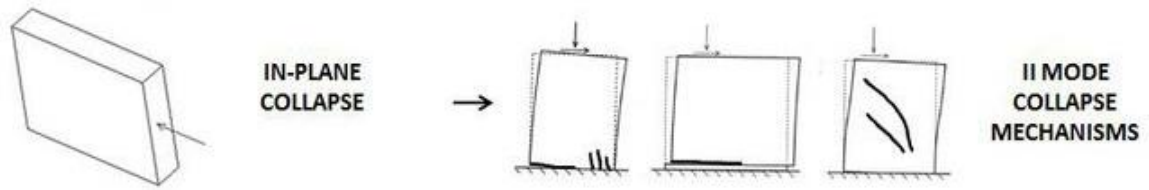


Figure 2.2 - In Plane Collapse.

These mechanisms are a consequence of the building's box behaviour, so it is necessary to examine the building as a whole with a three-dimensional model and assessing the reliability of the program, TreMuri, through the 3D equivalent frame modelling. In the following, the choice of the study case is presented, and the modelling technique adopted to study it are discussed more in deep.

2.2. Equivalent frame modelling of URM buildings

In the field of structural element models the “equivalent frame” ones is the most widely diffused (Lagomarsino S. et al., 2013). It considers the walls as an idealized frame, in which deformable elements connect rigid nodes, parts of the wall which are not usually subjected to damage. Usually, two main structural components may be identified: piers and spandrel, where the non-linear response is concentrated. This idealization starts from the earthquake damage observation that shows as usually cracks and failure modes are concentrated in such elements. Piers are the main vertical resistant elements carrying both vertical and lateral loads; spandrel elements, those parts of walls between two vertically aligned openings, are secondary horizontal elements (for what concerns vertical loads), which couple the response of adjacent piers in the case of lateral loads.

In the Fig.2.3 different schemes are illustrated according to very simplified models which represents the idealization of a wall with openings as an assemblage of structural elements, for which the actual modelling of spandrels behavior is not requested, and the Equivalent Frame (EF) discretization that considers both pier and spandrel elements. In particular, the idealization of a “strong spandrels-weak piers” model (SSWP) assumes that piers cracked first, thus preventing the failure of spandrels which can be then assumed as infinitely stiff portions, assuring a perfect coupling between piers. This corresponds to assuming a fixed-rotation boundary condition at the piers extremities and it is also known as “storey mechanism” (Tomaz'evic' M, 1987), the most critical failure mechanism. On the contrary, in case of the “weak spandrels-strong piers” (WSSP), the hypothesis of both zero strength and stiffness of spandrels is adopted then assuming the piers as uncoupled (this corresponds to the cantilever idealization). In most cases, may be correct to assume that horizontal displacement of the vertical structural elements is at least coupled at the floor levels by the presence of horizontal diaphragms, but they will be shaped only if the designer considers them adequately clamped to the walls, capable of transferring these forces.

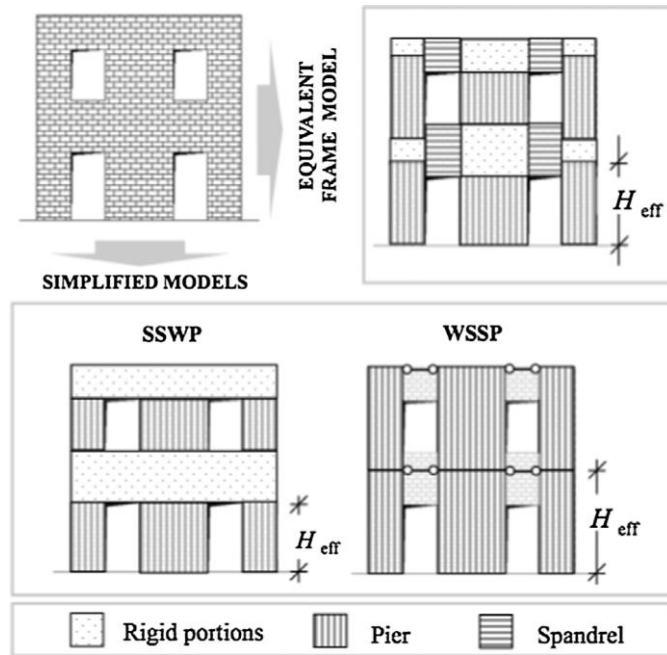


Figure 2.3. URM wall idealization according to simplified and equivalent frame models (Lagomarsino S. et al., 2013).

According to the assumptions of these simplified models, the designer can make a choice. since only pier elements are modelled, the definition of both their effective height and boundary conditions plays a crucial role for the reliable assessment of the overall capacity of the wall. For the letter mentioned reason, preliminary evaluations on the effectiveness of spandrels are requested to properly orientate the choice between these two extreme idealizations, knowing that both of these limiting cases are inappropriate for certain walls. The procedure for modelling the masonry wall as an equivalent frame is based at first in the idealization of the masonry wall into an assemblage of structural elements, previously introduced as piers and spandrels. Once having idealized the masonry wall in (§2.2.1), the reliable prediction of its overall behavior mainly depends on the proper interpretation of the single element response (modelling of structural elements, in §2.2.2 will be presented the TreMuri procedure).

Therefore, a modeling strategy implemented in the TreMuri program, can be schematized in the following steps (Fig. 2.4):

1. Identification of piers: the height of the piers may be assumed to be equal to the average height of the adjacent openings or limited by interlocking conditions or the presence of lintels;
2. Identification of the spandrel: the horizontal masonry beams are located at the overlapping of the openings;
3. Identification of rigid nodes: "non-deformable" portions, rigid precisely, where the elements are connected to form the equivalent frame.

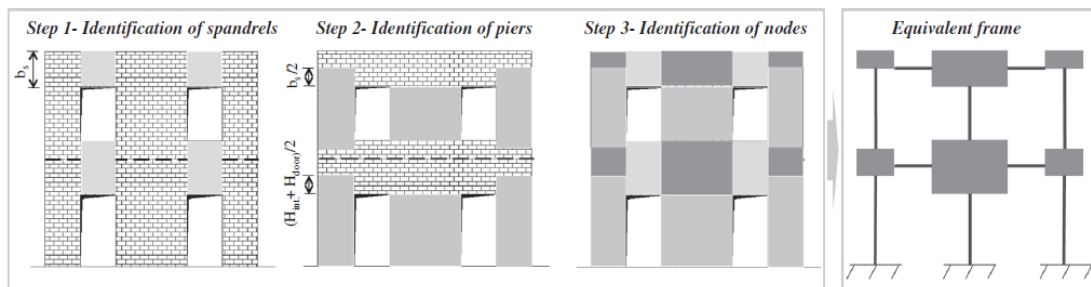


Figure 2.4 - Example of equivalent frame idealization in case of regularly distributed openings (Lagomarsino S. et al., 2013).

These steps were used to define the best model to implement in TreMuri that will be defined as function of the case of study, presented in this work. The operations of introducing data into the program are settled by the first phase of Input, where the geometry is defined and the structure characteristics are inserted, while the next steps of control of the results are divided into two other phases: Analysis and Verification, from which the data are derived for the analysis according to the TreMuri model, i.e. the equivalent frame (as shown in the following figure).

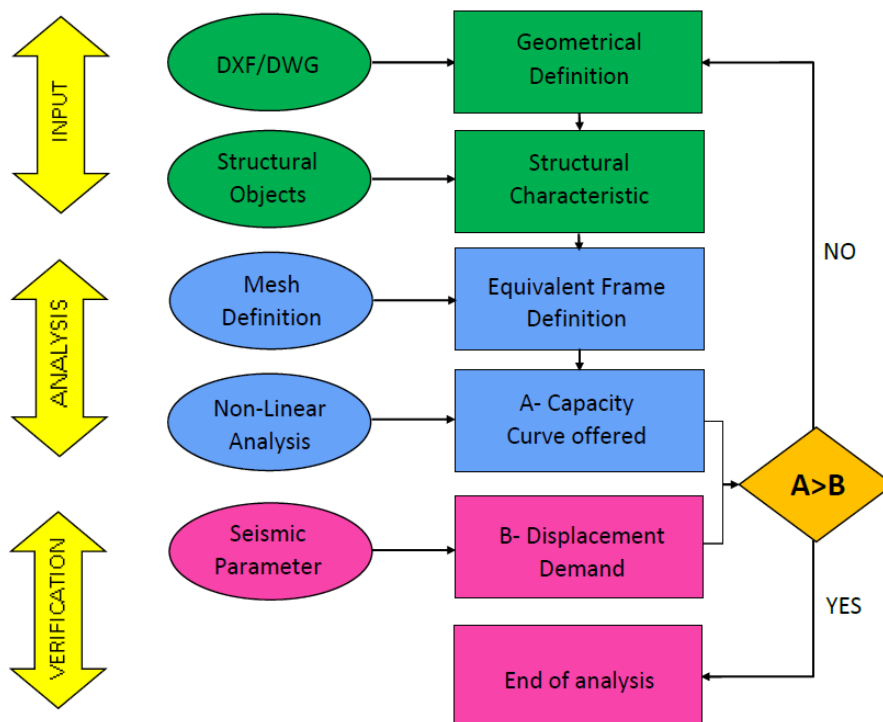


Figure 2.5 - General flow of data.

The analysis of the structure is divided into two phases: in the first phase the equivalent frame model is automatically generated which is followed by the nonlinear static analysis (push-over) from which the capacity curve of the structure is derived (stress curve - displacement of the point of control). While the verification consists, at global level, in the comparison between the displacement offered by the structure and that required by

the legislation. The verification at local level, for which masonry element is not able to bear gravity loads, is implicitly made during the nonlinear static analysis, by considering force-deformation relationships with strength degradation and the consequence at global level may be directly detected on the capacity curve.

2.2.1. Masonry elements

To properly describe the masonry type behavior a specific characterization of the force-displacement relationship starts from the knowledge and interpretation of the different failure modes which may occur. Observation of seismic damage to complex masonry walls, as well as laboratory experimental tests, have shown that a masonry panel subjected to in-plane loading may show two typical types of behavior:

- *The Flexural behavior*, that may be associated to the failure modes of *Rocking*, where panel starts to behave as a nearly rigid body rotating about the toe and *Crushing*, where panel is progressively characterized by a widespread damage pattern, with sub-vertical cracks oriented towards the compressed corners;

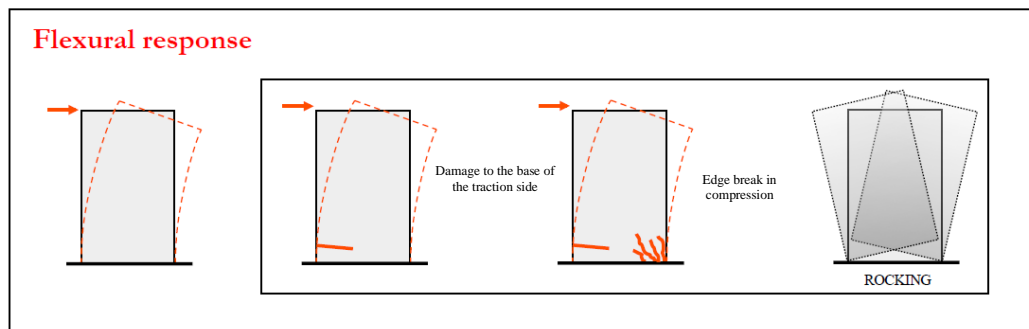


Figure 2.6 - Flexural failure.

- *The Shear behaviour*, that may be associated with the failure modes of *Diagonal Cracking*, where panel usually develops cracks at its center, that after propagate towards the corners and *Shear Sliding*, in which failure is attained with sliding on a horizontal bed joint plane.

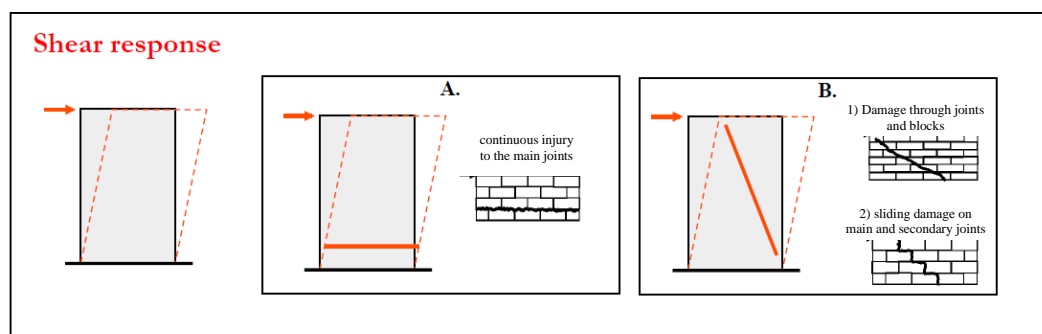


Figure 2.7 - Shear failure.

Despite this classification, it is evident that also mixed modes are possible and quite common. On the basis of these failure criteria described above we can highlight the main failure for the vertical masonry element (piers) and for the horizontal one (spandrel).

For piers, different failure criteria can be taken into account from literature. However, should be always considered the flexural failure, with partialization at the end sections and crushing at the tip, due to normal force and bending. For the irregular masonry, typical failure is characterized by diagonal cracking at the center of the panel element, mainly related to the diagonal tensile strength (masonry assumed as isotropic behaviour material), while, in the case of regular masonry, it depends on the mortar joint strength, the local friction and the interlocking between units. In the latter case, also shear sliding on a horizontal mortar joint should be considered. For better understanding a schematized table is presented below.

Table 2.1 - Distinction between irregular and regular masonry strength criteria.

REGULAR MASONRY			IRREGULAR MASONRY	
Flexural/Toe Crushing	Bed Joint Sliding	Diagonal Cracking	Flexural/ Toe Crushing	Diagonal Cracking

For spandrels, fewer experimental tests are available, and failure should also take into account the horizontal tensile strength of the masonry (due to interlocking and vertical compressive stress) and the characteristics of lintels and other horizontal coupled elements (tie rods, ring beams). It should be noted that the normal force in spandrels is usually very low, as horizontal seismic actions are distributed to each node in proportion to the tributary mass; normal forces are generated only when there is a redistribution of shear forces between masonry piers or if the elongation of the spandrel is countered by elements, such as ring beams or tie rods. In addition, the 3D equivalent frame model may not be accurate.

2.2.2. Modeling of the structure

It should therefore be stated that in order to obtain a suitable structural model for global analysis, a correct choice in the distribution of masses and stiffnesses is important, possibly taking into account the effect of non-structural elements (in §3.3.3). For this purpose, especially in the case of existing masonry buildings, where the resistant structural system is not always immediately identified (presence of structural variations or different construction phases, change of the intended use with changes to the original scheme), a preliminary analysis phase is of fundamental importance (§3.2) which, in addition to providing information on the characteristics of the materials, can clarify which are the resistant elements (both for vertical actions and for the actions of the earthquake). The reference model is the box model, equivalent to a three-dimensional equivalent frame, in which the walls are interconnected by horizontal plane diaphragms (slabs). As already mentioned, in the specific of masonry buildings, the wall can be suitably schematized as a frame, in which the resistant elements (piers and spandrel) and the rigid knots are assembled. The coupling beams in ordinary masonry, or spandrels, can be modelled only if adequately softened on the walls, supported by structurally effective lintels and a strut resistant mechanism is possible.

It is known that a lack of perfect knowledge of mass positioning can lead to underestimate the stresses on the structure related to torsional effects: In fact, it is precisely the growing eccentricity present between the centre of the masses and the centre of the stiffnesses that emphasizes this aspect. The rules therefore propose to consider an accidental eccentricity to be applied to the center of the masses of each plane of the structure. The accidental eccentricity will be equal to $\pm 5\%$ of the maximum dimension of the considered plane of the building in the direction perpendicular to the action of the earthquake.

Many calculation and verification procedures, adopted in several countries in modern anti-seismic design legislation, provide a description of the structural response in terms of displacements rather than forces, having regard to the increased sensitivity of the damage to the movements imposed. The Italian legislation also proposes a method that uses non-linear static analysis.

In this context, nonlinear static procedures play a central role, among them the capacity spectrum method (Capacity Spectrum Method, originally proposed by Freeman et al. 1975) and the N2 Method (Fajfar 1999, 2000), in §5.1.1 are explicitly mentioned for their purpose. These methodologies are simplified procedures in which the problem of assessing the maximum expected response, resulting from the occurrence of a given seismic event, is linked to the study of a non-linear system with a single degree of freedom equivalent to the model with n degrees of freedom, which represents the real structure ("Substitutive Structure Approach" Shibata and Sozen, 1976). The common feature of these procedures is to rely on the use of nonlinear static analyses (pushovers). Therefore, the non-linear static procedure is explained and well-reasoned in the following section.

2.2.3. Non-linear static analysis (NLSA)

TreMuri studies the "global" behavior of the structure through non-linear analysis which proposes a description of the structural response in terms of displacements, taking into account the increased sensitivity of the damage to the displacements imposed (fig. 2.9).

NLSA (pushover) characterizes the seismic system resistant through capacity curves. They are "static" as the external forces which are applied statically to the structure and "non-linear" due to the behavioral model assumed for the resistant elements of the

structure that pass from the elastic phase to the plastic phase and finally to rupture. These curves are intended to represent the envelope of the hysteresis cycles produced during the execution of the earthquake and can be considered as an indicator of the post-elastic behavior of the structure.

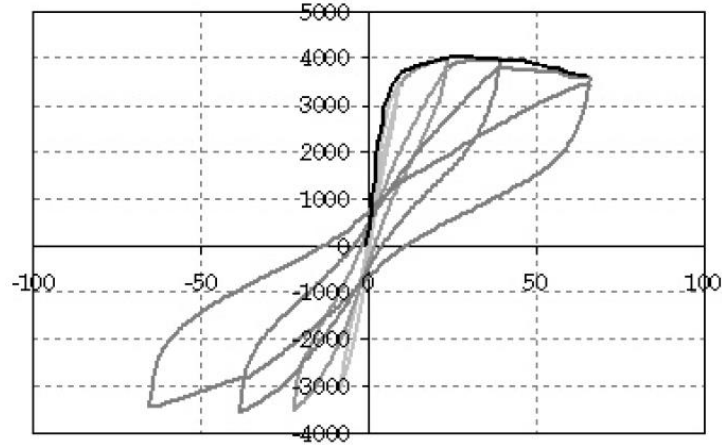


Figure 2.8 - Hysteresis cycles.

Nonlinear static analysis allows us to understand the evolution of the structural response as individual elements evolve in the non-linear field, providing information on the distribution of demand for inelasticity.

The curve thus obtained from pushover analyses (which will be, then, transformed into a capacity curve, taking into account the characteristics of the system equivalent to a degree of freedom, see §5.2.1) conventionally reports the trend of the resulting shear at the base with respect to the horizontal displacement of a control point of the structure. Each point of the curve can be associated with a specific state of damage of the entire system, and it is therefore possible to associate to certain levels of displacement the expected degree of functionality and the corresponding damage.

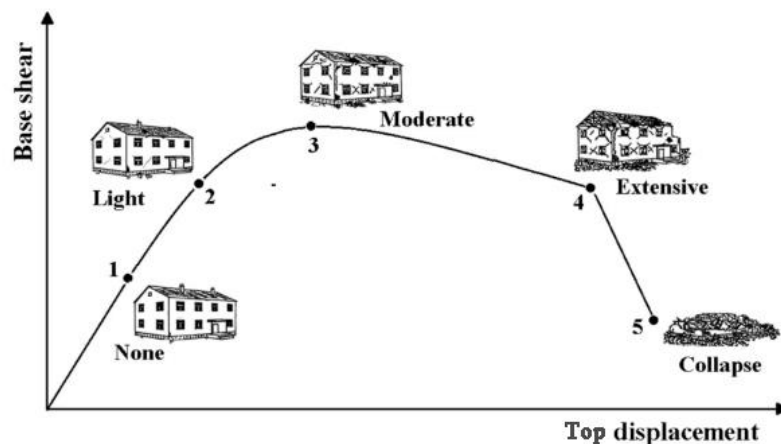


Figure 2.9 - The curve represents the full nonlinear response of the structure including all damage states as well as its collapse.

This curve, known as pushover (capacity), tells the behaviour of a structure subject to a horizontal load application. The load distribution applied is intended to represent the distribution of inertial forces induced by the seismic event. The proposed profiles will then be discussed later (in §5.3.2), but the intent is to better understand the response of the structure in the elastic field and then in the non-linear field (the NTC propose a distribution proportional to static forces, first way, and proportional to the masses, second way). Therefore, we monitor the force to the foot (overall shear) and the displacement of a summit point (control point) assumes the common name of capacity curve. In the first steps of application of this force, the structure, remains in the elastic field, the slope of this first stretch is defined as initial stiffness or elastic stiffness (1). This stiffness is what it has in the absence of damage. By increasing the external forces, some elements begin to stretch, the first yield strength is reached (2). The stiffness, that is, the slope of this curve, begins to decrease (increasing the displacements, also increase the entities of the applied forces). By increasing, we reach a level of damage (3), for which, the curve assumes a pseudo-horizontal tangent, in other words, we have reached the maximum possible action, that is, the maximum strength resistance. Having reached the maximum possible action, the external forces begin to reduce, the displacement increases, until the limits of deformation are reached. Then, we will have local collapses or local breakdowns, this stage is known as loss of resistance (4). At this point the overall resistance to horizontal forces has now been reduced a lot, but the structure is still able to support vertical loads. If we continue to push, even with a lower force, the structure will collapse (5).

The resulting capacity curve of a full structure can therefore be idealised to represent a non-linear force-deformation relationship. This relationship is assigned to an equivalent single-degree-of-freedom (SDF) system which is then expected to represent the detailed nonlinear structural model. This concept is illustrated in the following figure (fig. 2.10), where an approximated form of a capacity curve is used as the governing force-displacement relationship of an equivalent SDF system. These concepts will be explained more in deep in the §5.

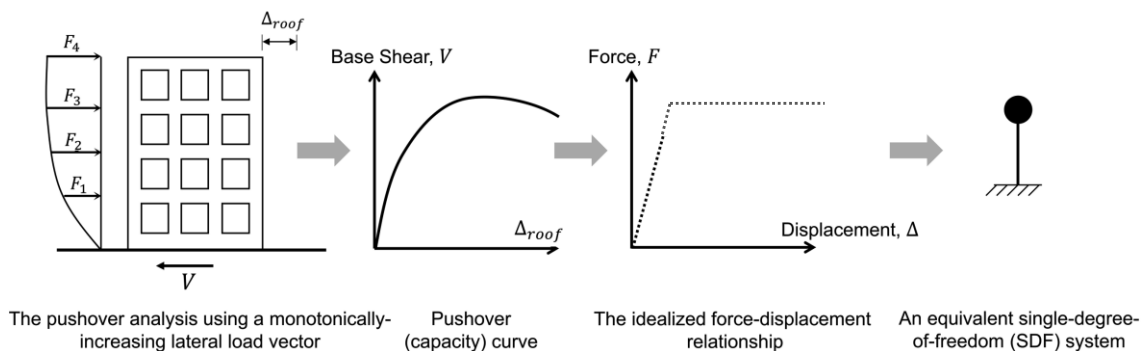


Figure 2.10 - Conversion of a detailed structural model in to an equivalent SDF system.

The "capacity" offered by the structure must then be compared, in view of a seismic verification, with the "demand" required by the external forcing, that is, by a certain seismic event. The effects of energy dissipation, which offer an additional margin of resistance that cannot be explained by using linear elastic theory alone, are especially relevant in the field of non-linear structure response, reason why demand shall be reduced.

As mentioned, the practical observation of damage on existing structures, led to the formulation of the masonry macroelement as an element that in its central part captures the shear behavior and that in the peripheral areas the die-casting behavior from which the appropriate theoretical formulation his macroelement have emerged.

2.2.3.1. Masonry macroelement

A non-linear beam element is implemented in the solver to meet the requirements required by current regulations. As reported in the User Guide, the main features are:

1. Initial stiffness according to the elastic characteristics of the material;
2. Bilinear behaviour with maximum shear and bending values consistent with the ultimate limit state values;
3. Redistribution of internal stresses to ensure equilibrium;
4. Damage state setting according to global and local parameters;
5. Degradation of stiffness in the plastic branch;
6. Ductility control by the definition of maximum drift (δ_u) differentiated according to the provisions of the regulations in force depending on the damage mechanism acting on the panel. For example, for existing buildings according to the Italian standard:

$$\delta_m^{DL} = \frac{\Delta_m}{h_m} = \delta_u = \begin{cases} 0.004, & \text{Shear} \\ 0.006, & \text{Combined compressive and bending stress} \end{cases} \quad (2.1)$$

7. Elimination of the element, to the attainment of the ultimate limit state (ULS) without interruption of the analysis.

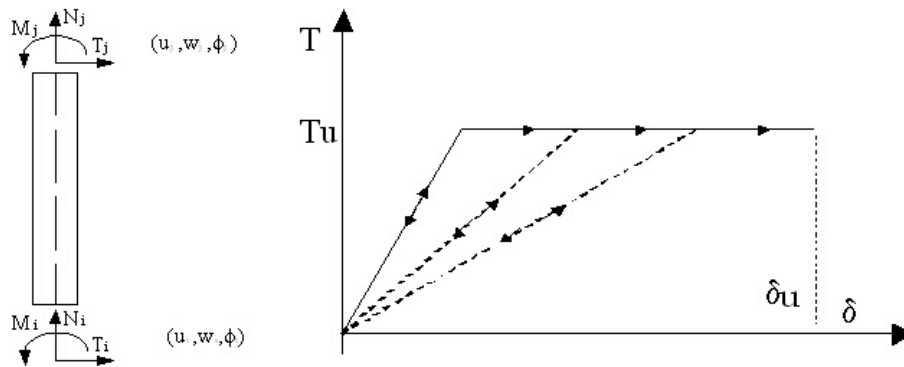


Figure 2.11 - Non-linear beam degrading behavior.

The elastic behavior of this element is governed by local constitutive relationships described through the following matrix of elastic stiffness (2.2):

$$\begin{Bmatrix} T_i \\ N_i \\ M_i \\ T_j \\ N_j \\ M_j \end{Bmatrix} = \begin{bmatrix} \frac{12EJ}{h^3(1+\psi)} & 0 & -\frac{6EJ}{h^2(1+\psi)} & -\frac{12EJ}{h^3(1+\psi)} & 0 & -\frac{6EJ}{h^2(1+\psi)} \\ 0 & \frac{EA}{h} & 0 & 0 & -\frac{EA}{h} & 0 \\ \frac{6EJ}{h^2(1+\psi)} & 0 & \frac{EJ(4+\psi)}{h(1+\psi)} & \frac{6EJ}{h^2(1+\psi)} & 0 & \frac{EJ(2-\psi)}{h(1+\psi)} \\ -\frac{12EJ}{h^3(1+\psi)} & 0 & \frac{6EJ}{h^2(1+\psi)} & \frac{12EJ}{h^3(1+\psi)} & 0 & \frac{6EJ}{h^2(1+\psi)} \\ 0 & -\frac{EA}{h} & 0 & 0 & \frac{EA}{h} & 0 \\ -\frac{6EJ}{h^2(1+\psi)} & 0 & \frac{EJ(2-\psi)}{h(1+\psi)} & \frac{6EJ}{h^2(1+\psi)} & 0 & \frac{EJ(4+\psi)}{h(1+\psi)} \end{bmatrix} \begin{Bmatrix} u_i \\ w_i \\ \phi_i \\ u_j \\ w_j \\ \phi_j \end{Bmatrix} \quad (2.2)$$

Where:

$$\psi = 24(1+\nu)\chi \left(\frac{r_i}{h} \right)^2 = 24 \left(1 + \frac{E-2G}{2G} \right) 1.2 \frac{b^2}{12h^2} = 1.2 \frac{E}{G} \frac{b^2}{h^2}. \quad (2.3)$$

Nonlinear behavior is activated when a nodal force value reaches its maximum value defined as the minimum of the following resistance criteria: Combined compressive and bending stress, shear-sliding, diagonal shear-cracking. The solutor shall ensure the overall and local balance as set out below.

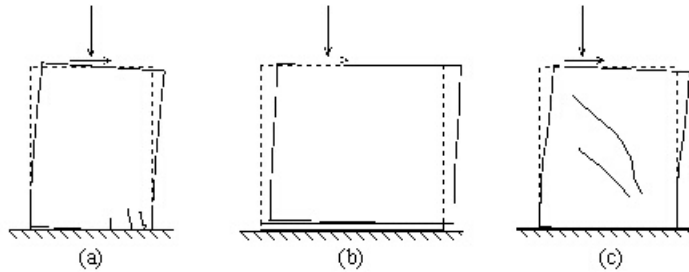


Figure 2.12 - Damage mechanisms in the masonry plane: Flexural, Combined compressive and bending stress (a), Shear and sliding (b) and shear and diagonal cracking (c) (Magenes et al., 2000)

Failure criteria for masonry piers and spandrel are based on the approximate evaluation of local, or mean, stress state induced by applied forces on predefined points (or sections) of the panels, to be compared with proper limit strength for constitutive material (and the panel itself). It means that for the flexural response the failure mode is associated to the attainment of the ultimate bending moment (M_u), calculated on the basis of the beam theory. Instead, for the case of shear response the failure is associated to the achievement of shear strength (V_u), many criteria are related to this behaviour and literature propose different models (for the Italian code refers to NTC 2018, §7.8, and some criteria in the Application Circular of Technical Standards as indicated in §C8.7). All the aforementioned criteria are extensively integrated in TreMuri and in-depth explained in the user manual integrated in the program (Stadata, 3Muri-User Guide).

3. Case Study

3.1. Choice of case study

This thesis deals with the seismic assessment of existing masonry structures carried out through non-linear static analyses implemented with TreMuri software applied to a case study of a typical Ligurian building. This kind of structures are characterized by a seismic behavior which is governed by the structural response of the many interacting units which form the whole building. This interaction can be relevant especially if the units are characterized by various architectural features that lead to different dynamic properties, stiffness, and strength of the units such as an eccentric tower incorporated in the building structure.

The choice of the case study that will be presented below was made precisely to go to investigate these special interactions, considering the presence of a tower element of the said structure. This features, which represent in plan and elevation irregularities, often constituted critical issues for the application of the nonlinear static approach. First, the implementation of a pushover analysis requires the availability of proper nonlinear models, therefore, within this context, this work intends to provide a contribution to the seismic analysis of masonry buildings, proposing TreMuri program. Then, it is necessary to choose the load pattern to use, the most reliable, considering the difficulty in knowing in advance the inertial forces that a seismic event may activate on a given building. Once pushover analyses have been performed, the results have been compared with the NLDA to identify the proper load pattern (it will be discussed in §6.3). The procedure requires the identification of displacements related to the attainment of different Performance Levels (PLs) or Limit States. In general, codes do not distinguish between PLs and DLs and the definition of PLs may be treated by checking the corresponding DLs in each single element. It turns out to be too conservative, often inadequate in the case of buildings with plan and elevation irregularities since it cannot take into account the localization of damage in single walls. For this reason, special investigation on each wall has been performed to check the local damage and some anticipated displacements have been identified.

Although NLSA represents a very suitable tool for the seismic analyses of masonry buildings, an extensive validation of this procedure in case of irregular structures is still lacking, and it is the object of this thesis for which the analysis results were compared with the results derived from the NLDA. Therefore, specific directions were provided on the most appropriate load patterns to be used in the pushover analysis and specific considerations were made to choose the most faithful equivalent frame model, especially for the presence of the tower, to obtain reliable results.

3.1.1. Masonry towers

The masonry towers are elements that constitute architectural heritage and are widely used in Italy, are appreciable representative elements for their prevalent high-rise peculiarity. They were seen a symbol of richness and power of the great families. Unfortunately present a huge seismic vulnerability. The seismic behavior of these structures depends on specific features such as the presence on the top part of vulnerable elements (such as cornices or parapets) and on the presence of adjacent shorter structural

elements. These features affecting the seismic performance of towers, directly, and the whole building. The presence of horizontal constraints at different heights of a tower may deeply change its structural behaviour. On one hand, they can reduce the oscillating period by restricting the actual slenderness. On the other hand, they can induce local stiffening which may produce stress state concentrations and, therefore, severe localized damages.

How already said, the idealization of every model starts from the earthquake damages observation. The seismic assessment of such complex structures shows several critical issues. The first problem deals with the definition of the best modeling choice to be adopted. It must balance the need of a reasonable computational effort with the need of guaranteeing a reliable assessment able to catch the interaction effects. The second problem is instead connected to the lack of tools and standardized procedures to perform the seismic analysis and verification of such quite complex masonry structures.

By considering the modelling choice issues, two different approaches can be adopted: i) decomposition of the whole asset into different units, ii) considering the entire structure realizing an unique global model. The second one is considered the most reliable for the structure mentioned, characterized by an aggregation of adjacent units because it account for the interaction between them (mutual boundary conditions), as TreMuri works (Macroelements). Afterwards, once defined the most suitable model, the second further critical issue deals with the procedure for the analysis and verification, which is not manageable a priori.

In the following section the study case will be presented (§3), starting by a preliminary analysis which consist in the data acquisition, through investigation. These are performed first from the historical point of view collecting the appropriate documents, then through on-site inspections. Once created the 3D model, will be explained the procedure for performing both NLSA and NLDA: the load pattern used in NLSA and the seismic input adopted in NLDA, the approach adopted for the definition of the performance levels and the comparison between results.

3.2. Preliminary feasibility study

Knowledge and characterization of materials are necessary and increasingly essential data in the world of consolidation. It follows the importance of knowing how to choose the most appropriate investigation depending on the case study and knowing how to correctly interpret the experimental data. The following chapter presents the results of the diagnostic campaign conducted on a three-stories stone and concrete building in Chiavari, proposing the TreMuri program for the seismic calculation of the structure.

3.2.1. Data collection

The preliminary investigation phase was conducted by researching the original projects deposited in the institutional offices and analysing the architectural surveys carried out. The documents were analysed with the aim of understanding the design logic of the building, the loads with which it was designed, the construction details used and the construction phases.



Figure 3.1.– Building's frontal view.



Figure 3.2 – Building's lateral view..

3.2.2. Acquisition and analysis of archival documentation

Given the time of construction, early 1900s, and the technique used for the construction of the main body of the building, any architectural or structural projects were not researched. Any search for these documents will be evaluated retrospectively.

3.2.3. Building description and data analysis

The building is settled in Chiavari, In Corso Lima, metropolitan city of Genoa, nearby La Spezia (geographical coordinate 44°32'08.32"N 9°32'47.84"E, in decimal degree 44.320832, 9.324784). The construction seems has not been subjected to modification by times, the only doubt is related on the tower element.



Figure 3.3- Satellitar view.

3.2.4. Main body

The main body was built around the early 1900s and consists of three residential floors above ground, with an articulated plan, inscribed in a rectangle of 14.55 m x 12.47 m. The roof is flat and walkable from which you can access the tower (fourth floor above ground)

From a structural point of view, based on the preliminary investigations, the walls were made of regular stone, with a gross thickness of about 40/55 cm for the perimeter walls and about 40 cm for the internal load-bearing walls. The internal secondary brick walls of different thicknesses (10 for the partitions, 15, 22, 35 cm the others). A separate discussion is made for the roof tower which was made up of perforated bricks 24x12x8 cm and reinforced concrete slab.

Table 3.1- inventory of the materials investigated

REGULAR STONE BEARING WALL	INTERSTOREY SLAB
	
INTERNAL STONE WALL	INTERNAL BRICK WALL
	
ROOF COVERING SLAB	TOWER SLAB
	

The ground floor has an inter-floor height of approximately 2.95 m. Presumably, the tread and roofing floors were made of concrete (structural part 10 cm and then the flooring, grit in the first and second floors).

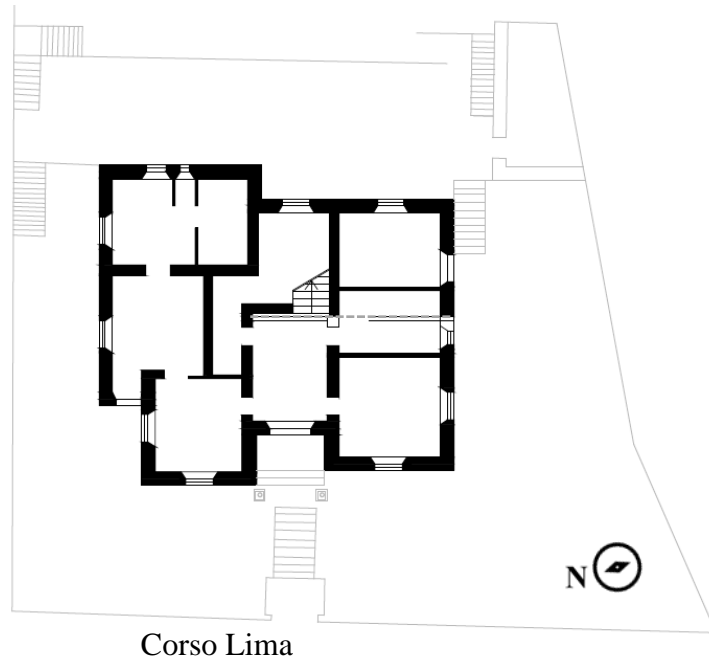


Figure 3.4 - Ground floor structural plan.



Figure 3.5 - Ground floor interior, beam detail.

On the upper floor, compared to the ground floor, the perimeter walls in stone remain (with a thickness that tapers off passing from a gross thickness of 55 to 50 up to 45 cm), while internally the spatial arrangement between the first and the second floor. (see figures 6 and 7).

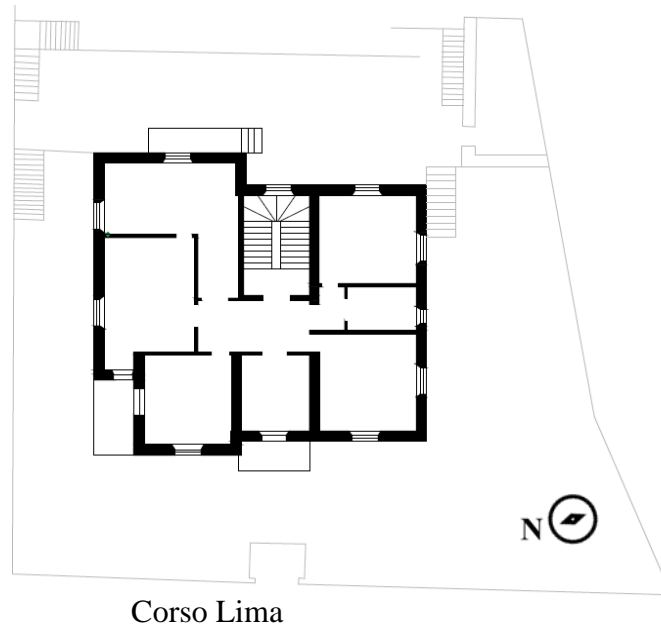


Figure 3.6 - Structural plan ground floor.

The structure of the slab was made of concrete, as previously mentioned. Above the screed there was the Genoese grit flooring.

On the second level, the layout and size of the walls remains like the lower level.

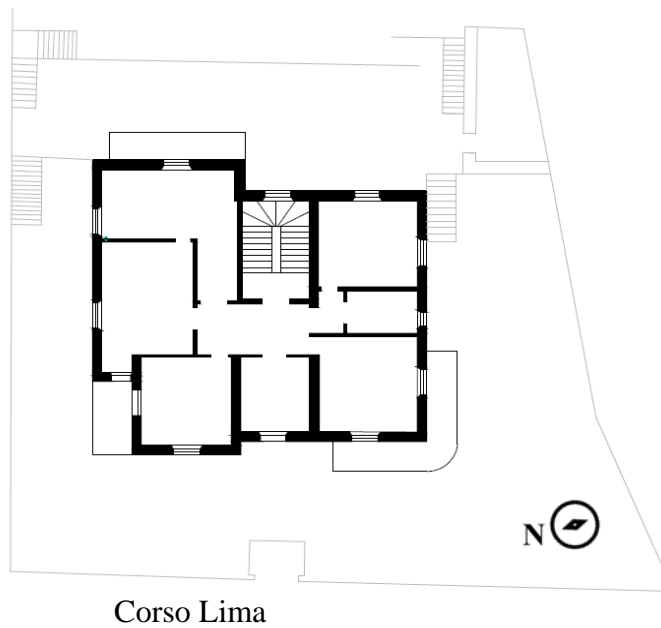


Figure 3.7 - First floor structural plan.

On the third level, the flat roof houses the tower.

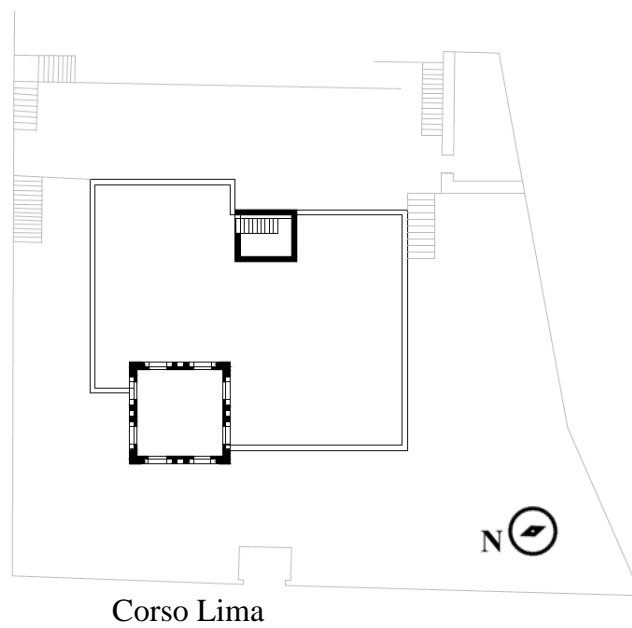


Figure 3.8 – Third floor structural plan.

The roof structure was made of concrete, a tile flooring was probably added later as shown in figure.



Figure 3.9 – Flat Roof and tower

3.3. Property inspection done

On Tuesday, April 13, the preliminary inspection of the property was carried out to ascertain the consistency of the architectural projects, the conditions of the structural elements and identify all possible causes of danger from a static and seismic point of view.

3.3.1. Verification of structural coherence

On 13 it was possible to access the building's premises to view the main elements of the structure.

3.3.2. Overall state of the structural elements

The control of the structural elements was not carried out in the preliminary phase, but it is considered to proceed with some investigations to look into the position and size of inter-floor slabs, pillars, walls and partitions. The acquired data are however sufficient to conduct a preliminary safety analysis. Further considerations can be made in the following phases when the structural role of each element will be clear.

Through the survey, is possible announce that a non-significant structural damage is present.

Firstly, by considering the **foundation** we can say:

- It was not possible to view this portion of the structure, but no deformation or significant settlement are visible.

For **load-bearing masonry walls**:

- No significant crack patterns were found;
- No deformation or settlement phenomena were detected;
- No degradation or deterioration phenomena of the material that could compromise its mechanical properties have been detected.

For the **first-floor concrete slab**:

- It was not possible to see this portion.
- No deformation or settlement phenomena were detected.
- No degradation or deterioration phenomena of the material that could compromise its mechanical properties have been detected.

For the **second-floor concrete slab**:

- It was not possible to see this portion of the structure in a satisfactory way, but it was possible to deduce its stratigraphy from visible surveys.
- No deformation or settlement phenomena were detected.
- No degradation or deterioration phenomena of the material that could compromise its mechanical properties have been detected.

For the **hedging structure** it can be stated that:

- No deformation or settlement phenomena were detected.
- No degradation or deterioration phenomena of the material that could compromise its mechanical properties have been detected.
- A new floor tiles is probably added in more recent years.

3.3.3. State of non-structural elements

With regard to non-structural elements, Circular NTC2018 points out that, when it is necessary to carry out a safety assessment of a building, it is essential to check not only the health status of the structural elements, but also investigate all evident causes of danger. In this context it is necessary to focus attention on the parapets on the roof, on the perimeter of the building, whose connection to the underlying structure must be controlled and eventually integrated, to verify that, in case of seismic event, no overturning or falling to the ground.



Figure 3.10- Particular parapet on the roof

It also required to evaluate the ledge and all the projecting elements such as balconies and attached decorations.

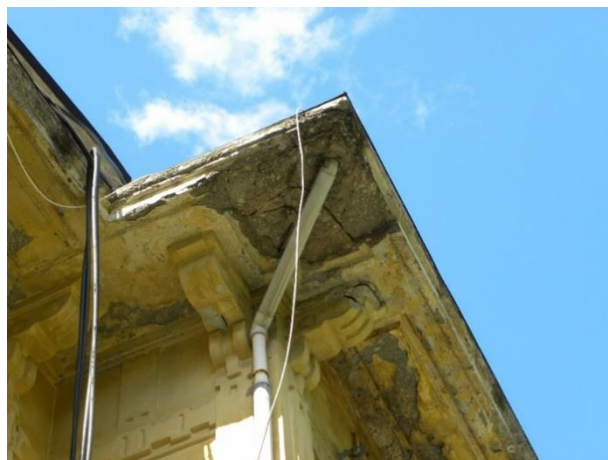


Figure 3.11 - Particular ledge



Figure 3.12 - Particular balconies



Figure 3.13- Particular coverage

3.3.4. Investigation of the tower



Figure 3.14 - Tower element

Based on the surveys, reasonable doubts have been raised up on data of construction of the tower. Therefore, it will be deepened the role of the tower once the analyses are launched, as can be seen in the next chapters (in §5.1).

In any case for this element have been made assumptions that will highlight the peculiarities of the building subject of this thesis, which in some way reflects those situations that often involve existing buildings, especially in the Italian territory, which are mainly characterized by irregularities in plant and elevation.

3.3.5. Surveys of slabs and floor

Through a preliminar investigation, the visual inspection performed, was possible understand the slab stratigraphy and composition.



Figure 3.15 - Investigation on the interfloor slab.

Step 1: Structure input

4. Modelling phase

A preliminary model of analysis of the structure was created to evaluate the feasibility of seismic improvement interventions. The model was created with STA Data's 3Muri software. The main parameters of the structure have been defined, necessary for the calculation model.

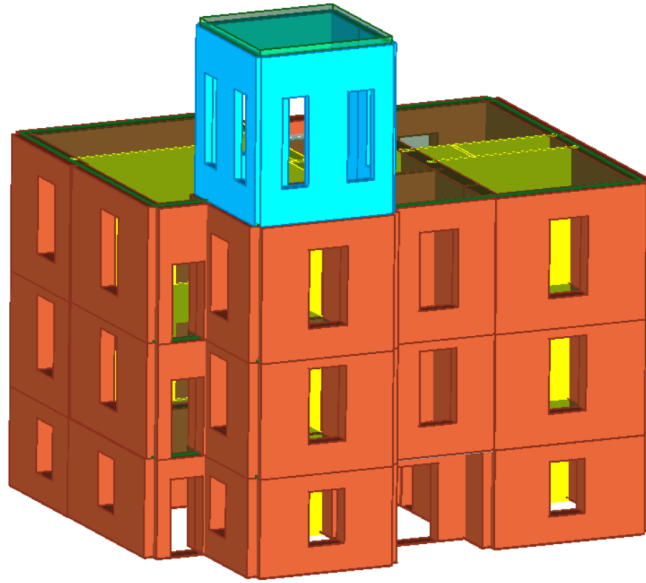


Figure 4.1 - Tremuri 3D model of building.

For the mechanical characterization of materials, the knowledge level was also taken into account, which determines the assignment of a confidence factor (FC), which acts as an additional partial safety coefficient, reducing the value of the resistance used in the calculations by the program. For the seismic safety calculation of a structure, the parameters defined by partial safety coefficients γ_m and confidence factors shall be used. It applies that is:

$$f_d = \frac{f_m}{(FC \times \gamma_M)} \quad ; \quad f_{vd} = \frac{\tau_0}{(FC \times \gamma_M)} \quad (4.1)$$

where:

f_d is the characteristic compressive strength of the masonry;

τ_0 is the characteristic shear strength of masonry;

γ_m is the partial safety coefficient on the resistance of the masonry.

The confidence factor, to be used as a partial safety coefficient to consider deficiencies in the knowledge of the design parameters of the model, varies between 1 and 1.35 depending on the level of knowledge (KL) of the different parameters involved in the model (geometry, construction details and materials).

Table 4.1- Knowledge levels based on available information and resulting confidence factor values for masonry buildings.

Knowledge level	Geometry	Constructive Details	Materials Properties	KL
KL1	Relief masonry, vaults, floors, stairs. Detection of loads on each wall element.	Limited in situ verifications	Limited in situ investigations	1.35
KL2	Identification type foundations.	<i>Extensive and exhaustive in situ verifications.</i>	In situ extended surveys	1.2
KL3	Detection of any cracking and deformative picture.		In situ comprehensive surveys	1

Since for the present case study, a limited in situ inspection were performed, therefore the knowledge level adopted was the first.

In general, the materials are characterized by three parameters: the stiffness expressed as inclination of the portion in which the behavior is elastic (elastic modulus), the resistance to yield strength and the ultimate displacement of the material before rupture. In the following section the mechanical parameter of the material detected in situ will be presented. To carry out nonlinear analyses, both static and dynamic, considering the stiffness of the cracked materials, with the ratio of elastic stiffness to secant stiffness equal to 1.6.

4.1. Mechanical masonry parameters

For the definition of the mechanical characteristics of the stone and brick masonry, we started from the characteristics of the materials detected in situ. Starting from these characteristics, the indications present in the NTC2018 were followed for the definition of all the necessary parameters and what is reported in the Application Circular (Ministerial Circular No. 7 of 21/01/2019). For the external walls stone masonry was detected, while for the internal walls it is assumed that simple solid bricks and lime mortar were used, and its mechanical characteristics are summarized in Table 4.2, where f_m is the average compressive strength of masonry, τ_0 is the average shear resistance of masonry, E is the elastic modulus, G is the shear modulus and w is the specific weight of the element.

Table 4.2 - Mechanical characteristics of masonry.

MASONRY WITH HEWN SEGMENTS, WITH FACING OF UNEVEN THICKNESS		SOLID BRICKWORK AND LIME MORTAR	
EXTERNAL WALLS		INTERNAL WALLS	
E [N/mm ²]	1,230.00	E [N/mm ²]	1,500.00
Eh [N/mm ²]	1,230.00	Eh [N/mm ²]	1,500.00
G [N/mm ²]	410.00	G [N/mm ²]	500.00
w [kN/m ³]	20	w [kN/m ³]	18
f _m [N/cm ²]	200.00	f _m [N/cm ²]	260.00
f _{hm} [N/cm ²]	150.00	f _k [N/cm ²]	134.81
f _k [N/cm ²]	103.70	f _b [N/mm ²]	7.5
τ [N/cm ²]	3.50	f _{v0} [N/cm ²]	13.00
FC	1.35	Φ	0.50
γ _m	3.00	μ	0.58
Maschio drift taglio	0.0050	f _{bt} [N/mm ²]	0.8
Maschio drift flessione	0.0100	FC	1.35
Fascia drift taglio	0.0150	γ _m	3.00
Fascia drift flessione	0.0150	Maschio drift taglio	0.0050
Fascia accoppiata drift	0.0200	Maschio drift flessione	0.0100
Stato	Esistente	Fascia drift taglio	0.0150
Descrizione	Muri esterni in pietra	Fascia drift flessione	0.0150
Libreria		Fascia accoppiata drift	0.0200
		Stato	Esistente
		Descrizione	muri interni mattoni pieni
		Libreria	

In addition to the load-bearing masonry and partitions of the three above-ground floors, thanks to the surveys, it is presumed that, for the tower, perforated bricks have been used, the mechanical characteristics are summarized in Table 4.3.

Specifically, for the modelling in commercial 3Muri, are used the following parameters:

$E=4200$ Mpa, $G=1400$ Mpa

$f_m=2$ Mpa

$\tau_0=0.14$ Mpa (with the criterion of Turnšek and Cacovic¹, or that for the irregular masonry)

$w=15$ kN/m³

The parameters assumed were derived from some experimental tests, in particular simple compression tests on wall panels made in the laboratory, drawn up by the University of Genoa in which it was experimentally characterized the masonry in blocks with horizontal holes, typical of the '50s-'60s in the northern Italian area.

¹ The Turnšek Cacovic criterion represents a type of diagonal cutting breakage (when the masonry element is subject to the combined action of cutting and bending) and its use is recommended in particular for existing irregular masonry (§2.3.3.4).

Table 4.3 - Mechanical characteristics of masonry's tower.

PERFORATED BRICK MASONRY	
WALL'S TOWER	
E [N/mm ²]	4,200.00
Eh [N/mm ²]	4,200.00
G [N/mm ²]	1,400.00
w [kN/m ³]	15
f _m [N/mm ²]	2.00
f _{hm} [N/mm ²]	1.50
f _k [N/mm ²]	1.00
τ [N/mm ²]	0.14
FC	1.35
γ _m	3.00
Maschio drift taglio	0.0060
Maschio drift flessione	0.0100
Fascia drift taglio	0.0150
Fascia drift flessione	0.0150
Fascia accoppiata drift	0.0200
Stato	Esistente
Descrizione	mattoni forati torre
Libreria	

4.2. Mechanical concrete parameters

The mechanical parameters of the concrete are used in line with the resistance parameters defined by the codes and its characteristics are summarized in the Table below.

Table 4.4 - mechanical parameters of concrete.

CONCRETE	
Nome	C8/10
E [N/mm ²]	25,331.00
G [N/mm ²]	10,555.00
w [kN/m ³]	25
f _{cm} [N/mm ²]	16.0
f _{ck} [N/mm ²]	8.0
γ _c	1.50
α _{cc}	0.85
Stato	Nuovo
Descrizione	
Libreria	Italia (NT18 circolare)

Some specific assumptions were made for the small unreinforced concrete pillars in the tower. For this element a new masonry material called “CLS” was defined. As regards this material used, irregular masonry rupture criteria has been defined (because it is a criteria for isotropic breakage, diagonal cracking, as well as concrete, which does not have an orthotropic structure in blocks and joints).

Since it is not known with which construction sequence the pillars were made, there may be a problem in the analysis phase, typical in all finite element analyses (or equivalent frame): the model calculates the stresses as if everything were built simultaneously and then "disarmed". Therefore, following this premise, a value comparable to that of the masonry is used to avoid this effect and are used the following parameters:

$E=5000 \text{ Mpa}$, $G=2000 \text{ Mpa}$
 $f_m=16 \text{ Mpa}$
 $\tau_0=1.0 \text{ Mpa}$
 $w=22 \text{ kN/m}^3$ (not reinforced concrete)

Table 4.5 - mechanical parameters of tower's concrete.

TOWER'S CONCRETE PILLARS	
E [N/mm ²]	5,000.00
Eh [N/mm ²]	5,000.00
G [N/mm ²]	2,000.00
w [kN/m ³]	22
f _m [N/mm ²]	16.00
f _{hm} [N/mm ²]	5.00
f _k [N/mm ²]	8.00
τ [N/mm ²]	1.00
FC	1.35
γ _m	1.50
Maschio drift taglio	0.0050
Maschio drift flessione	0.0100
Fascia drift taglio	0.0150
Fascia drift flessione	0.0150
Fascia accoppiata drift	0.0200
Stato	Esistente
Descrizione	simulazine di un pilastro i...
Libreria	

4.3. Mechanical steel parameters

The mechanical parameters of the steel were defined on the basis of the STIL database data for a common steel category for the building's construction years, the significant mechanical parameters are described in the figure 4.2.

Table 4.6 - Mechanical characteristics of steel bars.

STEEL BARS	
Nome	B450
E [N/mm ²]	206,000.00
G [N/mm ²]	79,231.00
w [kN/m ³]	79
f _{ym} [N/mm ²]	484.0
f _{yk} [N/mm ²]	450.0
γ _s	1.15
Stato	Nuovo
Descrizione	NTC08
Libreria	Italia (NT18 circolare)

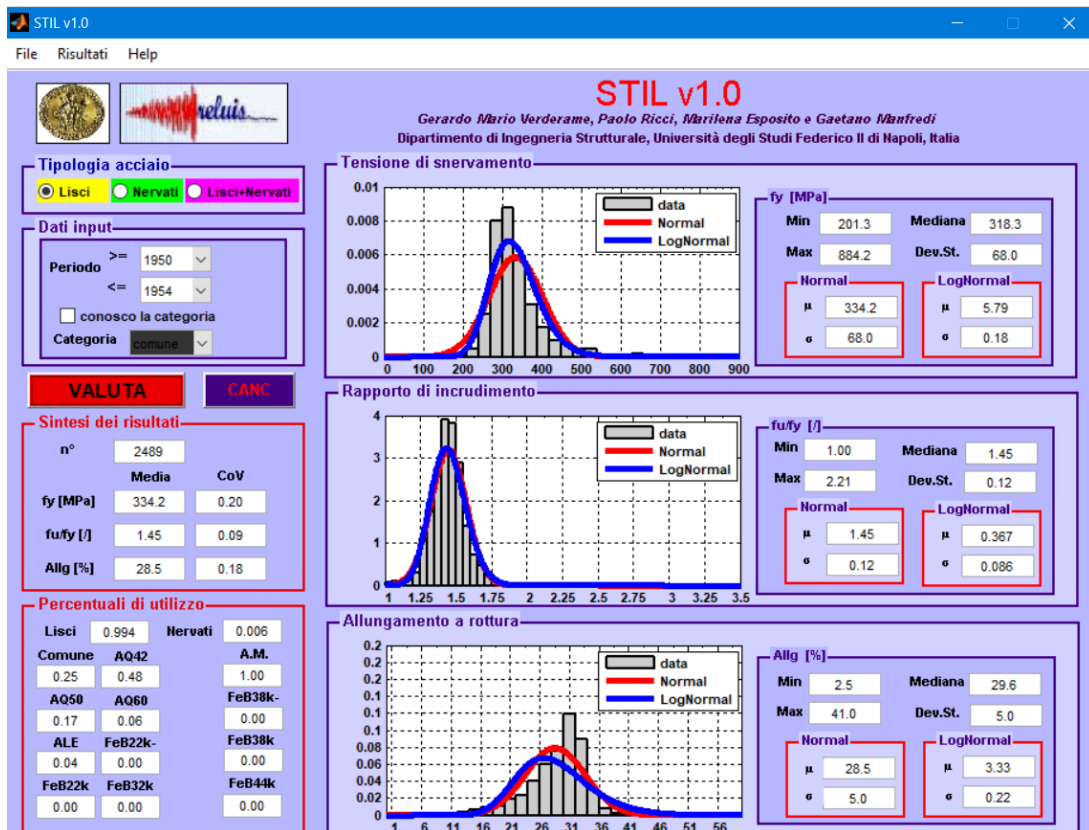


Figure 4.2 - Mechanical parameters from the 1950s / 54s.

4.4. Mechanical parameter of the slabs

The floors interact with the walls by transferring the seismic loads generated on them thanks to their stiffness in the plane and tangential.

In the software TreMuri, diaphragms are modelled as finite elements of type "orthotropic membrane" (plane stress element) of triangular or quadrangular shape (3 or 4 nodes). They are identified by a principal direction (floor spanning direction), with two values of Young Modulus along the two orthogonal directions (parallel, E_1 , and perpendicular, E_2 , to the spanning direction), Poisson ratio (ν) and the in-plane shear modulus (G_{eq}). This latter represents the shear stiffness of the floor and influences the horizontal force transferred among the walls, both in linear and nonlinear phases. The mechanical characteristics of the floors aforementioned have been obtained by making some assumptions and thanks to on-site inspections. It is therefore assumed a slab with a structural part of 10 cm and characterized by different stratigraphies for the interstorey floors, floor covering and tower. For the definition of the structural part and its own equivalent slab, inside the modelling in commercial 3Muri, was considered a hollow-core concrete floor with the smaller size of the bricks, so that it was comparable to a full slab.

Table 4.7 - Structural slab definition.

Equivalent membrane	
Thickness (cm)	10
G (N/mm ²)	10400
Ex (N/mm ²)	25000
Ex (N/mm ²)	25000
ν	0,2

4.5. Reference parameters adopted in the design phase

During the design phase, the cracked stiffness of the elements was considered to simulate the structure under seismic actions, as suggested by NTC18. It should be noted that in the calculation performed by the program, the flexural and shear behaviour has been accounted for. The legislation suggests that, if specific analyses are not carried out, the bending and shear stiffness of the elements in masonry, reinforced concrete, concrete steel, can be reduced up to 50% of the stiffness of the corresponding elements not cracked. For this purpose, the parameters considered are listed below.

Table 4.8 - Reduced material properties used for modeling.

	Material N.	E (N/mm ²)	G (N/mm ²)	f _m	τ ₀
Rough-hewn	89	615	205	2	0.03
Solid brick	90	750	250	2.6	f _{v0} =0.13
Perforated brick	91	2100	700	2	0.14
Cls	92	2500	1000	16	1

Step 2: The Analysis

5. Preliminary seismic vulnerability results

After completing the construction of the model and inserting the characteristics of the elements, materials, constraints and loads it is possible to proceed with the phase dedicated to the analysis.

This phase includes two steps: the first is related to the definition of the equivalent frame, the second to the push-over analysis itself.

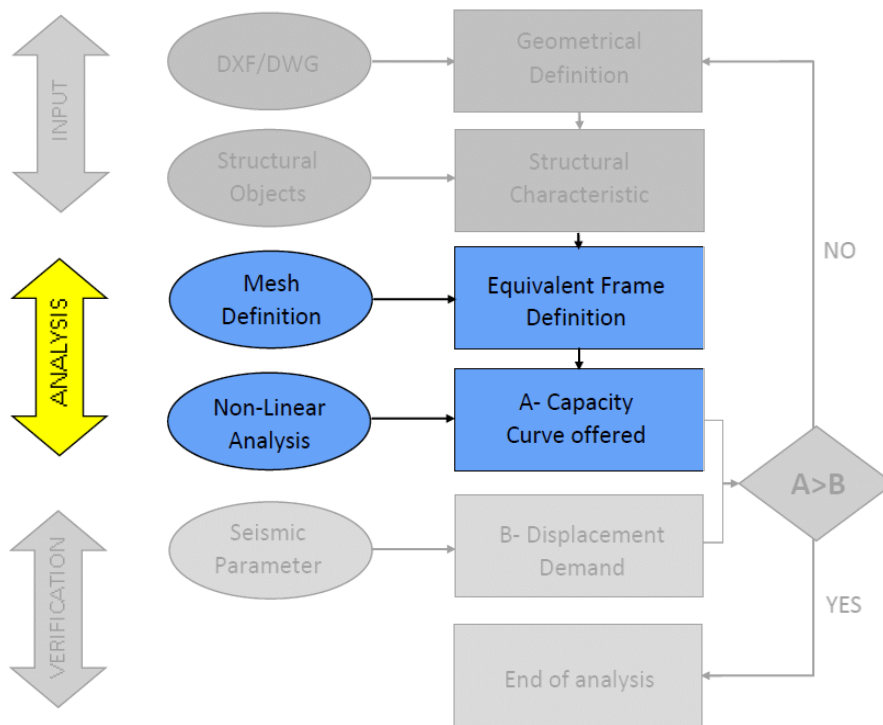


Figure 5.1 - Analysis phase

5.1. Equivalent frame definition

Starting from the geometry and inserted structural objects are derived data for analysis according to the 3Muri model, i.e. the equivalent frame. The result of this analysis is the presentation of a mesh that schematizes piers, spandrel, beams and pillars (figure 5.2). Some of these elements were modified manually to take into account the particular situation that occurred on the tower. We expect that the irregularities in the plan and in the elevation of this building will highlight several problems both in terms of modal analysis and pushover analysis.

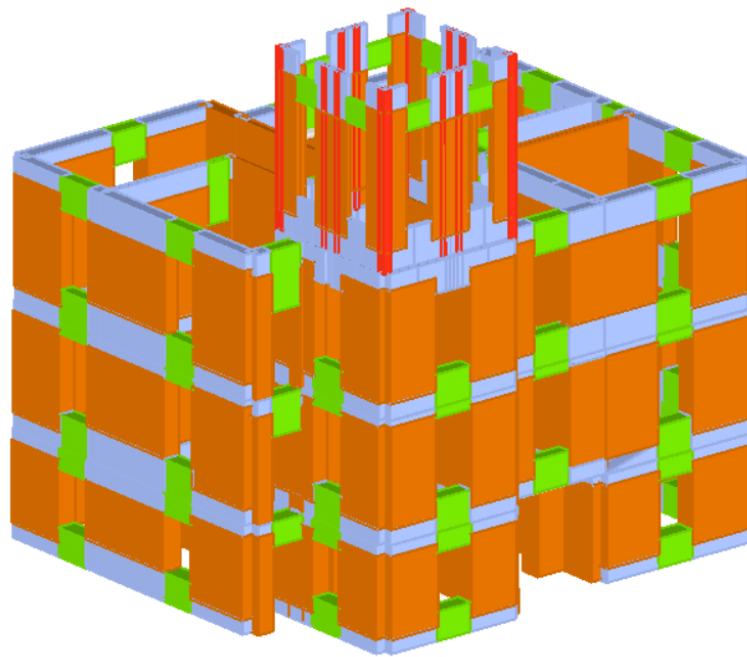


Figure 5.2 - 3D view showing the equivalent frame idealization (orange = piers; green = spandrels; blue = rigid nodes, red=pillars).

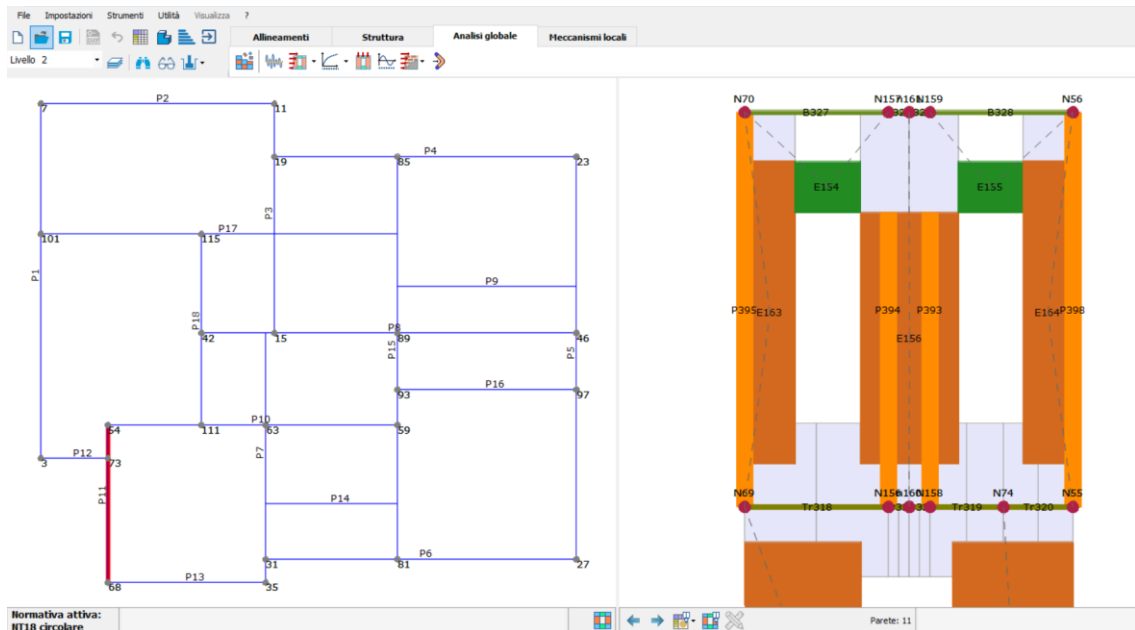


Figure 5.3 - TreMuri Tower's idealization.

5.1.1. Load analysis

In the preliminary study phase, it was necessary to trace the static loads acting on the structure. This phase was completed by carrying out an analysis of the loads for each element that characterizes it, starting from the definition of materials weight detected in situ summarized in Table 5.1.

Table 5.1 - Weights of the units of volume of materials used.

Weights of materials		
Concrete	22,0	KN/m ³
Light concrete	16,0	KN/m ³
Lime mortar	18,0	KN/m ³
Screed	18,0	KN/m ³
Tiles	0,4	KN/m ²
Pitch	0.03	KN/m ²

In addition, the load analysis performed are shown below for:

- Interfloor Slab;
- Roofing;
- Tower's Roofing.

Table 5.2 - Load analysis, interfloor concrete slab.

Interfloor Slab		
Permanent Loads		
Concrete Slab (G₁)	$(0,1*1,0*1,0)*22,00 = 2,20$	KN/m ²
Screed (G₂)	$(0,02*1,0*1,0)*18,00 = 0,36$	KN/m ²
Tiles (G₂)	0,40	KN/m ²
Variable Loads		
Residential Environments Cat. A (q_k)	2,00	KN/m ²

Table 5.3- Load analysis, roof concrete slab

Roofing		
Permanent Loads		
Concrete Slab (G ₁)	$(0,1*1,0*1,0)*22,00 = 2,20$	KN/m ²
Screed (G ₂)	$(0,02*1,0*1,0)*18,00 = 0,36$	KN/m ²
Tiles (G ₂)	0,40	KN/m ²
Screed (G ₂)	$(0,02*1,0*1,0)*18,00 = 0,36$	KN/m ²
Tiles (G ₂)	0,40	KN/m ²
Variable Loads		
Residential Environments Cat. A (q _k)	2,00	KN/m ²

Table 5.4 - Load analysis, tower's concrete slab.

Tower's Roofing		
Permanent Loads		
Concrete Slab (G ₁)	$(0,1*1,0*1,0)*22,00 = 2,20$	KN/m ²
Screed (G ₂)	$(0,02*1,0*1,0)*18,00 = 0,36$	KN/m ²
Pitch (G ₂)	0.03	KN/m ²
Lime (G ₂)	$(0,02*1,0*1,0)*18,00 = 0,36$	
Tiles (G ₂)	0,40	KN/m ²
Variable Loads		
Residential Environments Cat. A (q _k)	2,00	KN/m ²

5.2. Safety assessment

The safety assessment of existing buildings is an important topic for experts working in construction. It requires specific skills in order to meet economically (incremental cost for increasing structural safety), socially (reduction or disruption of serviceability and preservation of heritage values) and sustainably (reduction of waste and recycling) the reliability of the structures. Recent earthquakes have confirmed the high seismic vulnerability of this type of structures, which suffered damage even for low intensity earthquakes and undergone collapses for levels of intensity for which the life safety should be guaranteed. Especially for irregular structures characterized by elements of high vulnerability, such as a tower. Hence, the identification of a structural model for the

assessment is not straightforward, because in principle a clear distinction between structural and non-structural elements is not possible in the existing building field. In addition, material properties are inhomogeneous and difficult to be measured by in-situ non-destructive tests. As shown in the previous chapter some visual inspection has been performed, as suggest from the codes, to assign the most reliable characterization of materials.

On the basis of these premises, the model has been defined as shown in §4 and seismic safety is assessed by analysing the model and making the appropriate checks, well knowing that the seismic response of masonry buildings depends on the behaviour of masonry walls, both in plane and out of plane mechanisms (see §2.1), on the connection between walls, and on the interaction with horizontal elements. In any case, the safety verification is performed by checking at global level that the displacement demand is lower than the displacement capacity.

In the following sections some basic knowledge will be presented in a simplified way to understand better the steps needed to the define the linear force-deformation relationship and to understand how the software works.

5.2.1. From MDOF to equivalent SDOF systems

The NCTs propose analysis methods and verification criteria (in the administrative circular §C7.3.4.2). In the present case, non-linear static analyses were used to determine the capacity curve of the structure. As already mentioned, in the introduction, the pushover curve describes the relation between the applied overall base shear (V_{tot}) and the displacement, by assuming a control displacement usually at the top of the structure (d_{top}). Theoretically, the solution could only be found when the control node is on the 4th floor, the last floor of the building: I impose a displacement to the 4th floor, and I look for the deformed compatible with the distribution of forces. The pushover analysis (mixed control of displacement and forces) is used to understand the structure behaviour and, to do that, we must introduce the displacement and acceleration response spectra.

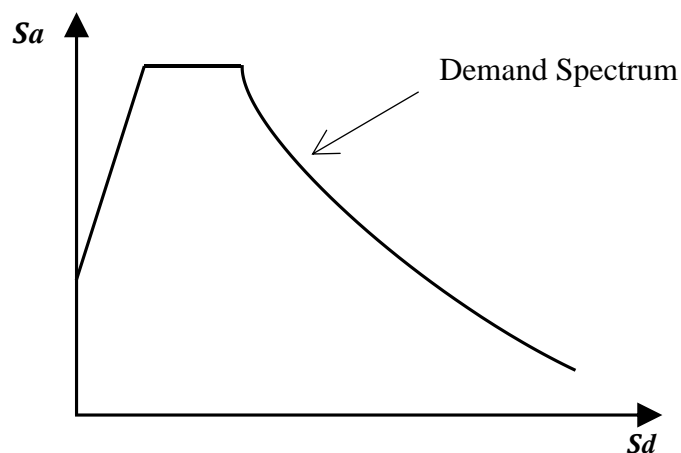


Figure 5.4 - Acceleration Displacement Response Spectrum.

The applied overall base shear (V_{tot}) is considered as an approximate representation of the inertial forces that a building may be subjected during an earthquake. In the case of study, the pushover analyses in the X and Y directions (positive and negative directions) were

taken into account, using the uniform the triangular distribution (proportional to the static forces) and also the modal distribution, limiting themselves to the situation without eccentricity.

According to the non-linear static procedure, we need to compute the seismic demand through a given seismic action (see §5.3.1) by comparing the pushover curve and the seismic action (described by the response spectrum). For each limit state considered, the comparison between the capacity curve and the displacement demand allows to determine the level of equilibrium reached. To this end, a structural system equivalent to a single degree of freedom (SDOF) is usually associated with the real structural system (MDOF). That is possible by introducing some factors (Γ and m^*) associated to dynamic response of the structure. We introduce the participant factor (Γ) and the participant mass (m^*).

$$\Gamma = \frac{\sum m_i \phi_i}{\sum m_i \phi_i^2} \quad ; \quad m^* = \sum m_i \phi_i \quad (5.1)$$

Where m_i is the mass of the i -floor and ϕ_i represent the expected deformed shape of the building due to the horizontal forces. The participant factor (Γ) is normalized in order to be 1 at the top.

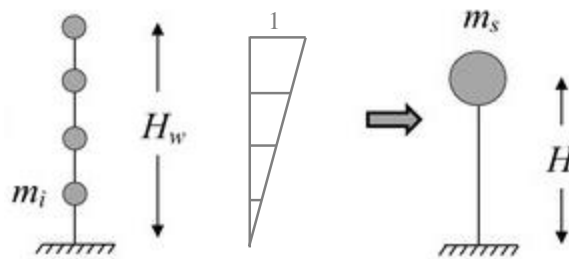


Figure 5.5- Schematisation of the transformation of a MDOF model of a structure to the equivalent SDOF model.

Can be demonstrated that their product is equal to the product of total dynamic mass of the building (M) and the fraction of the activated mass (e^*), equation (5.2) which represents the participant mass of the equivalent SDOF system.

$$\Gamma m^* = \frac{(\sum m_i \phi_i)^2}{\sum m_i \phi_i^2} = \dots = M \cdot e^* \quad (5.2)$$

With

$$m^* = \phi^T M = \sum m_i \phi_i \quad (5.3)$$

So, the first step required is to transform the pushover curve (representative of the MDOF system) into a capacity curve (representative of an equivalent SDOF system). As proposed in such conversion is made through the following expressions (5.4):

$$V_b^* = \frac{V_b}{\Gamma} \quad ; \quad d^* = \frac{d}{\Gamma} \quad (5.4)$$

Where “*” indicates that the quantity refers to an equivalent SDOF system.

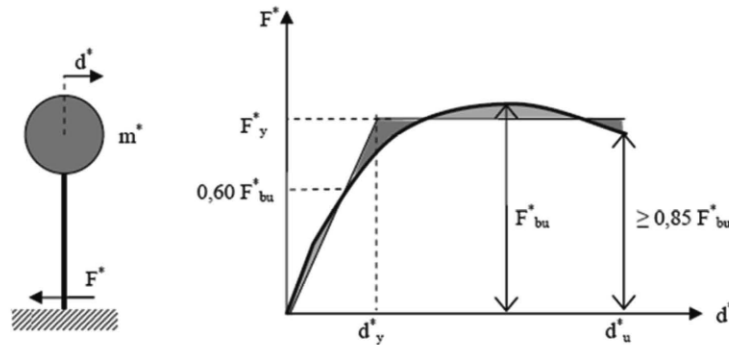


Figure 5.6 - Equivalent bilinear system and diagram, in §C7.3.1 of Circular application C.M. 21 January 2019.

Different procedures exist to account for the structure capacity; most of them require converting the capacity curve in an equivalent bilinear.

According to the Italian code²:

- the initial slope is the one for which the two lines intersect at $0.6 \cdot V_{b,max}$;
- the ultimate displacement capacity is set in correspondence of maximum base shear decay equal to 20% ;
- the bi-linear maximum base shear is defined imposing the areas subtended by the pushover and the bilinear curves are equal (until the ultimate displacement).

Once the displacement demand has been found, d^*_{max} , for the limit state under consideration the compatibility of the displacements might be verified. This methodology is implemented into TreMuri. Through the equivalence expressed before, the ultimate displacement and the maximum displacement are accounted and easily figured out into the pushover analysis (in the overall analysis section of the program).

² Circular application C.M. 21 January 2019, n.7, §C7.3.4.2, **Method A**, based on the identification of inelastic demand through the principle of equal displacement or equal energy.

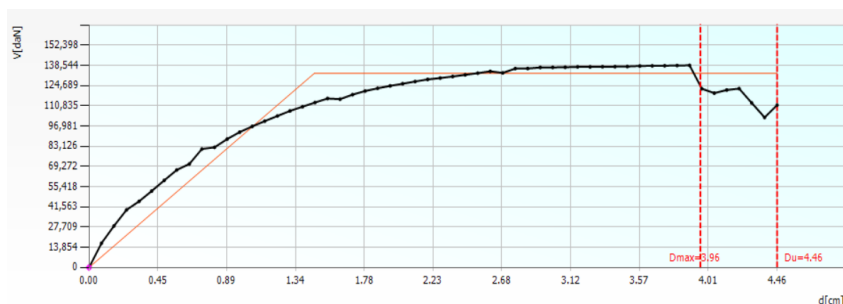


Figure 5.7- Pushover curve and relative displacements in TreMuri.

For operational purposes, literature provides different approaches to account for the non-linearity of the response that led to a reduction of the elastic response spectra, and then for the evaluation of the performance point (PP) of the structure, through the ductility (μ), the so called N2-Method, or through equivalent damping (ξ_{eq}), the Capacity Spectrum Method³.

To determine the spectral acceleration value (S_a) necessary to express the capacity diagram in Acceleration Displacement (AD) format, the force V_b^* from Eq. (5.4) must be divided by the equivalent mass m^* of the system obtained from Eq. (5.3) as shown below:

$$S_a = \frac{V_b^*}{m^*} = \frac{V_b}{\Gamma m^*} \quad (5.5)$$

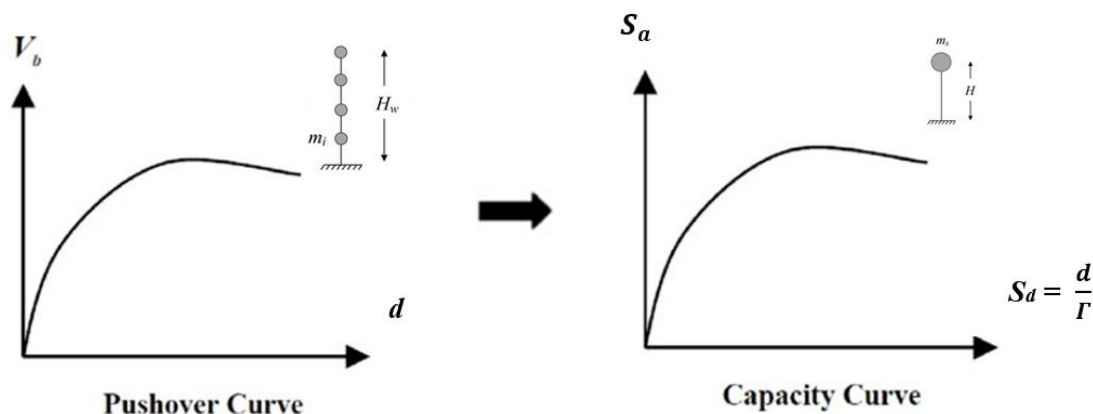


Figure 5.8 - Conversion Procedure from Pushover Curve to Capacity Diagram.

³ In literature exits some approaches to achieve the reduced spectra (Non-Linear Static Procedure): The N2-method, proposed by Fajfar (2000) and adopted by Italian code (NTC2018-MetodoA) and Eurocode8, based on the identification of inelastic demand through the principle of equal displacement or equal energy; The Capacity spectrum method, proposed by Freeman (1973-78) and adopted by American document (ASCE 41/3), New Zealand code (NZEE) and Italian code (NTC 2018-MetodoB), based on the construction of a capacity spectrum.

Then, it is possible to compare the two curves (demand and capacity spectrum as in figure 5.4) to define the “performance point”, which represents the expected displacement demand with a given seismic demand (associated to fixed return period T_R , PGA and the amplification factor S).

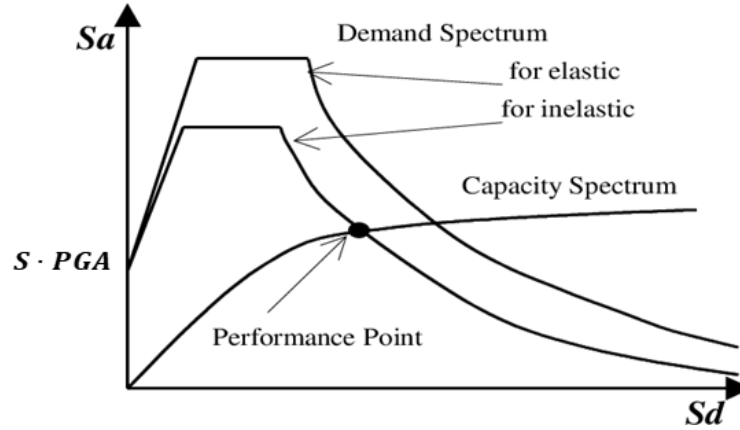


Figure 5.9 - Capacity Spectrum and demand spectrum.

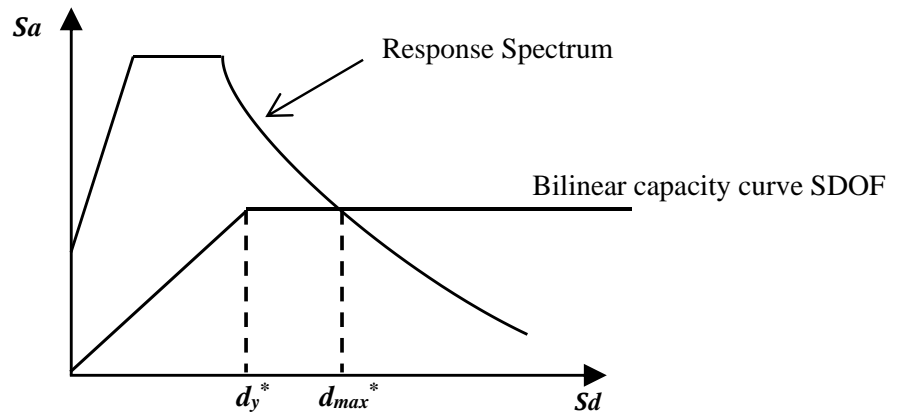


Figure 5.10 - ADRS Format and displacement demand.

Hence, a new performance point is obtained using the reduced elastic response spectrum and the verification consists in checking if the displacement expected for a given seismic demand (d_{PP}^*) is lower than the displacement capacity associated to the Limit State under consideration (d_{SLC}^*).

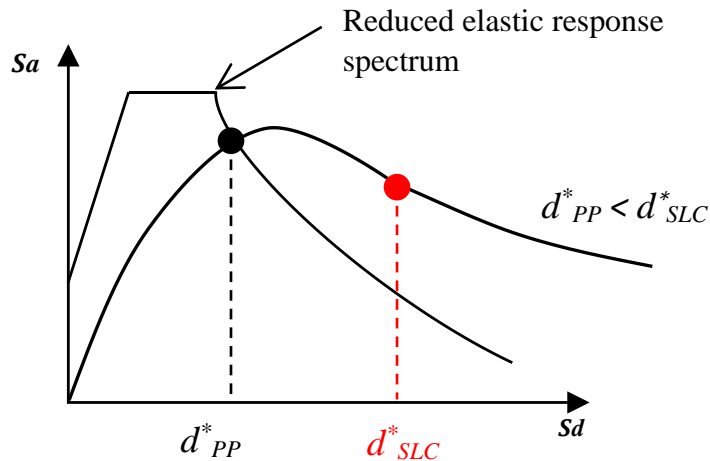


Figure 5.11 - Reduced Elastic Response Spectrum displacement associated to the Limit State under consideration.

At this point, may be compute the maximum peak ground acceleration (PGA) associated to the considered limit state (LS), threshold point who need proper criteria to be defined, by imposing a response spectrum properly reduced. As already mentioned, in the first chapter of this thesis, it constitutes a critical point. The codes provide different approaches based on Global Scale, where the monitored parameter (EDP= Engineering Demand Parameter) is the global base shear. The Near Collapse (LS) is defined according to the ultimate displacement capacity (in correspondence of a strength decay of the overall base shear equal to 20%).

The new version of the Italian and European code, especially for masonry building, suggests combining the global check with local one, in this way we can also monitor the walls that may collapse even before reaching the 20% threshold (local collapse). Thus, if some walls collapse before the global 20% threshold, the new actual displacement demand associated to that LS can be identified as follow (Eq. 5.6).

$$d_{NC} = \min\{d_{NC,G} ; d_{NC,L}\} \quad (5.6)$$

This procedure can be chosen by the technical engineer ticking the box "perform angular deformability check" for the calculation of the overall analysis of the structure (In TreMuri).

5.3. Nonlinear Static Analysis – Pushover

Nonlinear static analysis involves static application of loads. Nonlinearity comes from taking into account the constitutive laws of materials that are intrinsically non-linear, from which the resistance varies according to the level of load due to the degradation suffered (Ref.§ 2). The regulation indicates the criteria of resistance of the masonry that is the conditions whose overcoming means the inability to withstand further loads. These criteria are expressed in terms of displacement divided by the height of the element itself (ultimate drift). The previously defined structural model (in §4) is subject to increasing loads in a progressive way and the control of the reaction of the structure is carried out through the measurement of the displacement of a known control node usually placed at

the top of the structure. The verification of the whole structure is therefore reduced to the comparison between the movements offered by the structure and required by the legislation. The displacement offered is an intrinsic characteristic of the structure because during the push-over analysis no seismic localization hypotheses have been made, but the structure's response to increased load is studied. The required displacement, instead, depends of local seismic conditions that take into account all the characteristics of the soil, the use of the structure (normal, strategic or relevant) and consequently the useful life.

5.3.1. Selection of seismic conditions

To proceed with the analysis, it was necessary to set the seismic load by selecting the seismic zone and the Class of the site according to the Standard. In the Technical Regulations of January 2008, seismic spectra no longer depend on the area seismic (as in the previous regulations) but by the geographical coordinates of the site. This is possible by directly selecting the municipality by using the internal Database that relies on World Geodetic System 84 (WGS 84)⁴ as shown in figure 5.12.

The software calculates the values necessary to define the shape of the spectrum for each limit state by means of the inserted site parameters.

	SLC	SLV	SLD	SLO
a_g [m/s ²]	1.319	0.996	0.397	0.322
F_0	2.4	2.45	2.54	2.51
T_C^* [s]	0.29	0.29	0.23	0.2
T_R	975	475	50	30

Figure 5.12 - seismic load as a function of site parameters.

⁴ The World Geodetic System (WGS) is a standard for use in cartography, geodesy, and satellite navigation including GPS. This standard includes the definition of the coordinate system's fundamental and derived constants, the ellipsoidal (normal) Earth Gravitational Model (EGM), a description of the associated World Magnetic Model (WMM), and a current list of local datum transformations.

Carico sismico

Forma spettro: Parametrica Diagramma Spettro

Classe suolo: D Calcola

	SLC	SLV	SLD	SLO
► Verifica	<input checked="" type="checkbox"/>	<input checked="" type="checkbox"/>	<input checked="" type="checkbox"/>	<input checked="" type="checkbox"/>
a_g [m/s ²]	1.32	1.00	0.40	0.32
F_0	2.40	2.45	2.54	2.51
T^*_C [s]	0.29	0.29	0.23	0.20
T_R	975.00	475.00	50.00	30.00
S_S	1.80	1.80	1.80	1.80
T_B [s]	0.22	0.22	0.20	0.19
T_C [s]	0.67	0.67	0.60	0.56
T_D [s]	2.14	2.01	1.76	1.73

Categoria topografica: T1 S_T 1.0

Fattore di amplificazione: 1.000

OK Annulla ?

Figure 5.13 - Seismic load parameters weighted on site characteristics – TreMuri.

To defining the design seismic action the local conditions, that is the topographical and stratigraphic characteristics of the subsoil, the physical and mechanical properties of the soil with which it is constituted, must be evaluated. The stratigraphic conditions and properties of the soil are clearly attributable to the categories defined in Tab. 3.2.II of the Ntcs, for the subsoil categories, and Tab. 3.2.III, for topographical conditions.

Table 5.5 - From Tab. 3.2.II in NTCs - Subsoil categories that allow the use of the simplified approach.

Class	Description
A	Outcropping rock clusters or very rigid ground with shear wave velocities of more than 800 m/s, possibly including soils of poorer mechanical characteristics with a maximum thickness of 3 m.
B	Rocky clusters or very rigid terrain with cutting speeds exceeding 800 m/s emerge, possibly including soils with worse mechanical characteristics with a maximum thickness of 3 m.
C	Deposits of medium-sized coarse-grained soils or medium-sized fine-grained soils with a substrate depth exceeding 30 m characterized by an improvement in mechanical properties with depth and equivalent speed values between 180 m/s and 360 m/s.

D	Deposits of low-density coarse-grained soils or low-density fine-grained soils with a substrate depth of more than 30 m characterized by an improvement in mechanical properties with depth and equivalent speed values between 100 and 180 m/s.
E	Soils with characteristics and equivalent velocity values as defined for categories C or D, with a substrate depth not exceeding 30 m.

Table 5.6 - from NTCs Tab. 3.2.III – Topographical categories.

Category	Characteristics of the topographical surface
T1	Flat surface, isolated slopes and ridges with an average inclination of $\leq 15^\circ$
T2	Slopes with an average slope of $> 15^\circ$
T3	Reliefs with width in crest much smaller than at the base and average inclination $15^\circ \leq i \leq 30^\circ$
T4	Reliefs width much smaller than at the base and mean inclination $> 30^\circ$

5.3.2. Calculation setting and load patterns

At this stage the calculation is performed with the active legislation. Since the accuracy of nonlinear static analyses depends heavily on a correct choice of the initial distribution of forces, it should be said that during an earthquake the redistribution of forces on the structure changes continuously. In general, in the early stages of damage the actions are amplified in the higher levels as the response is dominated by its modal characteristics. While, when the damage level increases, it is possible that the intermediate levels are not able to transfer more seismic actions from the base to the top of the building and the damage is concentrated in the lower ones.

However, according to NTC2018 (in §7.3.4.2), the pushover analysis must be performed considering at least two different distributions of horizontal forces, in the main distributions⁵ (proportional to the masses, to the first way of vibrating or SRSS) and the other in the secondary distributions⁶ (uniform, adaptive or multimodal distribution). In

⁵ Group 1 - Main distributions:

- If the fundamental vibrating mode in the considered direction has participant mass not less than 75%, one of the following two distributions is applied:
 - the proportional distribution to the static forces;
 - the distribution which corresponds to an acceleration pattern that is proportional to the principal modal shape (in the direction considered).
- In every case may be used the distribution which corresponds to the development of the plane forces acting on each horizon, calculated in a linear dynamic analysis, including in the considered direction a number of modes with total mass participation of not less than 85%.

⁶ Group 2 - Secondary distributions:

the present case study, pushover analyses in the X and Y direction (positive and negative) have been taken into account, using i) the uniform, ii) the inverted-triangular distribution and iii) the modal distribution, where three different contributions have been identified (in §5.4.1), limiting them to the situation without eccentricity.

The screenshot shows the 'Analisi' software interface. The 'Nodo di controllo' section is active, showing a table with 24 rows. The first 8 rows are selected (checked in the 'Calcola analisi' column). The table columns are: N., Calcola analisi, Dir. sisma, Carico sismico, and Eccentricità [cm].

N.	Calcola analisi	Dir. sisma	Carico sismico	Eccentricità [cm]
1	<input checked="" type="checkbox"/>	+X	Uniforme	0.0
2	<input checked="" type="checkbox"/>	+X	Forze statiche	0.0
3	<input checked="" type="checkbox"/>	-X	Uniforme	0.0
4	<input checked="" type="checkbox"/>	-X	Forze statiche	0.0
5	<input checked="" type="checkbox"/>	+Y	Uniforme	0.0
6	<input checked="" type="checkbox"/>	+Y	Forze statiche	0.0
7	<input checked="" type="checkbox"/>	-Y	Uniforme	0.0
8	<input checked="" type="checkbox"/>	-Y	Forze statiche	0.0
9	<input type="checkbox"/>	+X	Uniforme	62.6
10	<input type="checkbox"/>	+X	Uniforme	-62.6
11	<input type="checkbox"/>	+X	Forze statiche	62.6
12	<input type="checkbox"/>	+X	Forze statiche	-62.6
13	<input type="checkbox"/>	-X	Uniforme	62.6
14	<input type="checkbox"/>	-X	Uniforme	-62.6
15	<input type="checkbox"/>	-X	Forze statiche	62.6
16	<input type="checkbox"/>	-X	Forze statiche	-62.6
17	<input type="checkbox"/>	+Y	Uniforme	70.0
18	<input type="checkbox"/>	+Y	Uniforme	-70.0
19	<input type="checkbox"/>	+Y	Forze statiche	70.0
20	<input type="checkbox"/>	+Y	Forze statiche	-70.0
21	<input type="checkbox"/>	-Y	Uniforme	70.0
22	<input type="checkbox"/>	-Y	Uniforme	-70.0
23	<input type="checkbox"/>	-Y	Forze statiche	70.0
24	<input type="checkbox"/>	-Y	Forze statiche	-70.0

Other interface elements include: 'Livello' set to [4] Livello 4, 'Nodo' set to 65, 'Spostamento' set to Spostamenti Medi pesati, 'Definizione per angolo sisma' with 'Angolo' set to 0, 'Dati generali' with 'Piano Campagna' at 0.0000, 'Step critico' at 500, and 'Precisione p.p.' at 0.0050. 'Parametri di calcolo' includes 'Sottopassi' at 200 and 'Spostamento max' at 16.00. 'Abilita analisi' has dropdowns for 'Dir. sisma', 'Carico sismico', and 'Eccentricità'. 'Carico sismico' has radio buttons for 'Proporzionale forze statiche' (selected) and 'Distribuzione modale'. There is also an option for 'Esegui controllo deformabilità angolare'.

Figure 5.14 - Setting the loads applied to the model and choosing the control node for the pushover analysis in TreMuri.

The choice of the distributions of seismic forces (proportional to the masses or the first way of vibrating) is up to the designer and in the present study both were examined to have a wider characterization of the structure and its behavior. The execution of the pushover analysis presupposes then the choice of the control node and the setting of the control displacement to be plotted, aiming letter to be more representative of the displacement of the building during earthquake. Due to the non-homogeneous entities with significant inertial differences, the need arises to study the global response of the structure with the control node positioned in different altitudes.

- the distribution of forces, derived from a uniform pattern of accelerations along the height of the construction;
- adaptive distribution, which changes as the control point shifts as a function of structure plasticisation;
- multimodal distribution, considering at least six significant ways.

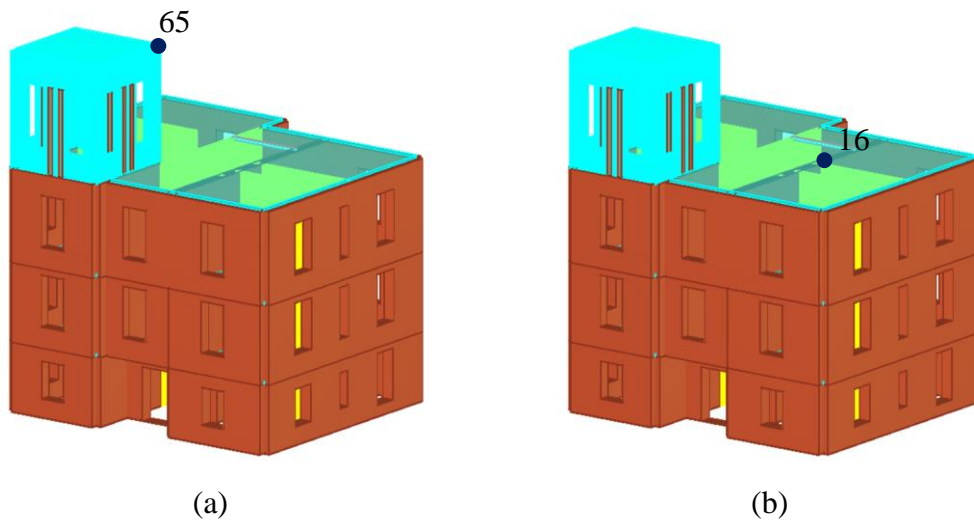


Figure 5.15 - Control Node positioning: (a) Control Node at the 4th Floor; (b) Control Node at the 3rd Floor.

The positioning of the control node with which the pushover will be executed must represent the average behavior of the structure under examination. The legislation suggests placing it at the top level, so in the present case it would mean on top of the tower (on the fourth floor). This choice risks to penalize, "distort", the results for the presence of this tower with a much smaller footprint than the rest of the building. Therefore, several analyses were carried out by placing the control node on both the tower and the floor below (with footprint of the largest building), by always imposing the weighted average displacements at the plane level (it is an option to choose in 3muri). The parameters of each analysis can be set using the appropriate area. To compute the analyses, accuracy, maximum displacement, and underpasses have been properly set in order to find the pushover without highly increase the computational effort.

5.4. Modal Analysis

Through modal analysis it was possible to calculate the modes of vibration of the structure. The modes of vibration are those deformed configurations for which the displacement of each point, left free to oscillate in the absence of damping, is proportional at any time to the displacement of any other point.

After carrying out the modal analysis of the building, it was possible to detect the modes of the structure. TreMuri presents a table with a list of modal shapes and the corresponding deformed shapes in plan and elevation. Below are presented the modal shapes of wall 13, for the modal shape in x-direction, and of wall 11, in the y-direction, which correspond to two walls of the tower. (Figure 5.18).

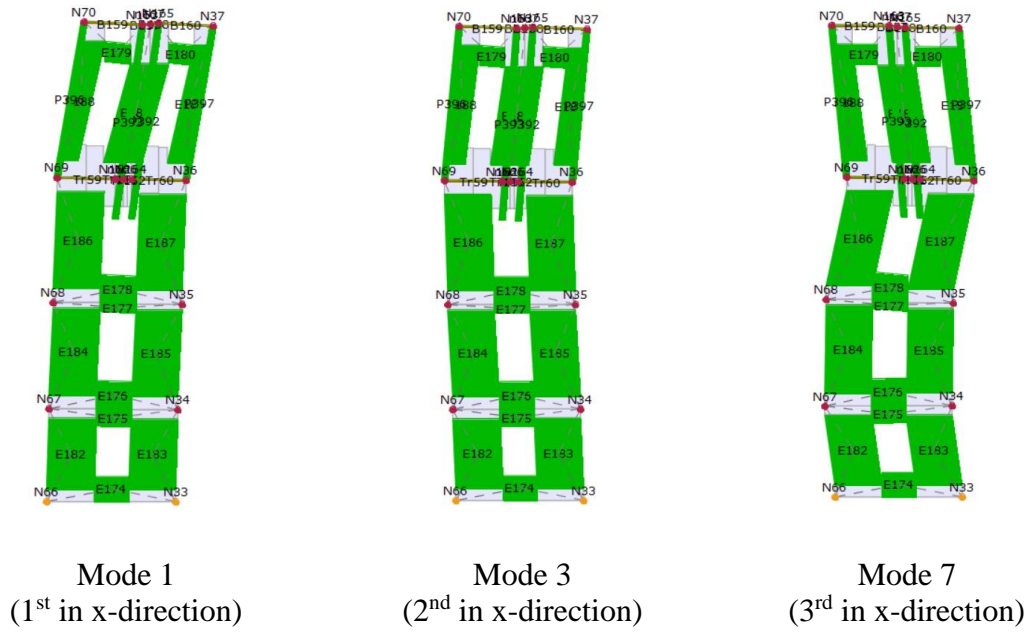


Figure 5.16 - X-direction vibration modes (wall 13).

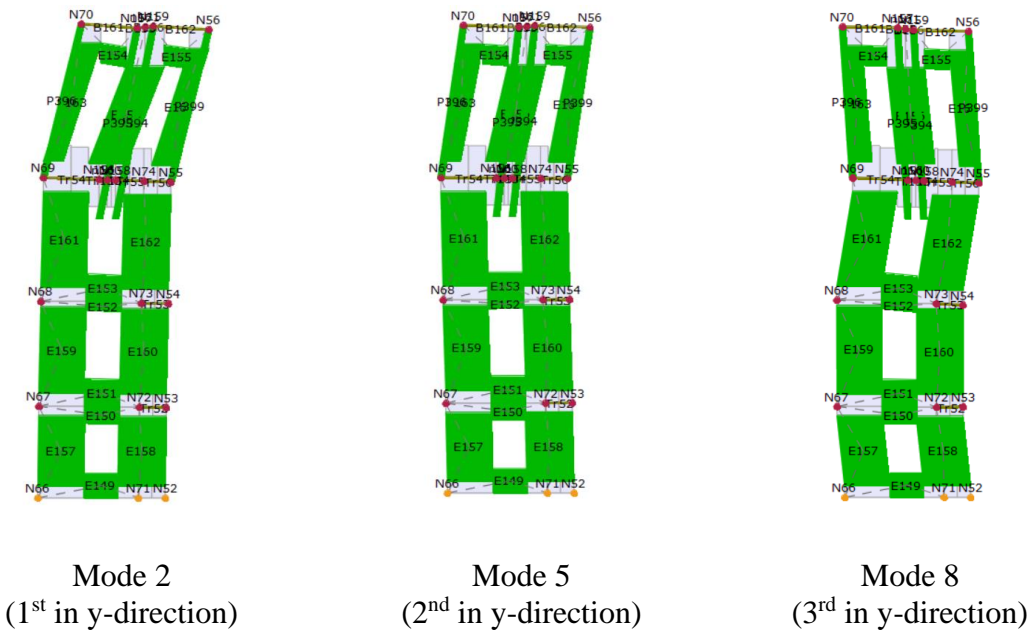


Figure 5.17 – Y-direction vibration modes (wall 11).

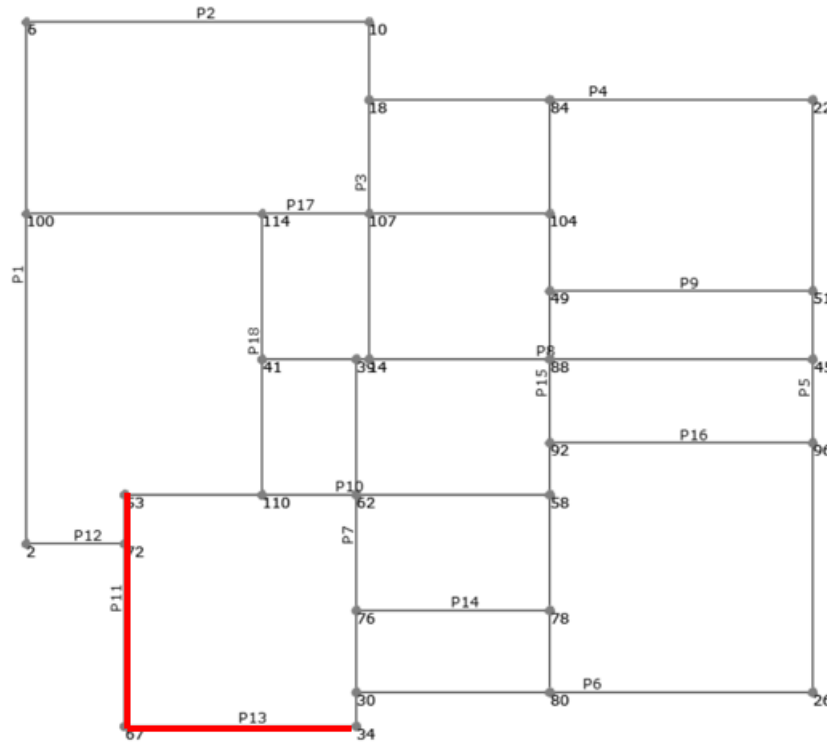


Figure 5.18 - Wall 11 and 13 identification (in red).

Each mode of vibration has its own period of vibration and participating mass. Vibration modes are ordered for periods of decreasing vibration (Table 5.7). The first way of vibrating will have the greatest period, the second way will have a shorter period than the first and greater than the third and so on. In general, buildings have three modes ("inflections"), in which for each wall all the nodes move in the same direction: a mode that mainly affects the walls oriented according to X, a mode in the Y direction and a torsional one.

Table 5.7 - Summary of the main results from modal analysis

Dir.	Mode	T [s]	mx [kg]	Mx [%]	my [kg]	My [%]	mz [kg]	Mz [%]
x	1	0.40567	267,732	34.46	7,982	1.03	15	0
y	2	0.37318	29,022	3.74	165,125	21.25	4	0
x	3	0.30894	162,455	20.91	734	0.09	21	0
x	4	0.28098	113,716	14.64	20,500	2.64	32	0
y	5	0.27363	15,954	2.05	382,260	49.2	29	0
	6	0.25189	10,069	1.3	30,094	3.87	17	0
x	7	0.12827	120,741	15.54	64	0.01	948	0.12
y	8	0.10985	85	0.01	126,873	16.33	249	0.03
	9	0.10257	11,189	1.44	62	0.01	56	0.01
	10	0.09122	1,624	0.21	177	0.02	258,545	33.28
	11	0.0857	36,718	4.73	181	0.02	18,457	2.38
	12	0.08063	40	0.01	627	0.08	232,006	29.86
	13	0.0791	1,169	0.15	135	0.02	43,343	5.58

14	0.07613	657	0.08	659	0.08	47,058	6.06
15	0.0749	21	0	1,604	0.21	7,166	0.92
16	0.07368	34	0	1,688	0.22	23,729	3.05
17	0.07114	132	0.02	47	0.01	330	0.04
18	0.07023	1	0	10,313	1.33	1,412	0.18
19	0.0681	197	0.03	24,758	3.19	42	0.01
20	0.06629	3	0	669	0.09	944	0.12

It is noted that the first modes of vibration have greater participating mass, but lower spectral accelerations because the period of vibration is greater. Therefore, in the table data generated by structural calculation software, for each mode of vibration it is possible to read the period of vibration and the participating mass expressed as a percentage of the total seismic mass (Table 5.8). It is possible to detect from the analysis that the first modes with higher translational participation factor in x and y direction are the first and the second (by detecting both percentages and the deformations).

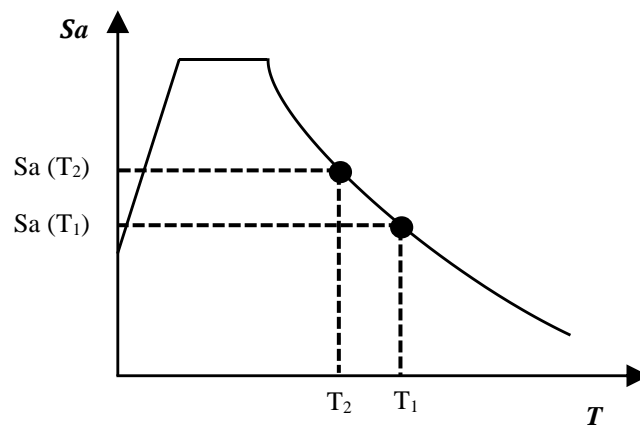


Figure 5.19 - Response Spectrum as a function of the vibration period.

From some research carried out (Lagomarsino, Sergio et al. 2018) it has been shown that when structure are characterized by irregularities, the 1st mode is not anymore purely translational but there is also a significant torsional component. In the present case study, six ways has been detected, because the tower and the first three floors of the building have very different stiffness and mass and therefore each way is split.

Consequently, has benn detected two "first" modes (without inflection) in the X direction, one with displacements prevalent in the tower and one that involves the first three floors, and similarly for the Y direction and the torsional mode. The torsional compound may be seen in the figure 5.15 in plan, but also in in the figures 5.13 and 5.14 shown before.

The main conclusions from modal analysis, when the buildings are not regular, are: (i) the 1st mode is not enough to represent the dynamic behaviour of the building, but also higher modes should be considered; they are also torsional.

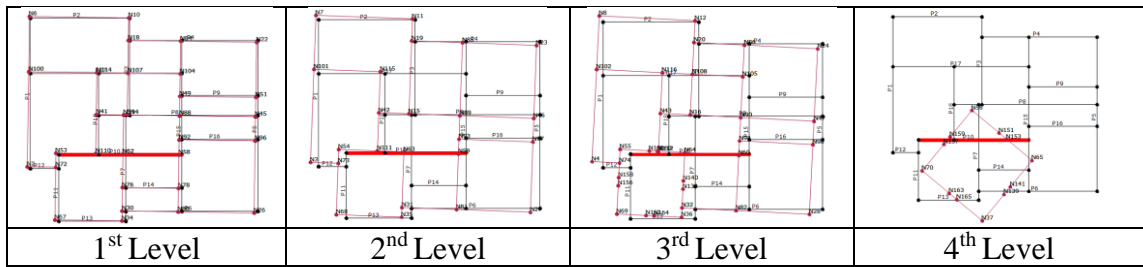


Figure 5.20 - Modal plan deformed shapes for the 3rd vibration mode (torsional).

5.4.1. Calculation setting

From this phase of calculation, it was possible to identify the contributions of those modal shapes to be activated in pushover. Therefore, three different contributions have been identified: the first one taking into account a set of modes which provides a cumulative mass participation factor around of 85% in both directions in x and y (named “*Combined Modal Distribution*”); a second which consider only the first modes with translational mode (mode 1 in x, and mode 2 in y) and finally a third identified as a tower-specific vibrating mode (mode 3 in x and 5 in y). For the second and third combination, refer to figures 5.22 and 5.23, through which we see the coherence between the three selected alignments (significant for the structure).

Table 5.8 - Set of Modes considered for the pushover analysis proportional to the modal distribution

	SRSS	1st Mode	3rd Mode
X [Mode]	1°, 3°, 4°, 7°	1°	3°
Y [Mode]	2°, 5°, 8°	2°	5°
MX [%]	85,55	34,46	21,25
My [%]	86.79	20,91	49,20

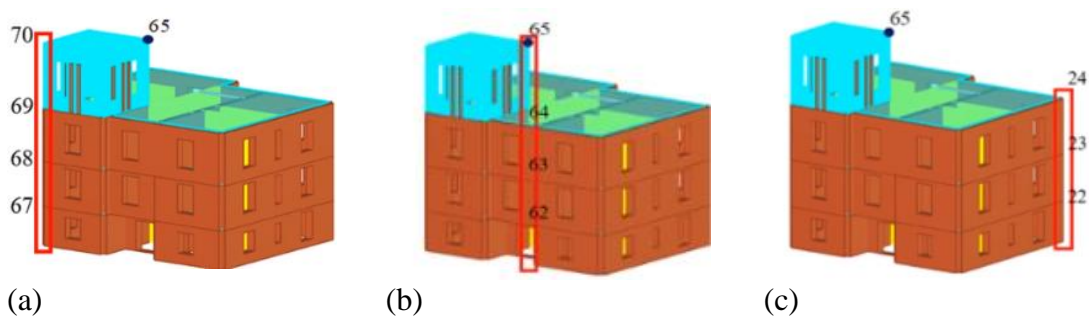


Figure 5.21 – Three alignment selected representative of the modal shape: (a) the four knots at the bottom left corner of the building; (b) knot 65 and the three below; (c) the three knots of the corner opposite the tower (extreme right of the building).

From the figure 5.21 is possible to see that all the three alignments move in the same direction, an almost purely translational modal form.

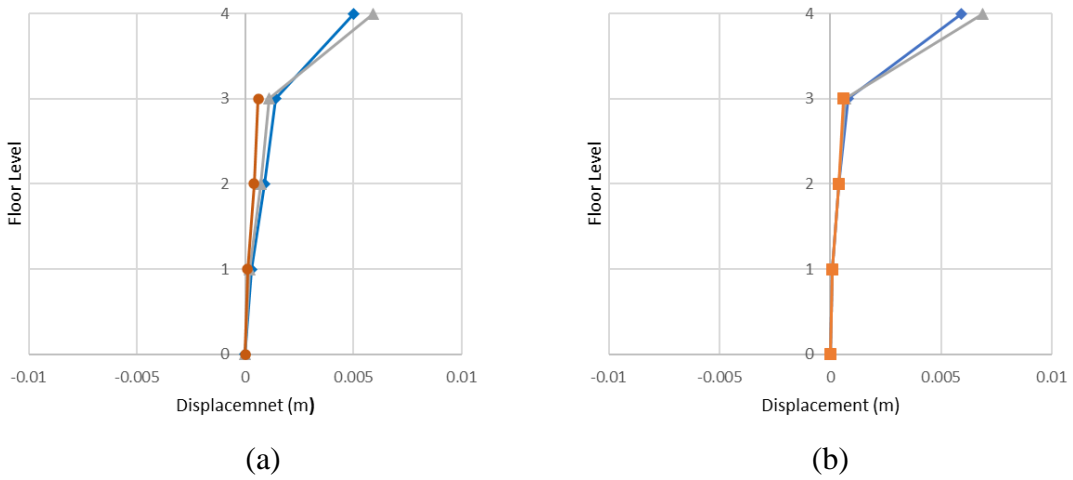


Figure 5.22 – 1st Mode: (a) x-direction; (b) y-direction.

From the figure 5.22 we can see the inversion of sign: for the first three floors the structure moves in one direction, while the fourth one goes on the opposite side (the “Tower Mode”), with also a much greater deformation, which is not aligned with the deformed planes below.

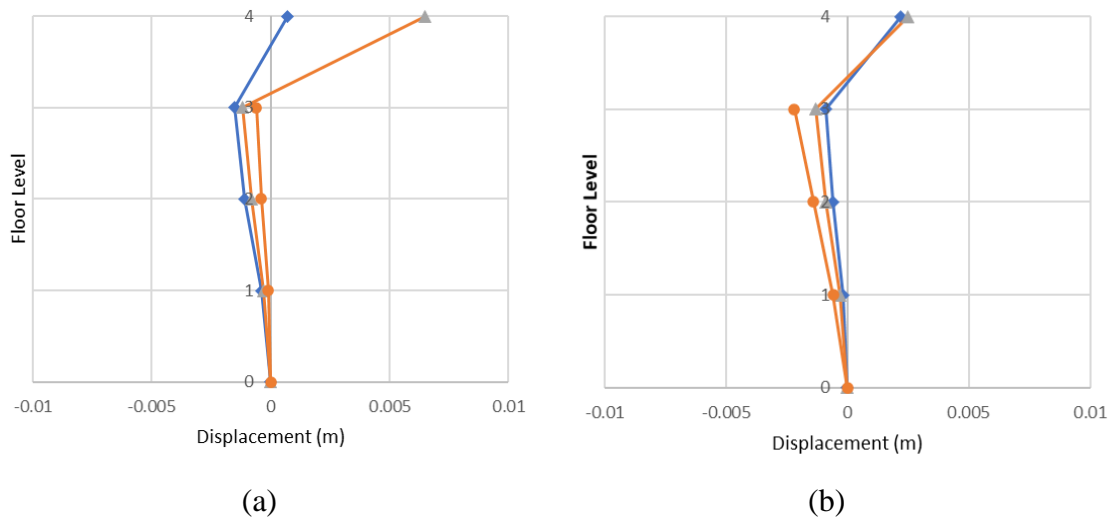


Figure 5.23 – 3rd Mode (“Tower Mode”): (a) x-direction; (b) y-direction.

The *Combined Modal Distribution* is based on SRSS model which involves a combination of effects rather than causes (e.g., load patterns themselves), used to combine higher modal response. The SRSS approach (proposed in 1953 by Goodman, Rosenblueth and Newmark) stay for *Square Root of the Sum of Squares* method. Therefore, it has been disproved that statistically the most likely maximum value for each mode of vibration of the Emax effect can be calculated by the following formula (5.6):

$$E_{max} = \sqrt{\sum_{n=1}^M (E_n^{max})^2} \quad M < N \quad (5.7)$$

This report provides well-approximated average values and is currently the most widely used, also implemented in TreMuri.

5.5. Summary analysis

The pushover analyses were carried out by using different load patterns, kept invariant during the analysis, in the Y and X directions. They are reported in the program in the outcome section, and thanks to this visualization it is possible to see roughly how the structure behaves according to the two directions and therefore to understand how much they affect the irregularity of the structure. According to the analyses carried out, the structure is strongly influenced on the irregularities. For this reason, five different load distributions (figure 5.24) were performed:

1. The Uniform distribution (in blue);
2. The inverse Triangular (in green);
3. Proportional to the 1st Mode (in magenta);
4. Proportional to the 3rd Mode (in cyan);
5. SRSS combination (in black).

Since several studies have identified the challenges associated with the applicability of NLS Analyses with reference to their accuracy in predicting the nonlinear response. This leads us to make new comparisons to understand which is the distribution that best represents the overall response of the building. The NLDA is always considered a benchmark to evaluate how well the simplified procedure aforementioned are able to capture various complex aspects of nonlinearity and it will be seen in in §6.2. Before comparing with the dynamics, the results obtained by the pushovers have been analysed (following section). This involved the identification of the various ultimate displacements (Du) and careful study of the damage of the various walls, those of the tower, for which the collapse occurs prematurely.

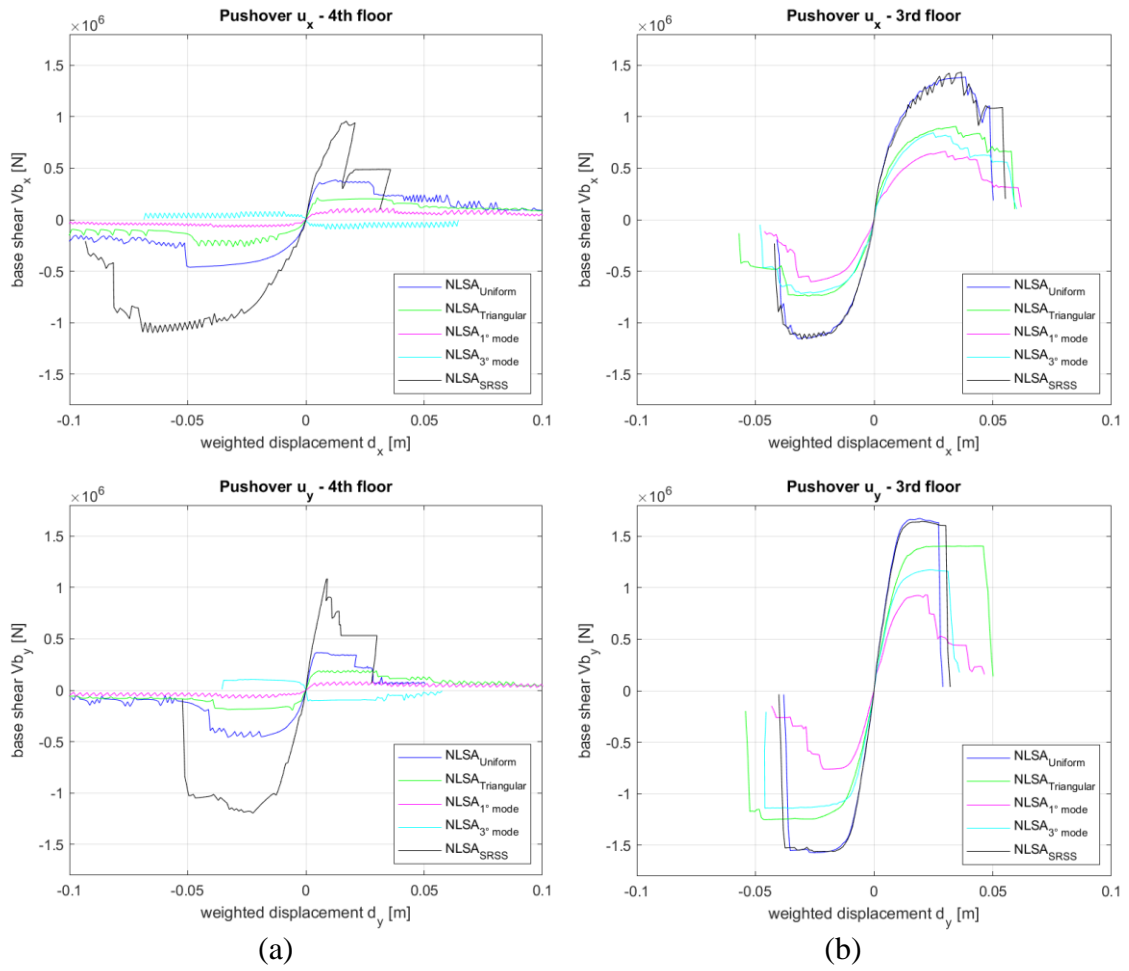


Figure 5.24- Pushover curve in x and y-direction (positive and negative): (a) 4th floor; (b) 3rd floor.

Step 3: The Verification

6. Analysis of results

6.1. Results of non-linear static analysis

Once completed the model and executed the calculation, the program supplies in output the pushover curve of the structure; this curve depends exclusively on the structure and is totally independent from the seismic spectrum. The spectrum will be used later for the verification. The latter, therefore, consists in the comparison between the two displacements, if the displacement supply is greater than the displacement demand, the structure is verified. From the curve is directly identifiable the displacement supply of the structure, the seismic parameters lead instead to define the displacement demand.

6.1.1. Definition of the limit states

Today, regulations provide controls to define limit states that also consider the location of damage in specific portions of the system. In the case of irregularities at elevation such as this one, these checks lead to retreat the ultimate displacement capacity on the pushover curve. To carry out these checks, hence to get information about the damage, the program shows the output of ".sta" files, or damage to the wall panels. Below is an image that is able to clarify the classification of damage that a building may suffer.






	<p>Grade 1: Negligible to slight damage (no structural damage, slight non-structural damage) Hair-line cracks in very few walls. Fall of small pieces of plaster only. Fall of loose stones from upper parts of buildings in very few cases.</p>
	<p>Grade 2: Moderate damage (slight structural damage, moderate non-structural damage) Cracks in many walls. Fall of fairly large pieces of plaster. Partial collapse of chimneys.</p>
	<p>Grade 3: Substantial to heavy damage (moderate structural damage, heavy non-structural damage) Large and extensive cracks in most walls. Roof tiles detach. Chimneys fracture at the roof line; failure of individual non-structural elements (partitions, gable walls).</p>
	<p>Grade 4: Very heavy damage (heavy structural damage, very heavy non-structural damage) Serious failure of walls; partial structural failure of roofs and floors.</p>
	<p>Grade 5: Destruction (very heavy structural damage) Total or near total collapse.</p>

Figure 6.1 - Classification of damage to masonry buildings (G. Grünthal, 1998)

By means of the damage's configuration, it was possible to identify the displacement associated with the collapse of the tower also for analyses conducted with control on the third floor. The mentioned displacements are anticipated with respect to the decay of 20% of the curves. For this purpose, the displacement said are proposed below:

Table 6.1 - Advanced ultimate displacements for each force distribution.

	3rd Floor $Du_{advanced}$ (cm)				
	Uniform	Triangular	1 Mode	3 Mode	SRSS
X_pos	1.55	1.06	0.5	0.25	/
X_neg	1.3	0.81	0.41	0.33	/
Y_pos	1.21	0.72	0.32	0.44	/
Y_neg	1.05	0.65	0.24	0.62	3.23

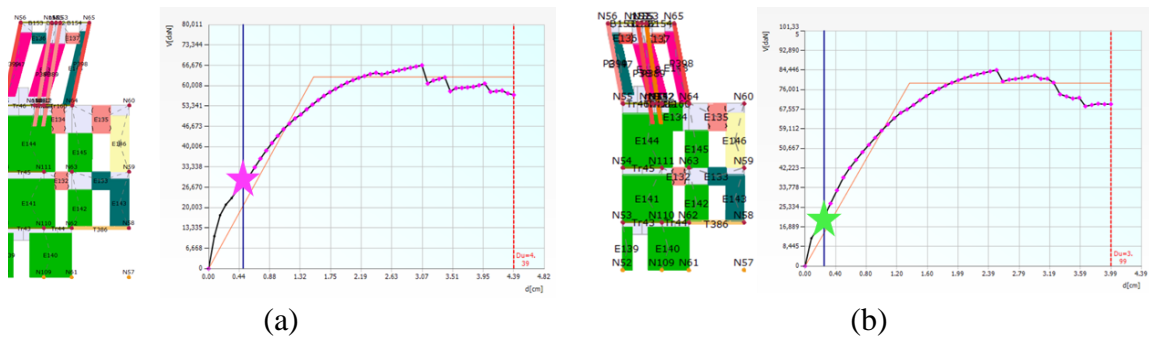


Figure 6.2 – Tower damage evolution in the early elastic phase: (a) 1st mode; (b) 3rd mode.

For completeness, the ultimate displacement associated to the pushover conducts with control node to the third floor are reported below.

Table 6.2 - Ultimate displacements for each force distribution.

	3rd Floor Du (cm)				
	Uniform	Triangular	1 Mode	3 Mode	SRSS
X_pos	4.38	4.63	4.39	3.99	4.33
X_neg	3.78	3.77	3.19	4.02	3.87
Y_pos	2.74	4.71	2.49	3.22	2.99
Y_neg	3.53	5.23	2.62	4.56	3.86

6.1.2. Influence of the applied load profile on the capacity curve

Comparing the pushover analyses in terms of load patterns distribution showed that the pushover analyses led with the combined mode (SRSS) provided an estimation of the load capacity in agreement with the uniform distribution, while the Triangular LP seems to behave like the 3rd Modal distribution. In the analyses conducted we can often find

problems of convergence, mainly related to the presence of the tower. The latter, in some cases, despite going into crisis, does not compromise the global structure which still has a structural capacity.

Pushover analyses conducted both proportional to static forces and according to the modal distribution, in general, lead to more hysterical curves. Hysteresis is the phenomenon that produces a dissipative cycle when an alternating stress is applied, so we can say that due to the presence of the tower the dissipations that come into effect are quite substantial. In the case of pushovers with control node on the fourth floor, we can say that sometimes they are very hanging with little deformative capacity and sometimes have for shear values at the base very small, a great deformative capacity. This gap depends on the tower, when it reaches its maximum strength for which the structure can no longer increase its deformations due to the load distribution applied. The Uniform distribution has a lower impact on the 4th floor compared with the Triangular. So theoretically, when this happens, the structure starts to lose load and the part below, not yet broken, should go back. From the graphs we can see that the load patterns that bear the most shearing values at the base are the Uniform and combined distribution (SRSS). For analyses with the control node on the third floor, the situation is much more homogeneous, but the convergence problems mentioned above are more frequent (visible from the pushover, figure 6.2, through the fuchsia dots).

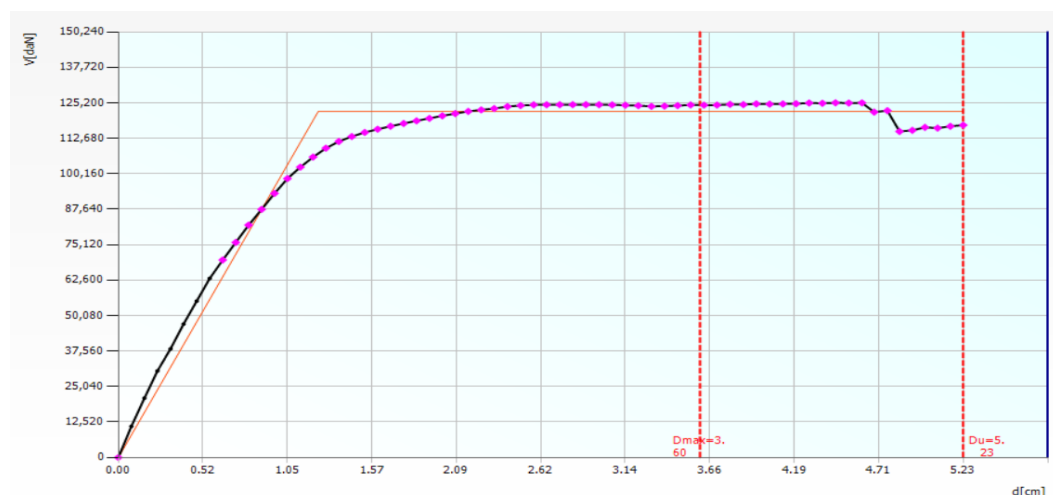


Figure 6.3 - fuchsia dots in TreMuri pushovers that say convergence has not been reached.

In this case, once the displacement for which internal forces are generated, balanced with the distribution of selected external forces, which produce the collapse of the tower, the analysis fails to find convergence. In fact, if I continue to increase the displacement to the 3rd floor, the shear at the base would continue to grow, but this is impossible because the tower has now collapsed (see figures from 6.4 to 6.7).

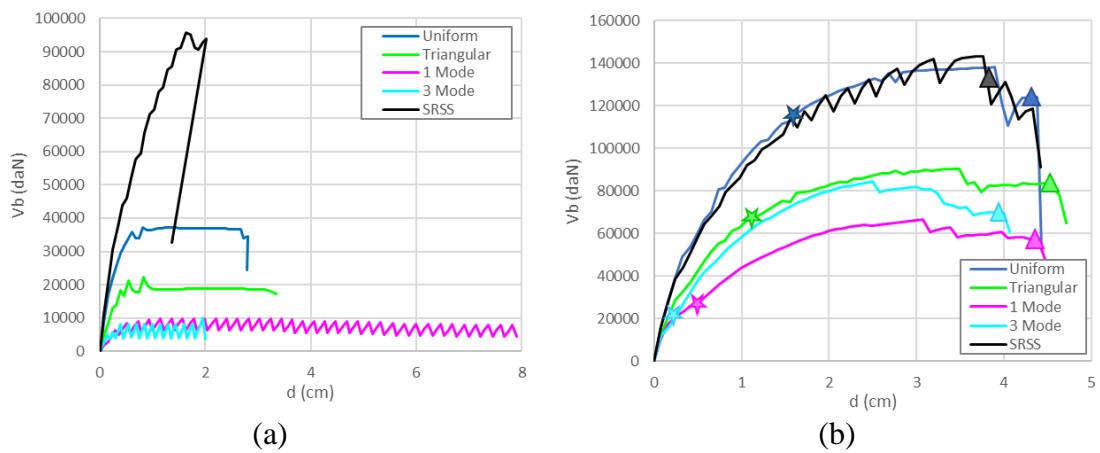


Figure 6.4 - Pushover curves in x-direction positive: (a) 4th Floor; (b) 3rd Floor.

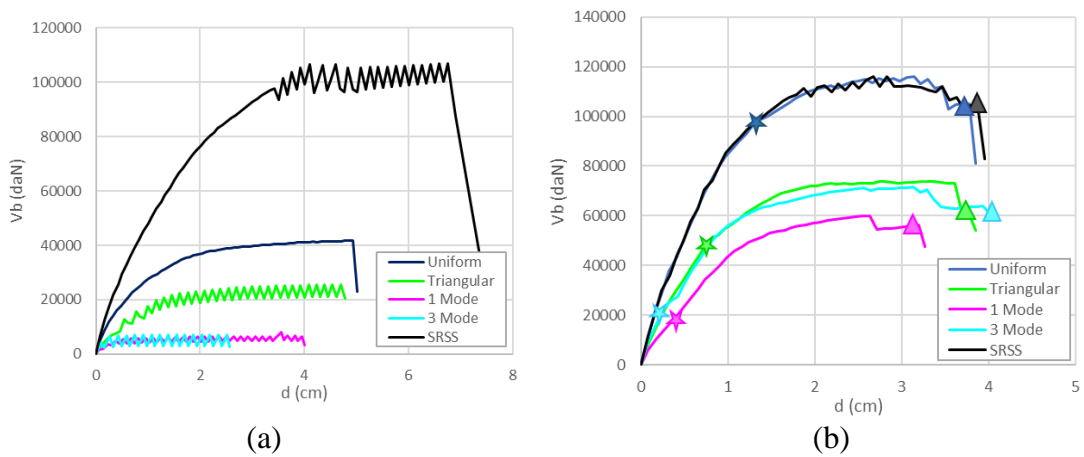


Figure 6.5 - Pushover curve in x-direction negative: (a) 4th Floor; (b) 3rd Floor

On the 3rd floor, we are not able to detect the collapse of the tower immediately, but if we check where the tower goes into crisis (damage), the two pushovers converge (on 3rd and 4th floor). It is worth noting that the curves on the 4th floor flatten where the anticipated ultimate displacement of the 3rd were detected (Table 6.1, page 61).

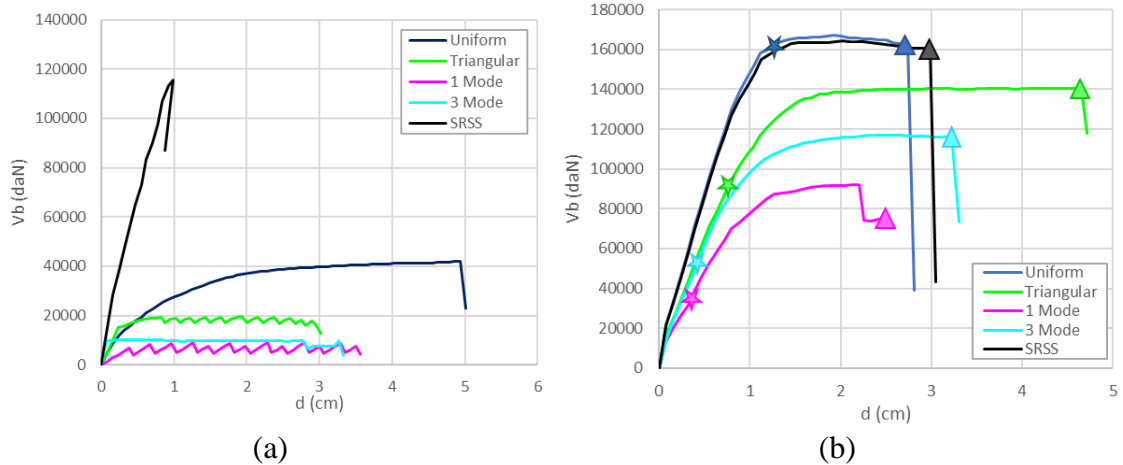


Figure 6.6 - Pushover curve in y-direction positive: (a) 4th Floor; (b) 3rd Floor

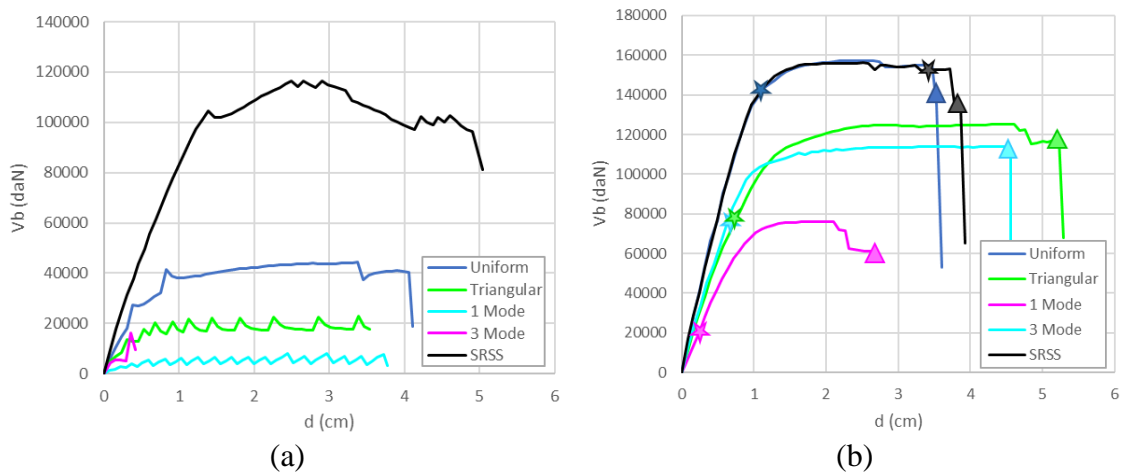


Figure 6.7 - Pushover curve in y-direction negative: (a) 4th Floor; (b) 3rd Floor

6.1.2.1 Capacity curve

At this point, it is a matter of understanding which distribution of forces is most reliable and how sensitive the verification is to the chosen distribution of forces. At first, watching only the different pushover curves depending on the force distribution taken into account, it would seem the 3rd Mode or the Triangular are the most reliable, but also the Uniform and the SRSS even if they give different results. Therefore, it was decided to convert each pushover curve into its capacity curve, representative of the equivalent SDOF, to see if the differences between the various distributions will be reduced.

To do this it was necessary to determine the Γ and m^* values as suggested by the NTC18 and shown in §5.2.1.

Since the pushover curves have been carried out considering the mean weighted displacement, we should calculate the floors' normalized weighted average displacements from the normalised eigenvectors Φ of the nodes' displacements; the eigenvectors Φ have

been normalized to the value 1 in correspondence with the absolute maximum displacement we had between all the nodes above ground and therefore with seismically activated masses.

So, it was necessary to identify the nodes of the third and fourth levels: all the 3D and 2D nodes of the walls in the direction of thrust (both in x and y-direction). Then it was calculated the sum of the products of the "dynamic mass of the node i " times the "displacement of the node i " (Eq. 6.1). Later, dividing the values calculated in Eq. 6.1 by the sum of the products of the "dynamic mass of the node i " times the "squared displacement of the node i " (Eq. 6.2), the gamma value was derived for each direction.

$$m_x^* = \sum m_{i,x} \phi_{i,x} \quad ; \quad m_y^* = \sum m_{i,y} \phi_{i,y} \quad (6.1)$$

$$\Gamma_x = \frac{\sum m_{i,x} \phi_{i,x}}{\sum m_{i,y} \phi_{i,y}^2 + \sum m_{i,x} \phi_{i,x}^2} \quad ; \quad \Gamma_y = \frac{\sum m_{i,y} \phi_{i,y}}{\sum m_{i,y} \phi_{i,y}^2 + \sum m_{i,x} \phi_{i,x}^2} \quad (6.2)$$

It is worth noting that can be strongly meaningful to see the results in terms of capacity curve, formulated in the acceleration-displacement format, for any performance considerations. This procedure is performed to combine the pushover analysis with the capacity spectrum approach and made the proper control. In general, once the load distribution is found (the most reliable one), the Codes require us to convert pushover curves into capacity curves to determine the level of performance achieved and then check the structure. This means to correlate the displacement capacity of the structure to the displacement demand of the expected earthquake.

Through this conversion, it could happen that pushover curve with the smallest base shear will becomes the curve with the highest capacity (representative of the equivalent SDOF). What said is since to get the capacity, the base shear needs to be divided for the mass of the equivalent SDOF (m^*), and if it is smaller compared with the ones obtained from the others load patterns it will becomes the curve with the highest capacity (Figure 6.6b, magenta and cyan curves).

Before talking about the capacity curves obtained for the fourth floor (figure 6.7b), we must remember that the resistances obtained in pushover did not reach the same values as those obtained with control node on the third floor, because of the tower collapse (Table 6.1, page 61).

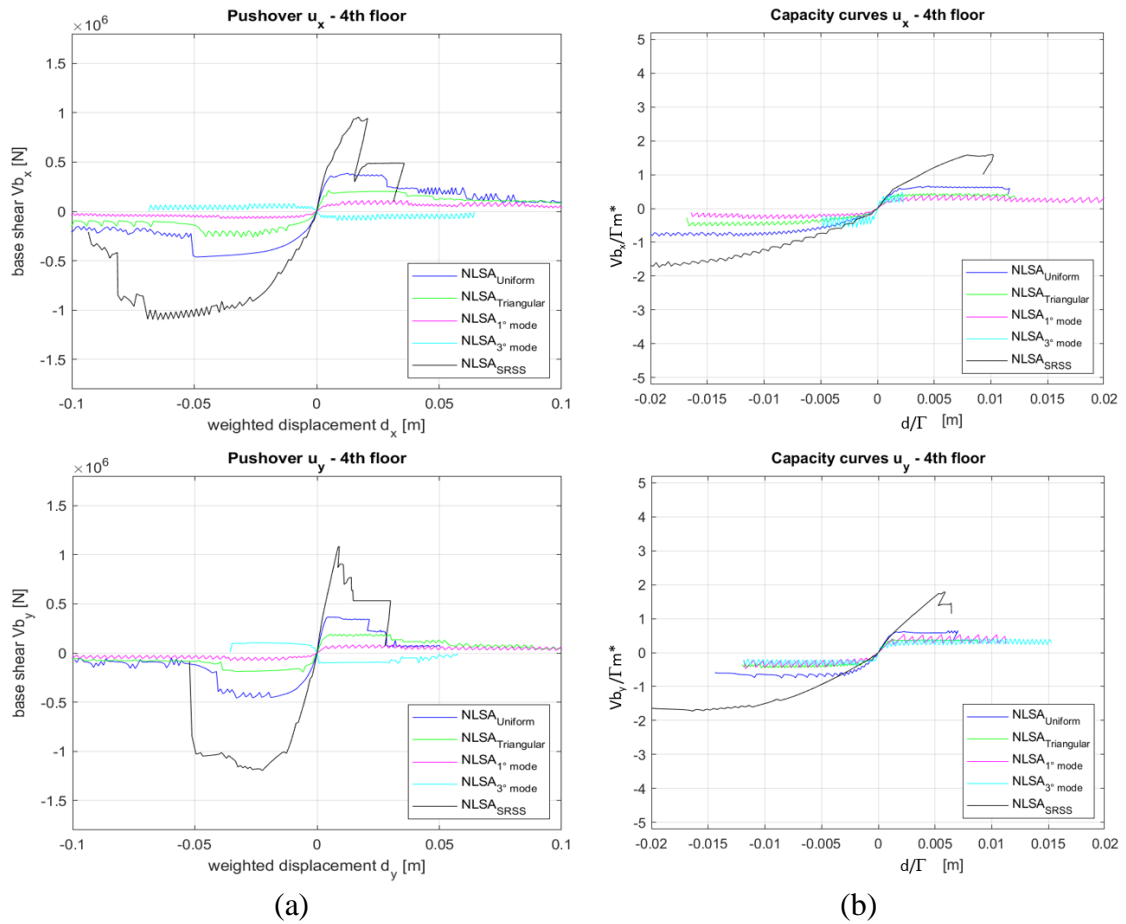


Figure 6.8 - Pushover (a) and capacity (b) curves associated to the 4th floor.

Instead, for the capacity curves obtained for the third floor, from the diagrams it is possible to observe the inversion of the curves which leads to more compact curves. By comparing the Uniform and the combined modal distribution (SRSS) it is possible to observe their overlapping, so they give the same resistance value. The Triangular distribution has always been reasonable outcome and nevertheless results conform with the other curves, but it is based on a linear deformation. For single-mode distributions (magenta and cyan curves), on the other hand, the capacity curves have characteristic values in terms of resistances: in Y the 1st Mode has high resistance, while in X the 3rd Mode. This inconsistency is due to the low participating mass that these distributions activate. Therefore, once converted into equivalent oscillators (SDOF), having a very low denominator, the accelerations values rise.

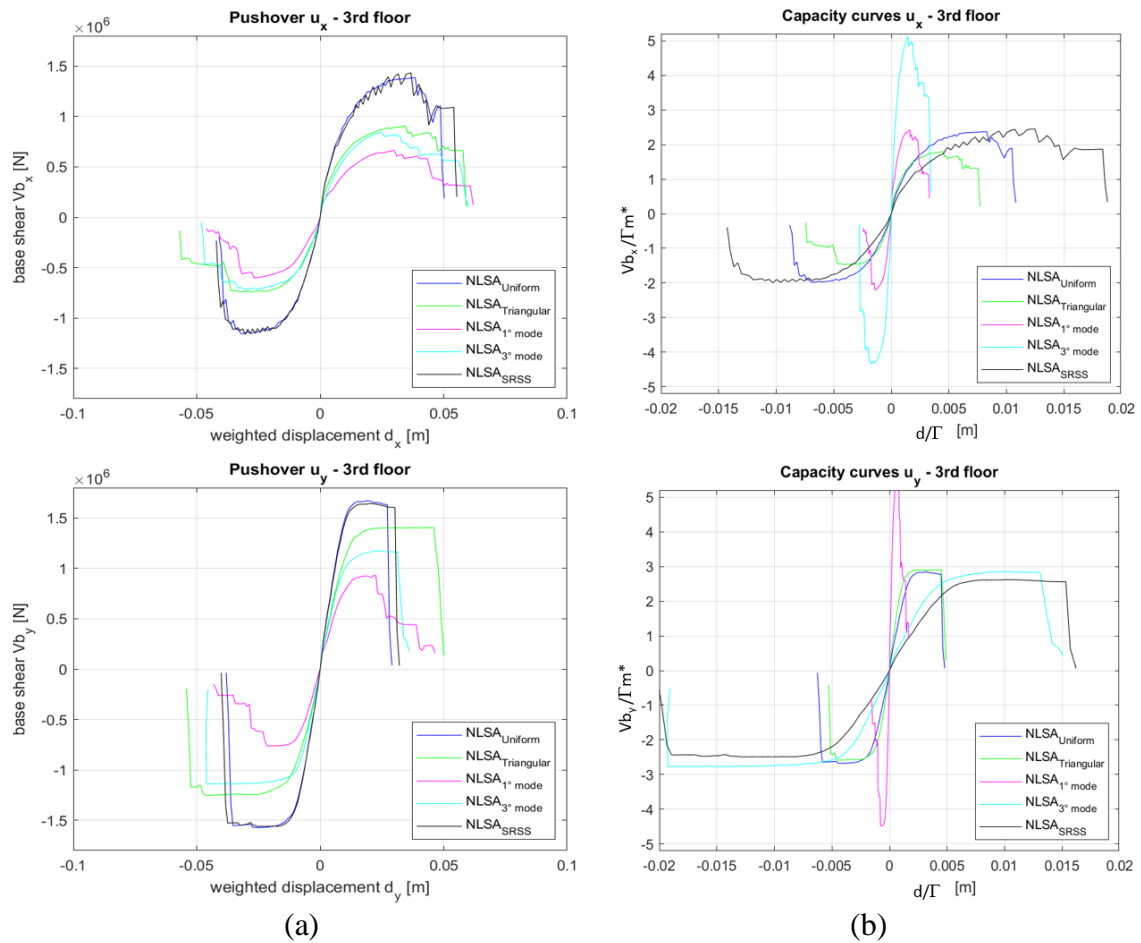


Figure 6.9 - Pushover (a) and capacity (b) curves associated to the 3rd floor.

Conversion into capacity curves, where the overall response is represented (pushover on 3rd floor), leads to overall consistent results, but highlights that the distributions on single modes are not representative of the overall response, but rather of the local system, and the proof is that when we convert a pushover curve into a capacity curve we get equivalent oscillators that are not reliable. This is because such distributions affect more a part, like the tower, but exclude many other situations, more representative of the global response. If we look at tables 5.8 and 5.9 (in §5.4.1), we can see that the participating mass is much lower than the distribution SRSS. Moreover, making the ratio between e^* (obtained as the product between Γ and m^*) divided by the dynamic mass of the building (M), we find the fraction of participant mass. In the case of Uniform and Triangular we are over 80%, while in the case of 1st and 3rd Mode we have much more modest fractions (around 20%).

Then (in §6.2), based on the observations made, it was decided to start some nonlinear dynamic analysis, to compare the dynamic response, which somehow represents the closest approximation to the real one, with the different pushover curves, to understand which distribution of forces is the most representative.

6.2. Nonlinear Dynamic Analysis (NLDA)

A valid alternative and most advanced seismic analysis method to pushover analysis is the Nonlinear Dynamic Analysis (NLDA). Due to its computational demand, it is not extensively used in common practice. To carry out an accurate evaluation of structural seismic response, NLDA requires an input accelerogram consistent with the seismic hazard at the site. For the present case, a selection of different accelerograms compatible with the structure has been selected, recorded in Visso (Marche), leading several analyses for which the collapse of the structure was reached at the peak ground acceleration variety (from a value of 0,05g up to the collapse), commonly defined record-to-record variability.

Perform a time history analysis, especially for the masonry structure, has computational limits, since there is a lack availability of software able to define cyclic constitutive model by means of damping and other significant properties. Moreover, select appropriate input ground motion records is a very difficult task. Records must be able to represent the actual structural behavior without being too punitive towards the structure, and vice versa. It has been pointed out that, the structural response in dynamic simulations, are significantly influenced by the damping, and for this purpose the Rayleigh damping model was used (in §6.2.1). In addition, it must be said that interpreting the results of nonlinear dynamic analysis in terms of performance limits is not easy. In the present case, the most representative results were used as a reference for static analyses.

To determine the dynamic analyses it was necessary to use the updated release of Tremuri, which is the program for the research that the laboratories of the University of Genoa have adopted. Therefore, modal analysis was relaunched with the Research version, modifying the file “.txt” by setting the analysis to be calculated and the necessary output parameters: frequency, period, modal participation coefficients in the three directions (x,y,z) and the participating mass. The modal analyses carried out allow us to define the alpha and beta parameters considering a specific period interval (Tab. 6.4). The inferior parameters are defined by assuming the period in which at least the 80% of mass was exited (until Mode 8).

Table 6.3 - Period that brings about the activation of 80% of mass

Mode	Mx_reached (%)	My_reached (%)
1	34	1
2	38	22
3	59	22
4	74	25
5	76	74
6	77	78
7	93	78
8	93	95

Table 6.4 - Defined range and relative frequency and angular velocity quantities.

T _{inf}	0.110
f _{inf}	9.103
w _{inf}	57.198
T _{sup}	0.811
f _{sup}	1.233
w _{sup}	7.744

If we indicate with T the period (time taken to complete an oscillation) and with f the frequency (number of complete oscillations accomplished in a second), the angular velocity is defined as:

$$\omega = 2\pi f \quad (6.3)$$

6.2.1. Rayleigh's coefficients adopted

With the NLDA the seismic action was defined by equivalent acceleration, constant in space and time, with parameters α and β properly derived. It was possible previously setting specific viscous damping and frequencies. According to the Rayleigh viscous damping model, the symmetric damping matrix $n \times n$ (C) is formulated as a linear combination of mass (M) and stiffness (K) matrices:

$$[C] = \alpha[M] + \beta[K] \quad (6.4)$$

The type of damping described by equation 6.4 is known as Rayleigh damping. Applying the transformation of modal coordinates, the modal damping matrix (c) becomes diagonal:

$$[\Phi]^T[C][\Phi] = [c] = \alpha[1] + \beta[\omega^2] \quad (6.5)$$

The modal damping matrix (c) is given by:

$$[c] = 2[\xi\omega] \quad (6.6)$$

The viscous damping coefficient c_i for i-th mode is calculated as shown below:

$$c_i = 2\xi_i\omega_i = \alpha + \beta\omega_i^2 \quad (6.7)$$

And the viscous damping ratio ξ_i , for the i-th mode, is expressed as:

$$\xi_i = \frac{\alpha}{2\omega_i} + \beta\frac{\omega_i}{2} \quad (6.8)$$

If we keep the lower and upper modes as reference (table 6.2), the Rayleigh coefficients will be calculated by the solution of the two algebraic equations. If we also consider the same damping ratio (as expressed in the table 6.3), we will have:

$$\alpha = \xi \frac{2\omega_{inf}\omega_{sup}}{\omega_{inf} + \omega_{sup}} \quad ; \quad \beta = \xi \frac{2}{\omega_{inf} + \omega_{sup}} \quad (6.9)$$

The viscous damping develops with the frequency as follows. The first line (in blue) is determined by assuming the damping that depends only on the masses of the system, while the second (in red) depends only on the stiffnesses.

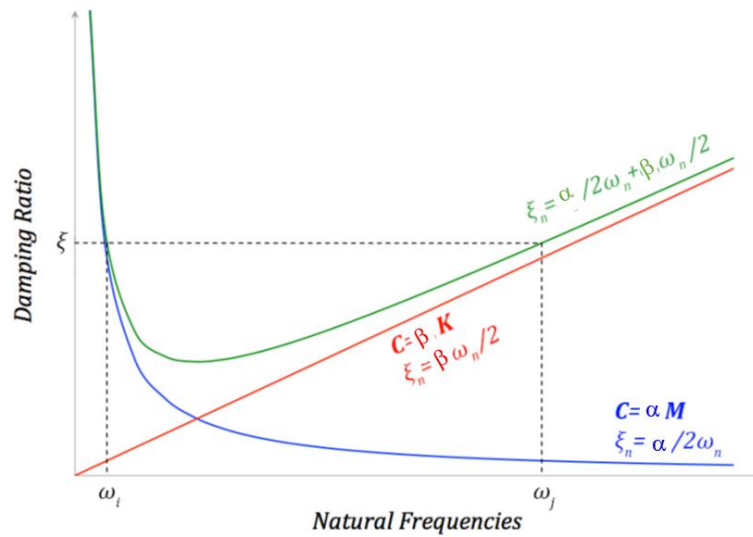


Figure 6.10 - Variation of the modal damping ratio with natural frequencies (in Green the Rayleigh viscous damping).

In the following, the parameters of ductility and viscous elastic damping were defined and the α and β values for Rayleigh damping were derived.

Table 6.5 - Assumed threshold parameters and α and β values for Rayleigh damping

T_{inf}	ω_{inf}	T_{sup}	ω_{sup}	ξ	μ	α	β
0.110	57.198	0.811	7.744	0.03	4	0.409244	0.000924

6.2.2. Selection of seismic conditions

The study of structural systems by dynamic analyses requires seismic action to be represented by accelerograms. In the present case, consideration was given to natural accelerograms: accelerometric records of different seismic events (Table 6.4). At first, 29 accelerograms were extrapolated from the 29 analyses of 125 (250 in both direction) that led to the near collapse state of a masonry building at Visso (Marche). To follow, the seismic input was defined by the accelerations of the ground recorded by the 29 accelerograms whose average gave us a spectrum compatible with code (figure 6.7).

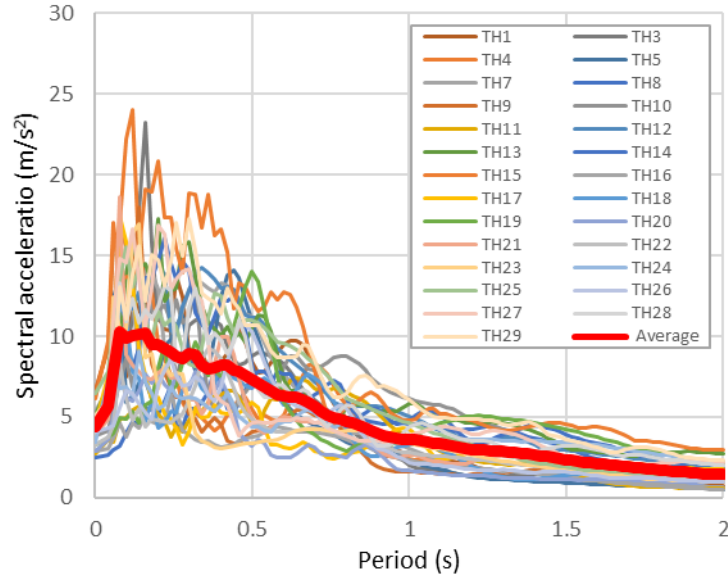


Figure 6.11 – Time History representation of the 29 accelerograms.

Typically, the response spectrum gives information about the effect of the ground motion on a structure and the acceleration levels depend on the geographical location and the type of soil. The shape of the spectrum is schematized according to four periods (NTC2018 §3.2.3). In the first, from 0 to T_B , the maximum acceleration increases with the period. In the second, from T_B and T_C , the maximum acceleration can be considered as average constant. In the third, from T_C to T_D , the maximum speed remains constant, while the acceleration varies inversely to the period. Finally, for T greater than T_D , the maximum displacement remains constant, and the acceleration varies inversely to the square of the period. In accordance with these indications, the Italian regulations report the following analytical expressions for elastic response $Se(T)$:

$$\text{For } 0 \leq T \leq T_B \quad Se(T) = a_g S \left(1 + \frac{T}{T_B} (2.5 \eta - 1) \right) \quad (6.10)$$

$$\text{For } T_B \leq T \leq T_C \quad Se(T) = a_g S 2.5 \eta \quad (6.11)$$

$$\text{For } T_C \leq T \leq T_D \quad Se(T) = a_g S \eta \left(\frac{T_C}{T} \right) \quad (6.12)$$

$$\text{For } T_D \leq T \quad Se(T) = a_g S \eta \left(\frac{T_C T_D}{T^2} \right) \quad (6.13)$$

The legislation also provides five distinct response spectra associated with a specific stratigraphic soil profile. They differ in the values of T_B , T_C , T_D and of the coefficient S which affects the improvement of motion (in §5.3.1). Since the pushover is not soil-conditioned, these accelerograms were used (although they may influence the verifications). In this way, it will be possible to make a comparison to see which distribution of forces was able to better represent the dynamic response of the structure.

Therefore, at first, in the analysis phase, we can say that the characterization of the ground counts little, provided that the period of the building itself is not very high.

Table 6.6 - 29 accelerograms used for the NLDA.

	N°/250	N° Process	Event	Mw	Corrected (Y(=1)/N(=0))	Waveform	PGAx (m/s ²)	PGAy (m/s ²)
1	15	70	NW-Kagoshima-Prefecture	6.1	0	19970326_0831_KGS005_NS_in_g.acc	4.213	4.930
2	17	80	Hector-Mine	7.1	0	19991016_0946_HEC_H1_in_g.acc	3.303	2.604
3	28	49	Bingol	6.3	0	20030501_0027_AI_049_BNG_EW_in_g.acc	2.872	5.109
4	36	82	Olfus	6.3	0	20080529_1545_113_Tr_in_g.acc	4.674	6.588
5	40	64	L'Aquila-mainshock	6.3	0	20090406_0132_AQA_WE_in_g.acc	3.947	4.338
6	42	73	L'Aquila-mainshock	6.3	0	20090406_0132_AQK_NS_in_g.acc	3.468	3.237
7	43	83	L'Aquila-mainshock	6.3	0	20090406_0132_AQV_WE_in_g.acc	6.442	5.352
8	50	68	S-Suruga-Bay	6.2	0	20090810_2007_SZO018_EW_in_g.acc	4.07	2.516
9	68	81	Christchurch	6	0	20110613_0220_LPCC_H2_in_g.acc	5.717	6.632
10	75	74	Norcia	6.5	0	20161030_0640_ACC_EW_in_g.acc	4.259	3.847
11	81	54	Norcia	6.5	0	20161030_0640_T1212_NS_in_g.acc	2.732	2.744
12	97	101	L'Aquila-mainshock	6.3	1	20090406_0132_AQV_WE_in_g.cor5000	7.321	5.775
13	98	103	MID-NIIGATA-PREF	6.2	1	20110311_1859_NIG023_NS_in_g.cor5000	4.936	5.077
14	103	93	Norcia	6.5	1	20161030_0640_NRC_EW_in_g.cor5000	5.109	4.404
15	116	122	Off-Noto-Peninsula	6.7	1	20070325_0042_ISK006_EW_in_g.cor10000	6.732	6.126
16	127	55	Friuli-2nd-shock	5.6	0	19760911_1635_GMN_NS_in_g.acc	3.219	2.926
17	138	77	Honshu	5.9	0	19960810_1812_MYG005_EW_in_g.acc	3.883	4.554
18	140	70	NW-Kagoshima-Prefecture	6.1	0	19970326_0831_KGS005_EW_in_g.acc	4.93	4.213
19	142	80	Hector-Mine	7.1	0	19991016_0946_HEC_H2_in_g.acc	2.604	3.303
20	153	49	Bingol	6.3	0	20030501_0027_AI_049_BNG_NS_in_g.acc	5.109	2.872
21	158	60	Off-Noto-Peninsula	6.7	0	20070325_0042_ISK003_NS_in_g.acc	5.248	3.929
22	160	51	Olfus	6.3	0	20080529_1545_112_Lo_in_g.acc	5.311	3.283
23	165	64	L'Aquila-mainshock	6.3	0	20090406_0132_AQA_NS_in_g.acc	4.339	3.947
24	167	73	L'Aquila-mainshock	6.3	0	20090406_0132_AQK_WE_in_g.acc	3.237	3.468
25	168	83	L'Aquila-mainshock	6.3	0	20090406_0132_AQV_NS_in_g.acc	5.352	6.443
26	175	68	S-Suruga-Bay	6.2	0	20090810_2007_SZO018_NS_in_g.acc	2.516	4.070
27	207	72	Norcia	6.5	0	20161030_0640_T1214_EW_in_g.acc	5.932	4.130
28	223	103	MID-NIIGATA-PREF	6.2	1	20110311_1859_NIG023_EW_in_g.cor5000	5.077	4.936
29	228	93	Norcia	6.5	1	20161030_0640_NRC_NS_in_g.cor5000	4.404	5.109

As can be seen from the following images, an excessive deformation of the 4th floor occurred. Even if the global structure do not reach excessive deformations, the tower is collapsed, where the maximum displacement at the 4th level is greater than 2 m (figure 6.11). Therefore, the dynamics often do not converge or at least have cycles that do not close, with large dissipations (figure 6.12).

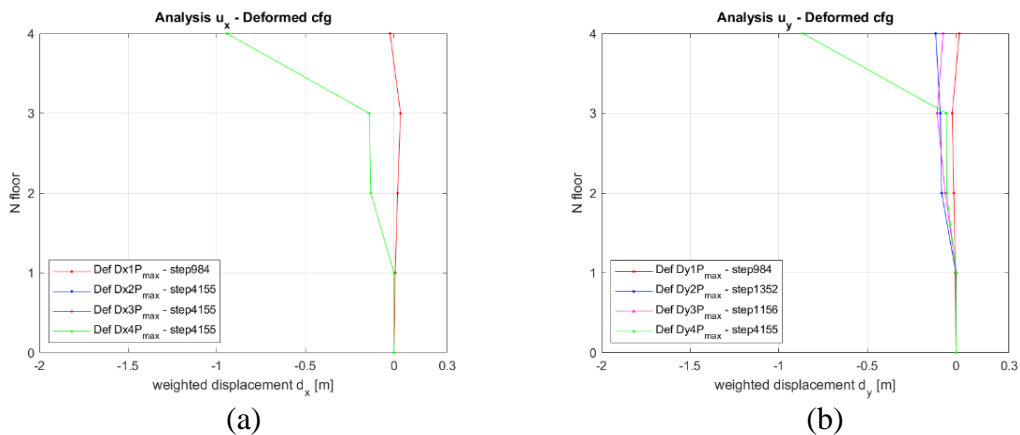


Figure 6.12 - Deformed configurations: (a) in x-direction; (b) in y-direction. (Acc_15, 1/29).

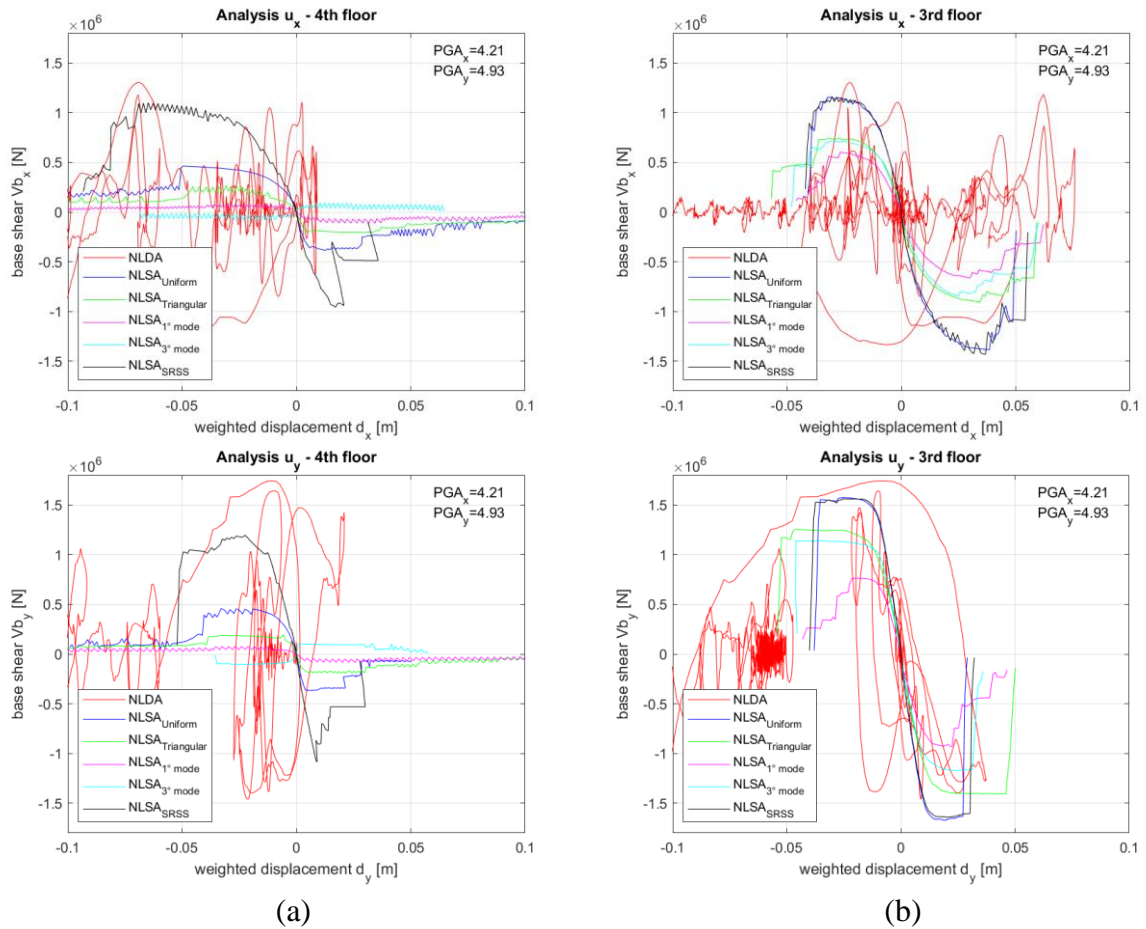


Figure 6.13 - Nonlinear dynamic analysis not reaching convergence in both control node choice: (a) 4th floor; (b) 3rd floor. (Acc_15, 1/29).

Analysing the results, the need arose to change the 29 accelerograms and use some more "light" of the 250 provided by the University, which had brought the building in Visso to lower damage levels.

6.3. Comparison between the results of static and dynamic analyses.

As mentioned in the previous sections it was necessary to consider other accelerometric recordings more correct for the present case study (problematic already found in the literature). Hence, the previous approach, NLSA, is compared with the results derived from the NLDA to better understand the influence of the choice of the load pattern used. Several analyses were performed in order to check the reliability of the static approach. The results obtained by the NLDA were considered as the reference actual behavior, to be compared with the results obtained in TreMuri with all the load pattern computed. From the 3rd Record, the Acc_3 (pga=0.1-0.12g), and the 5th ,Acc_5 (pga=0.05g), We can see that the overall response is still well below the maximum resistance. From the two plotted graphs with the control of the displacement on the third floor (figure 6.14b), we see that the cycles of the dynamics (in red) do not reach the maximum shear of the pushover. The figures on the left (figure 6.14a) show that the tower responds not in phase

with the global response, because the NLDA diagram is not cyclical. We will understand better this reaction from other records, but in any case the maximum displacement at the top of the tower remains inferior to that which has happened from the total pushover.

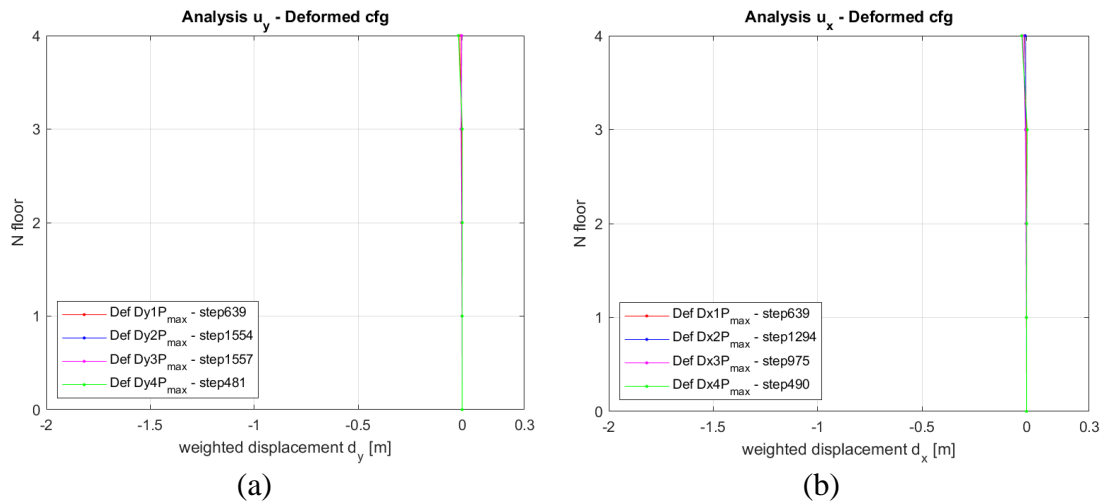


Figure 6.14 - Acc_3 deformed configuration: (a) x-direction; (b) y-direction

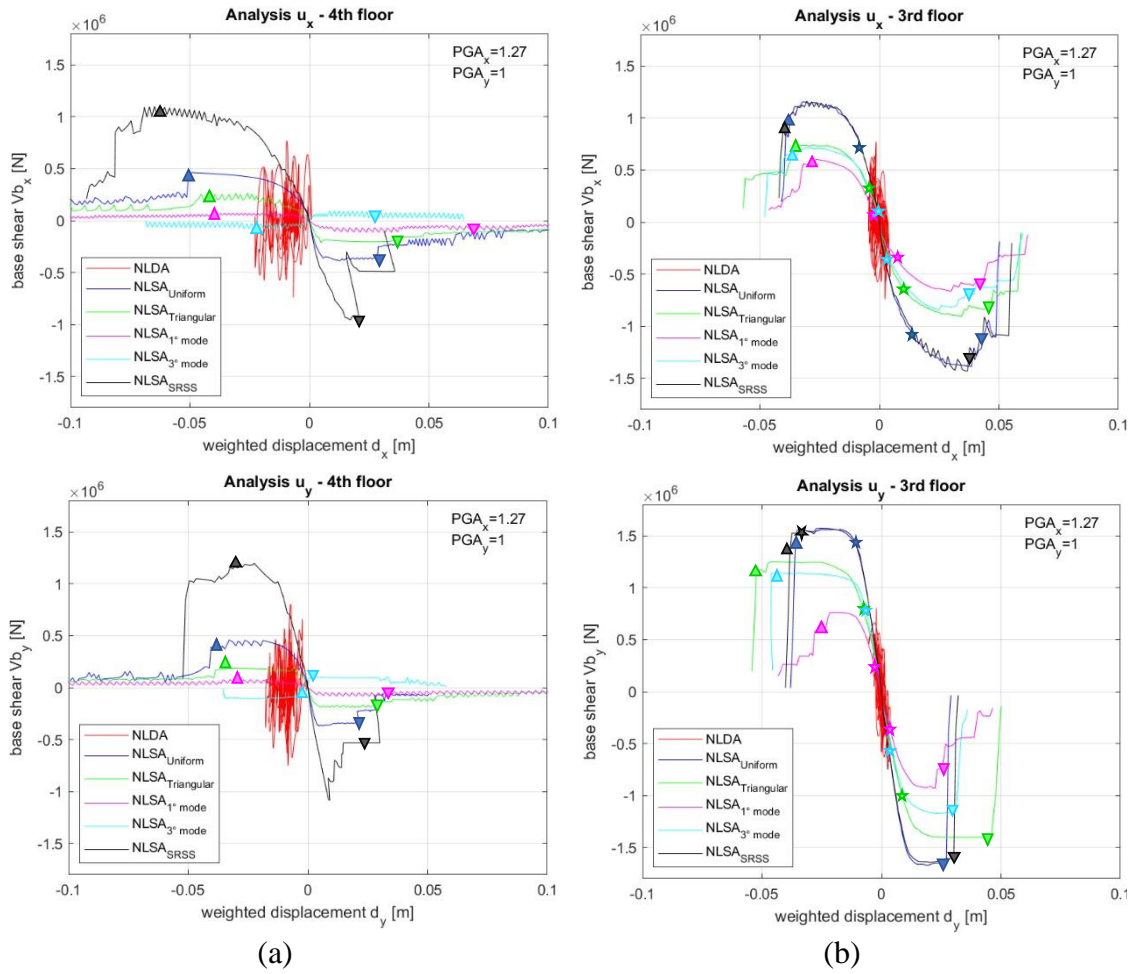


Figure 6.15 – Comparison between pushover and dynamic analysis for Acc_3, obtained at two different height: (a) at the tower level, (b) at the roof level.

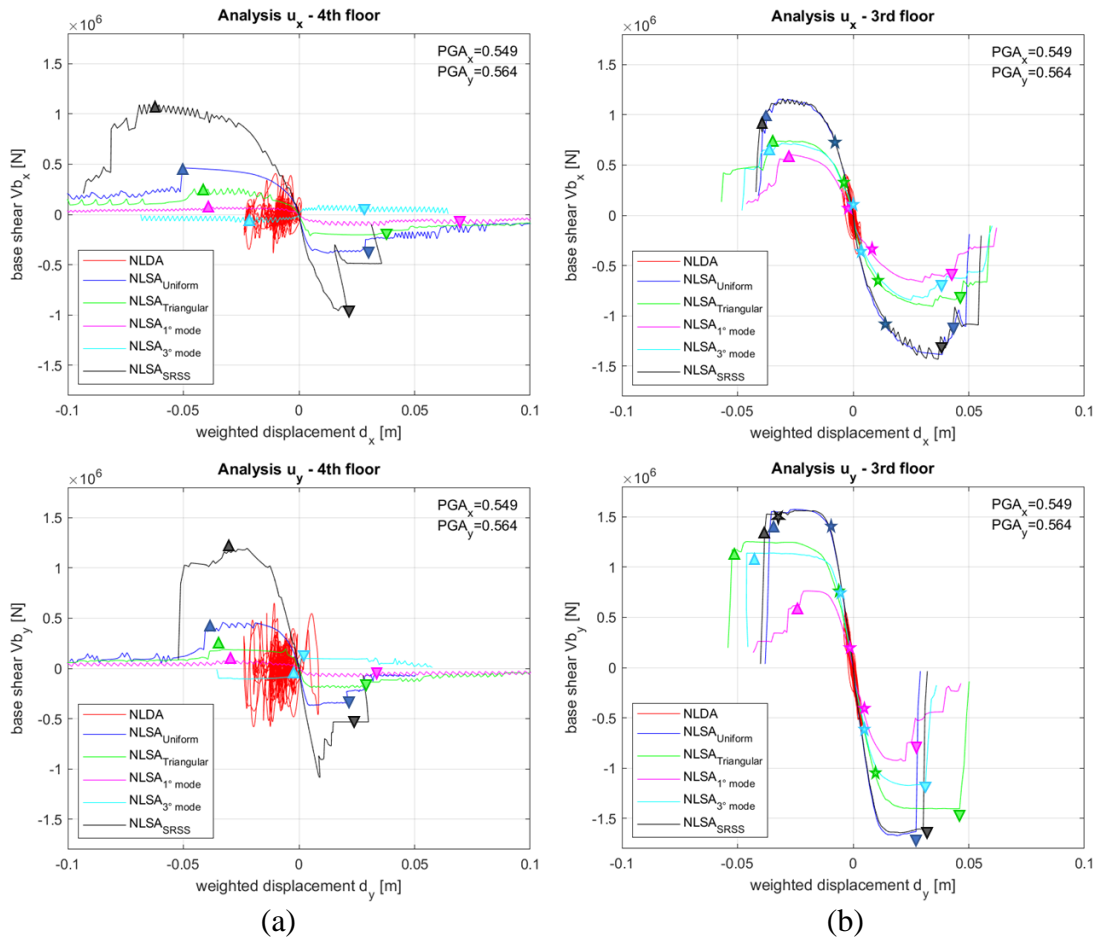


Figure 6.16 - Comparison between pushover and dynamic analysis for Acc_5, obtained at two different height: (a) at the tower level, (b) at the roof level.

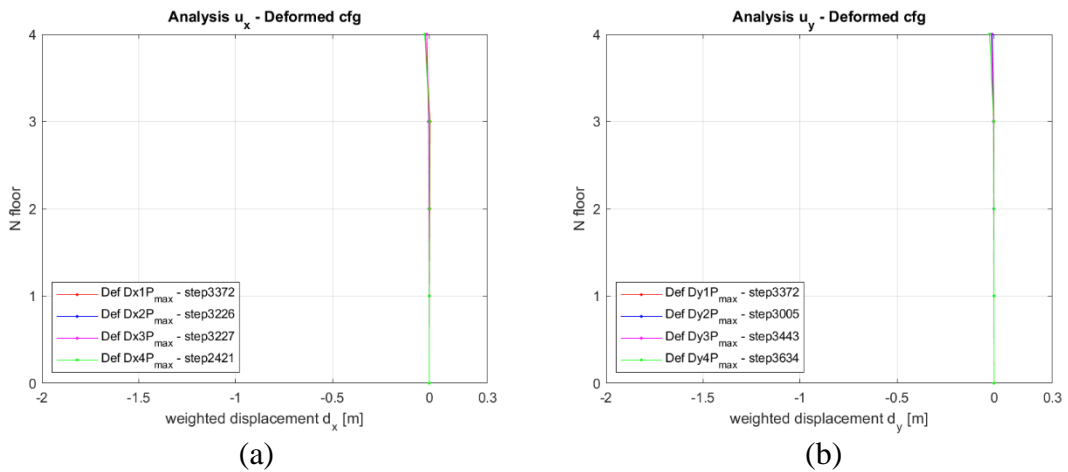


Figure 6.17 - Acc_5 deformed configuration: (a) x-direction; (b) y-direction.

In the records Acc_4 (pga=0.15-0.16g) and Acc_6 (pga=0.12-0.18g), the global structure has not collapsed (two figures 6.17a, on the left), but the tower yes, because the maximum displacement to the 4 ° level (figure 6.18) is greater than 2 m.

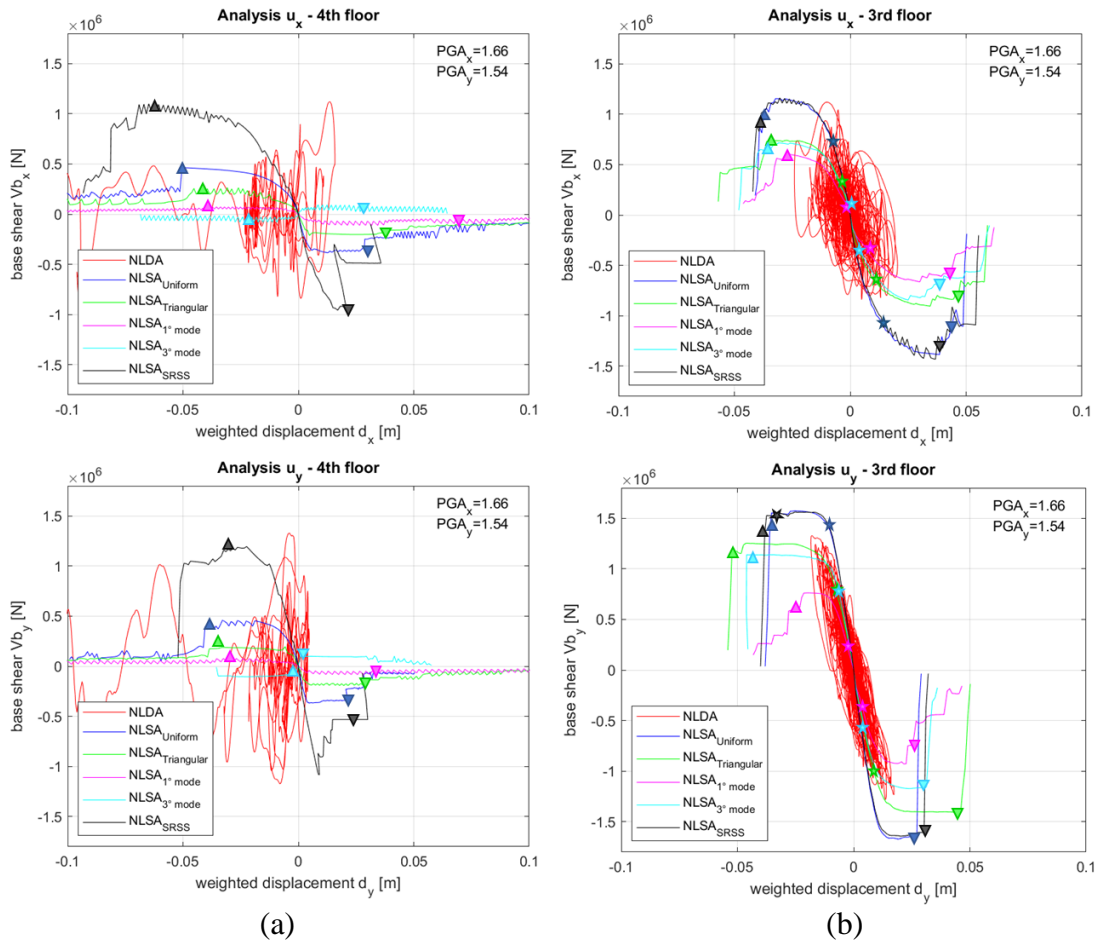


Figure 6.18 - Comparison between pushover and dynamic analysis for Acc_4, obtained at two different height: (a) at the tower level, (b) at the roof level.

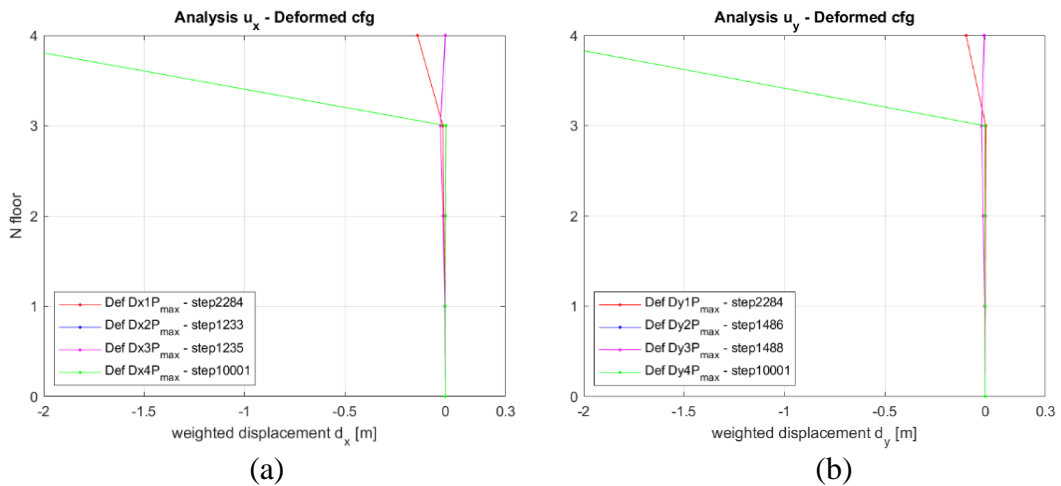


Figure 6.19 - Acc_4 deformed configuration: (a) x-direction; (b) y-direction

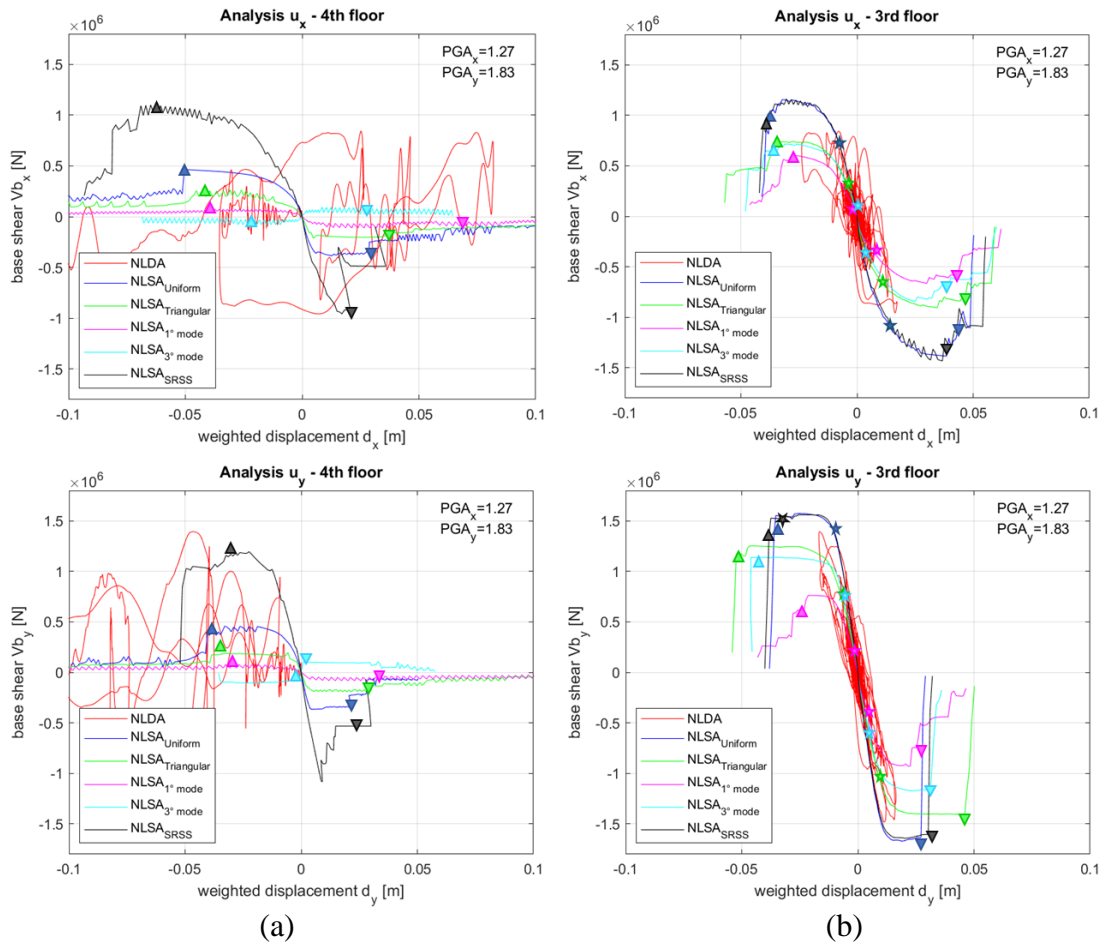


Figure 6.20 - Comparison between pushover and dynamic analysis for Acc_6, obtained at two different height: (a) at the tower level, (b) at the roof level.

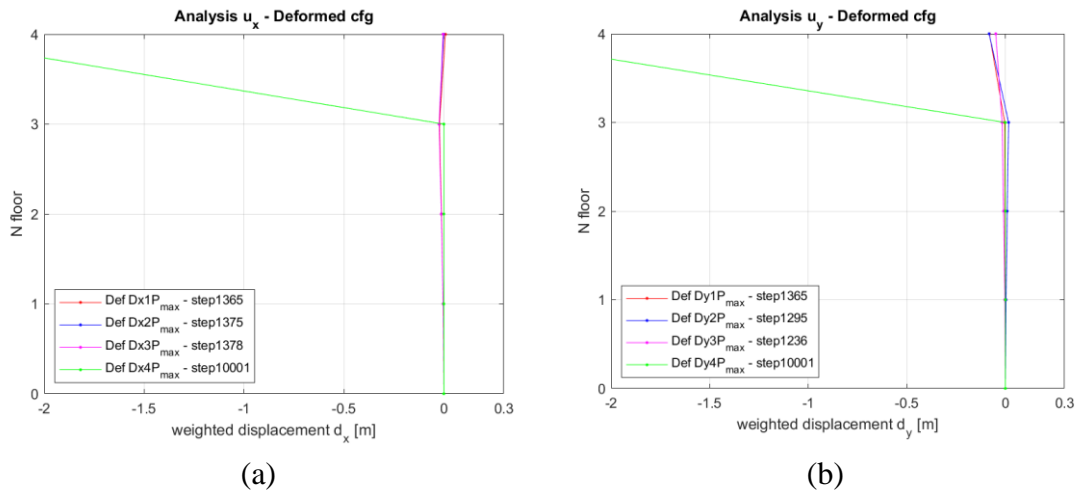


Figure 6.21 - Acc_6 deformed configuration: (a) x-direction; (b) y-direction

Looking at the maximum displacement at the coverage level, we can see that it is often lower than the last displacement obtained from the pushover. Therefore, the verification

would not be satisfied. It is also noted that the dynamic resistance seems to be lower than that of the blue pushover (Uniform), but often also of the combined SRSS, because the distribution always leads to an overestimation of the resistance. But we can see that in any case this distribution (SRSS) covers some dynamic cycle, and above all it reflects the behaviour of the structure also when seen in terms of last anticipated displacements (figure 6.21 and 6.22).

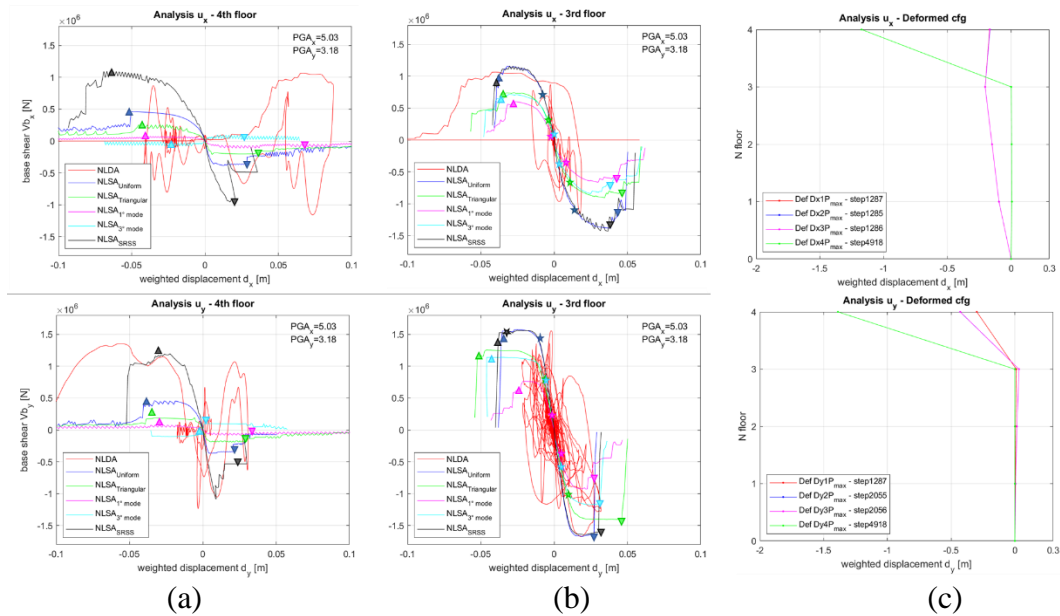


Figure 6.22 - Acc_10: (a) Analysis on the 4th Floor; (b) Analysis on the 3rd Floor; (c) Deformed configurations.

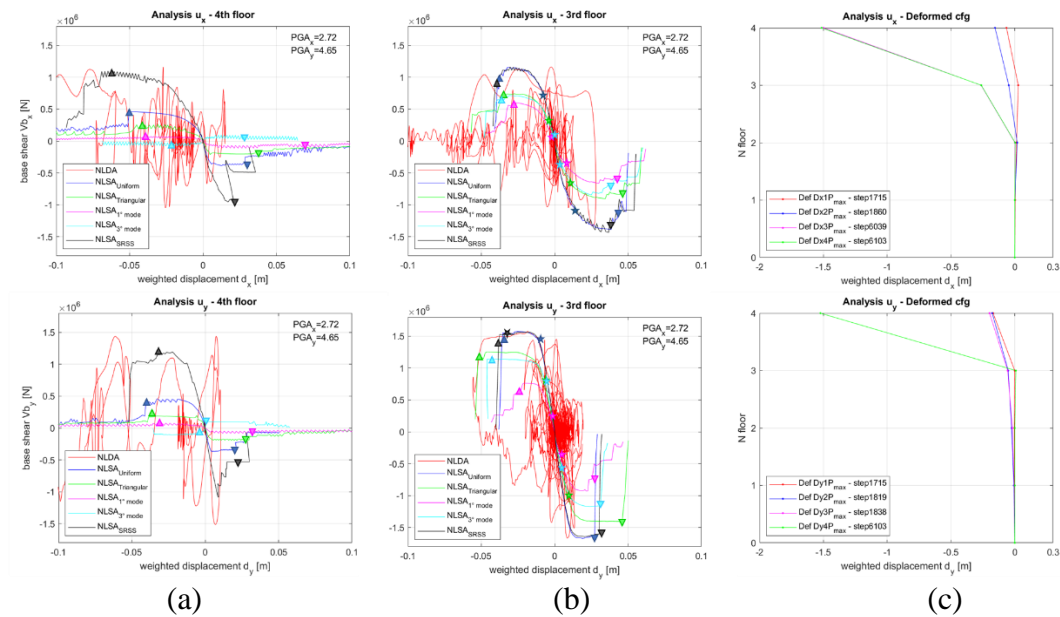


Figure 6.23 - Acc_11: (a) Analysis on the 4th Floor; (b) Analysis on the 3rd Floor; (c) Deformed configurations.

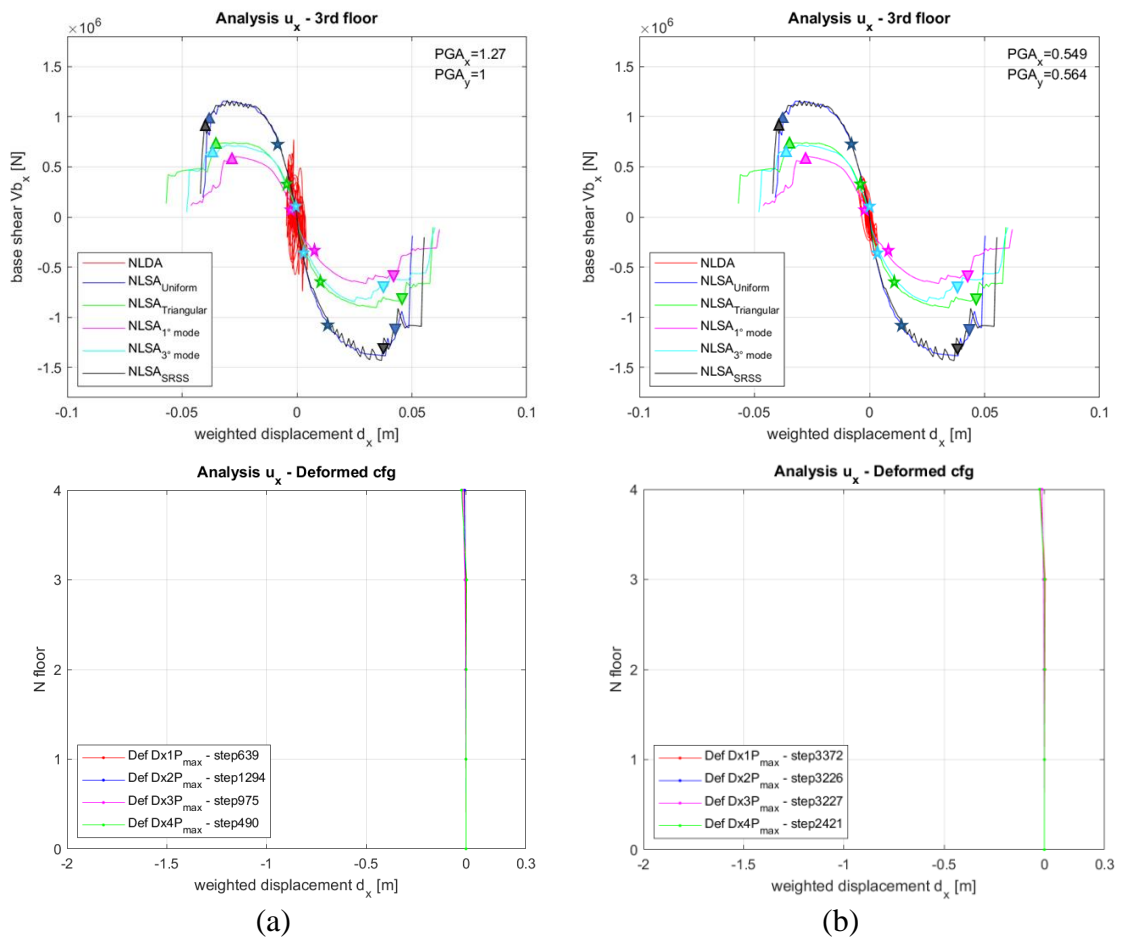


Figure 6.24 – Comparison between ultimate displacement in pushover and at the floor scale: (a) Acc_3 on third floor in x-direction; (b) Acc_5 on third floor in x-direction

From figure 6.23 and 6.24, it is clear again that the anticipated displacements are more representative also with respect to the dynamic response.

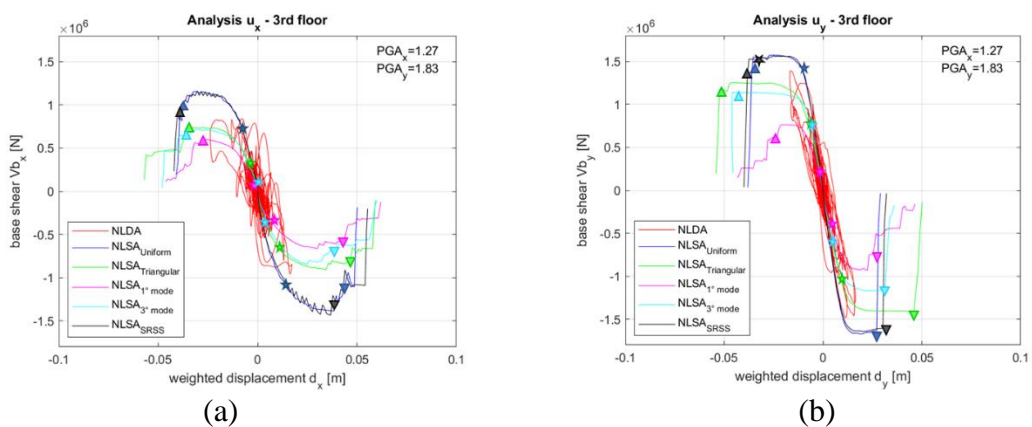


Figure 6.25 - Comparison between pushover and dynamic analysis for Acc_6 with ultimate displacements highlighted (a) in x-direction and (b) y-direction.

On the basis of the above considerations, it was interesting to see the response spectra of the input accelerograms. We remember that the typical shape of the spectrum has an initial "bell" that corresponds to a strong amplification of the spectral acceleration compared to that of the ground, the so-called mechanical phenomenon of resonance. It occurs when the forcing period (soil) is similar to that of the structural system. When at very high periods the spectrum has amplifications, it means that the structure is more deformable and therefore not appreciably affected by the effects of ground motion. This phenomenon can be appreciated in the present case study, because of the irregularities in plan and high that characterize this structure. The period is a value that we remember to be linked to the relationship between mass and stiffness of the structure, therefore if the structure is more deformable it means that it is less rigid and therefore it will have own greater periods.

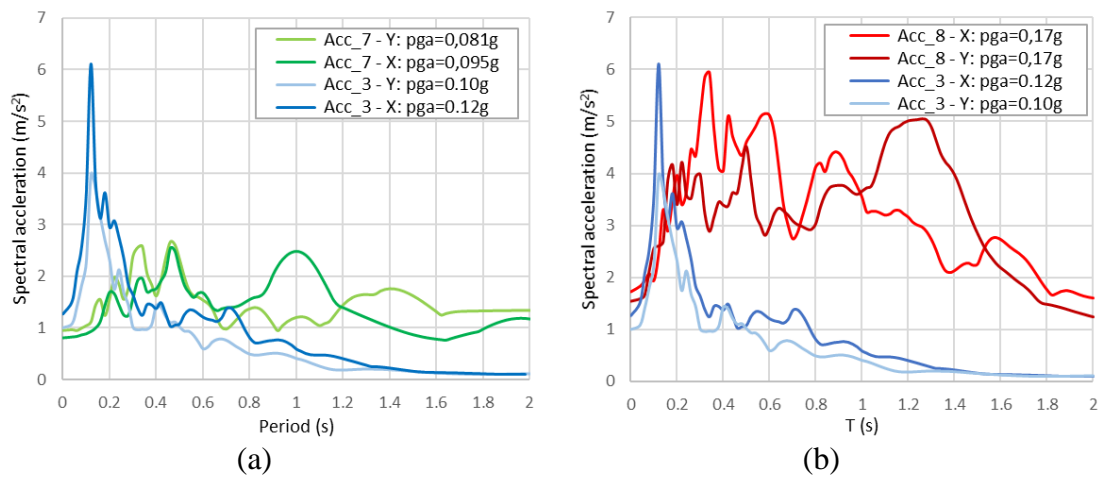


Figure 6.26 - Comparison between input spectra acceleration: (a) Records 3 and 7; (b) Records 3 and 8.

This phenomenon recurs often, as can be seen in Figure 6.25 where the inputs of records 7 and 8 are compared with 3rd. The accelerograms were supplied as pairs of time-acceleration values and therefore it was possible to trace the associated spectra. Taking a look to the spectra of the two records 7 and 3 is visible that the Acc_7, despite having a lower PGA, present much higher frequency at longer periods (the structure deforms much more). This means that after the tower starts to get damaged it generates amplifications and therefore a much greater demand for displacement.

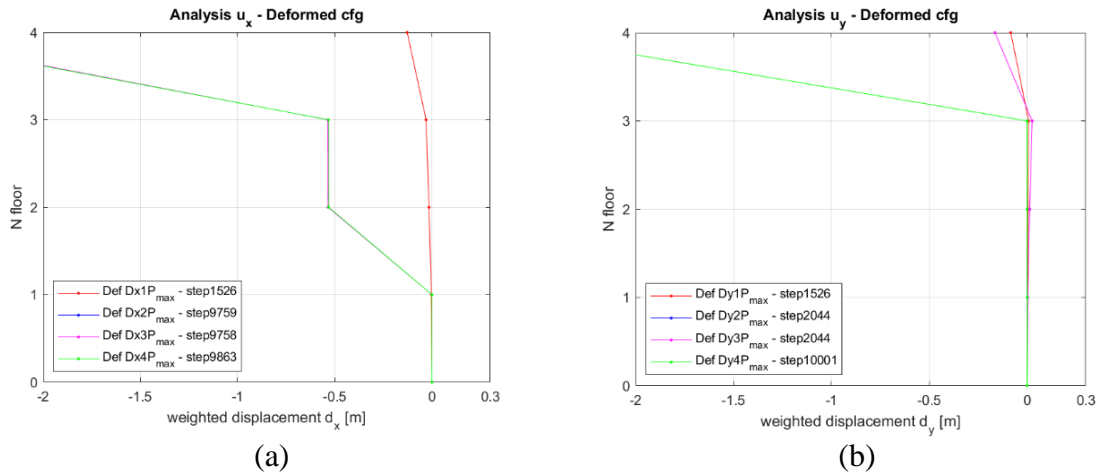


Figure 6.27 – Acc_7 deformed configuration: (a) x-direction; (b) y-direction

The same happens for Acc_8 (pga=0.15-0.17g), more clearly, the amplifications are much wider. In terms of dynamic response, we can say that the whole structure reaches collapse, with a mechanism on the second floor in the x-direction (figure 6.25a). In the direction y (figure 6.25b) instead it is noticed as the response of the tower is not in phase with that of the global structure: the maximum value to the 3rd floor in y-direction occurs when the tower is going on the other side.

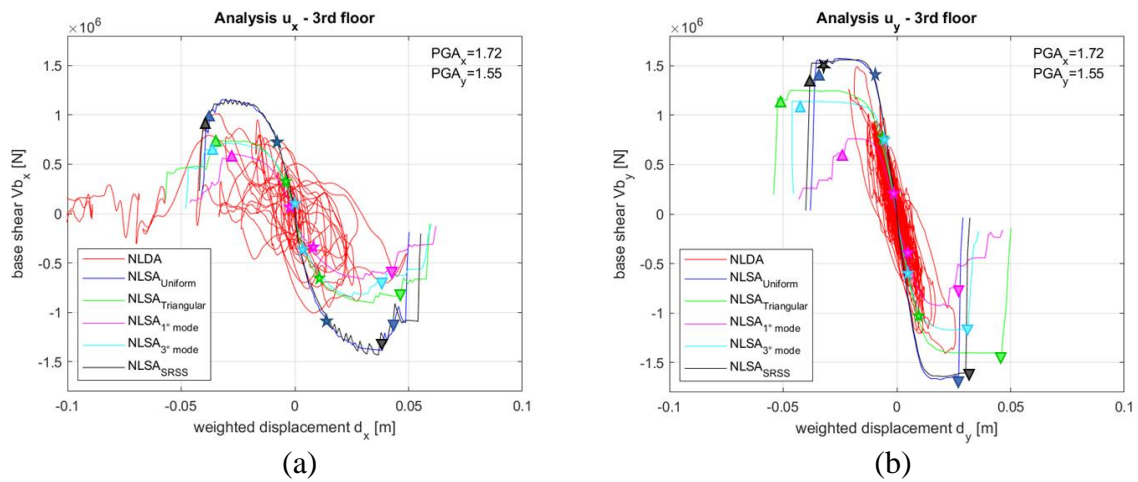


Figure 6.28 – Acc_8, 3rd floor analysis: (a) x-direction; (b) y-direction

6.3.1. Distinctive features of NLSA and NLDA

At this point we can say that the conversion into capacity curves, in the case where the global response is represented (pushover to the 3rd floor), leads to overall consistent results. In the case of structure like the one studied here, we cannot expect that an "approximate" method (pushover analysis) allows us to understand everything, or better to carry out evaluations with equal detail compared to a more accurate method (nonlinear dynamic analysis). In fact, using the nonlinear dynamic analysis (NLDA) that activates more precisely the inertial forces, and then comparing the hysteretic response obtained

by the NLDA with those of pushovers, simplified distributions obtained with the Uniform, the Triangular and the SRSS can be considered valid. The results provided by these three distributions seem to bring a result closer to what is suggested by non-linear dynamics. The comparisons made in the previous section have helped us to understand which distribution of forces was more representative and that the discourse to move back last seems to work.

7. Conclusions

The seismic assessment of existing masonry buildings is confirmed to be a relevant issue from different point of views: especially for an irregular building like the one we are dealing with. So, the reliability of the nonlinear static approach (NLSA, i.e. pushover analysis) may be debatable and in this study the comparison with the complete nonlinear dynamic analysis (NLDA) is adopted to verify this issue. The possibilities analyzed in the previous paragraphs, both on modeling and on analysis procedure, are certainly not exhaustive, but they try in some way to underline the importance of adopting appropriate precautions in the current seismic verification approaches, used by professionals to achieve reliable results as much as possible.

In this thesis the identification of the structural model has been confirmed not straightforward, since a clear distinction between structural and non-structural elements is not always possible. From the comparison made between NLSA and NLDA (assumed as benchmark solution), it was well established, once again, that the NLSA response is limited in its ability to capture the complex dynamic behavior of multiple-degree-of-freedom (MDOF) structures. However, the use of NLSA also in the case of irregular masonry building is an important result due to the easy applicability and speed in the results output, but also for a more than significant knowledge of the structure.

By converting the pushover curve into a capacity curve (in § 6.1.2.1, page 65), which is the essential step to pass to the safety verification, we have seen that in most cases the curves tend to be closer to each other when the deformed shape induced by the load pattern is used as reference. This highlighted the relevance of the criteria adopted to carry out such a conversion into the equivalent SDOF. For example, the inverse-triangular load pattern, as pushover curve, was much lower than the SRSS and the Uniform, but after the conversion they become practically equal. However, significant differences have been noticed when the deformed shape induced by using a single mode. Thus, we concluded that the conversion based on single-modes is not representative. This "incongruity" is associated to the fact that since these distributions (that of 1st Mode and 3rd Mode, for the examined case study) activate very small participating mass, they are not representative of the whole behaviour of the building. Therefore, for the 1st and the 3rd mode distribution, the meaning of this equivalent oscillator conversion falls. According to the 3rd mode, where we find the inversion of the sign, there is a higher possibility that this distribution supplies non representative results, due to the distribution of forces that push in different directions (figure 5.22, page 58). In the ending, we found out that when strong irregularities in the elevation are possibly associated to quite flexible diaphragms, it is preferable to avoid the use of load patterns based on single specific modes.

As a result, ratings with the Uniform, Triangular and SRSS distribution are more reliable and more robust. The SRSS is very similar to the Uniform distribution.

A further result concerns the effectiveness of some criteria recently introduced by the Italian Structural Code to consider the concentration of damage in specific portions and, thus, eventually alter the ultimate displacement capacity based on heuristic criteria that refer only to the overall base shear reduction in the softening phase.

The application of this approach to irregular buildings, as the one examined, may lead to a retraction of the ultimate displacement capability on the pushover curve. The comparison with the NLDA has proven this retraction quite realistic.

Actually, the results of NLDA showed that even if at a global level the building had not reached a significant damage, in some cases the tower had already collapsed. To consider the possible occurrence of these local effects in the definition of limit states displacement on the pushover curve allows to obtain more reliable results.

These conclusions about the reliability of NLSA approach could be integrated with the application to other irregular configurations. Moreover, other reference buildings, in terms of plan and elevation irregularities, should be considered in order to perform an accurate comparison and evaluation. Finally, starting from this technical analysis, a code for the seismic assessment of irregular building, which is still lacking, could be proposed in order to complete the legislation.

8. Bibliography

- ANIDIS, 2011. Italian National Conference on Earthquake Engineering, Un nuovo modello a telaio equivalente per l'analisi statica non lineare di pareti in muratura, Bari, Italy.
- Arianna Pavia et al. "Seismic Upgrading of a Historical Masonry Bell Tower through an Internal Dissipative Steel Structure." *Buildings (Basel)* 11.24 (2021): 24–. Web.
- Brencich A, Gambarotta L. Mechanical response of solid clay brickwork under eccentric loading. Part I: Unreinforced masonry. *Mat Str (RILEM)* 2005;38: 257-66.
- Casolo S., A three-dimensional model for the vulnerability analysis of a slender medieval masonry tower *Earthq Eng*, 2 (4) (1998), pp. 487-512
- Castellazzi G, D'Altri AM, de Miranda S, Chiozzi A, Tralli A. Numerical insights on the seismic behavior of a non-isolated historical Masonry tower. *Bull Earthq Eng* 2018;16(2):933–61.
- Degli Abbati S., Maria D'Altri A., Ottonelli D., Castellazzi G., Cattari S., De Miranda S., Lagomarsino S.: Seismic assessment of interacting structural units in complex historic masonry constructions by nonlinear static analyses, *Eng. Struct.*, 213 (2019) 51-71
- D'Ambrisi, V. Mariani, M. Mezzi, Seismic assessment of a historical masonry tower with nonlinear static and dynamic analyses tuned on ambient vibration tests, *Eng Struct*, 36 (2012), pp. 210-219
- EN 1998-3. Eurocode 8: design of structures for earthquake resistance-part 3: assessment and retrofitting of buildings. CEN (European Committee for Standardization), Brussels, Belgium; 2005.
- Galasco A., Frumento S., *Analisi sismica delle strutture murarie, calcoli strutturali*, Gruppo Editoriale Simone.
- G. Grünthal (editor). European macroseismic scale EMS. Technical report, European seismological commission, 1998.
- Gambarotta L., Lagomarsino S. "Damage models for the seismic response of brick masonry shear walls. Part II: The continuum model and its applications." *Earthquake Engineering & Structural Dynamics* 26.4 (1997): 441–462. Web.
- H. Bachmann, W. Ammann, F. Deischl *Vibration problems in structures: practical guidelines* Springer Verlag, Berlin (1997), pp. 50-55.
- Hummel, Johannes & Seim, Werner. (2016). Performance-based design as a tool to evaluate behavior factors for multi-storey timber buildings.

Jauregui, Juan Carlos. *Nonlinear Structural Dynamics and Damping*. 1st ed. 2019. Cham: Springer International Publishing, 2019. Web.

Lagomarsino S., Penna A., Galasco A., Cattari S., TREMURI Program Seismic Analysis Program for 3D Masonry Buildings TREMURI USER GUIDE.

Lagomarsino S., Penna A., Galasco A., Cattari S., TREMURI program: An equivalent frame model for the nonlinear seismic analysis of masonry buildings, *Engineering Structures*, Volume 56, 2013, Pages 1787-1799, ISSN 0141-0296.

Lagomarsino, Sergio et al. “Seismic Assessment of Existing Irregular Masonry Buildings by Nonlinear Static and Dynamic Analyses.” *Recent Advances in Earthquake Engineering in Europe*. Cham: Springer International Publishing, 2018. 123–151. Web.

Lagomarsino, Sergio et al. “Seismic Assessment of Existing Irregular Masonry Buildings by Nonlinear Static and Dynamic Analyses.” *Recent Advances in Earthquake Engineering in Europe*. Cham: Springer International Publishing, 2018. 123–151. Web.

Marino, Salvatore, Serena Cattari, and Sergio Lagomarsino. “Are the Nonlinear Static Procedures Feasible for the Seismic Assessment of Irregular Existing Masonry Buildings?” *Engineering structures* 200 (2019): 109700–. Web.

Minagawa, Masaru. “Nonlinear Dynamic Analysis of Frame Structures.” *Computers & structures* 27.1 (1987): 103–110. Web.

Najam, Fawad Ahmed. “Nonlinear Static Analysis Procedures for Seismic Performance Evaluation of Existing Buildings – Evolution and Issues.” *Facing the Challenges in Structural Engineering*. Cham: Springer International Publishing, 2017. 180–198. Web.

Preciado A., Sperbeck S.T., Ramirez-Gaytan A., Seismic vulnerability enhancement of medieval and masonry bell towers externally prestressed with unbonded smart tendons, *Eng. Struct.* 122 (2016) 50–61.

Preciado Seismic vulnerability reduction of historical masonry towers by external prestressing devices Doctoral thesis.

R. Meli *Structural engineering of the historical buildings* (in Spanish) Civil Engineers Association (ICA) Foundation, A.C., Mexico (1998).

Stadata, 3Muri_brochure, S.T.A. DATA SRL - C.so Raffaello, 12 - 10126 Torino.

Stadata, 3Muri_User Guide, v.10.9.0, S.T.A. DATA SRL - C.so Raffaello, 12 - 10126 Torino.

Tomaz'evic' M. Dynamic modelling of masonry buildings: storey mechanism model as a simple alternative. *Earthquake Eng Struct Dyn* 1987;15(6):731–49.

Appendix A

Response Spectra example:

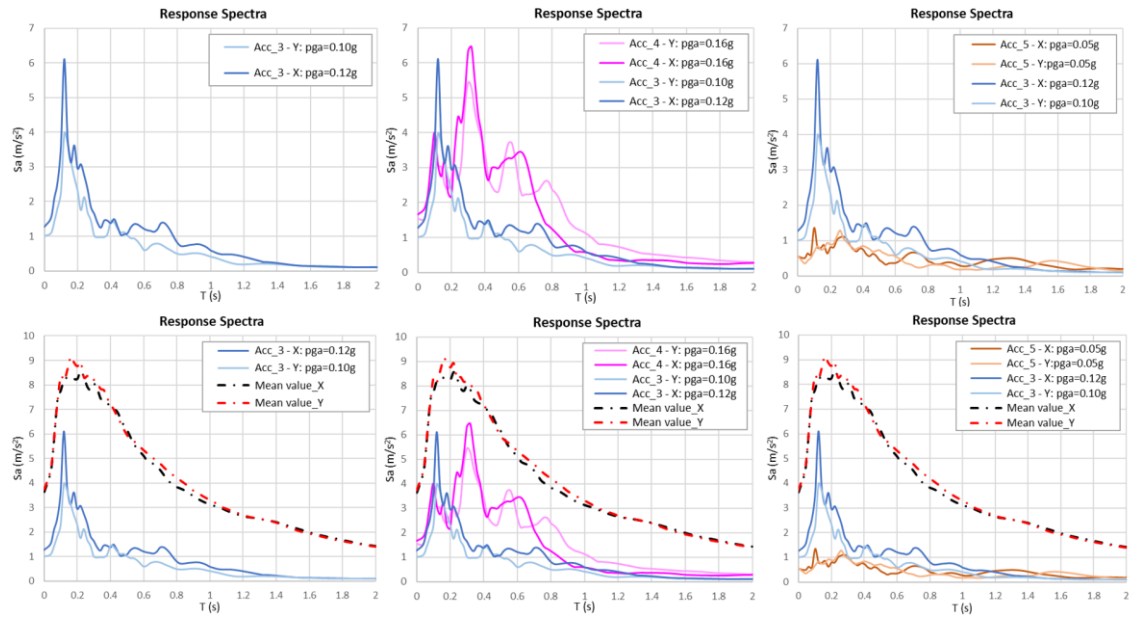


Figure 8.1 - Acc_3; Acc_4; A Acc_5

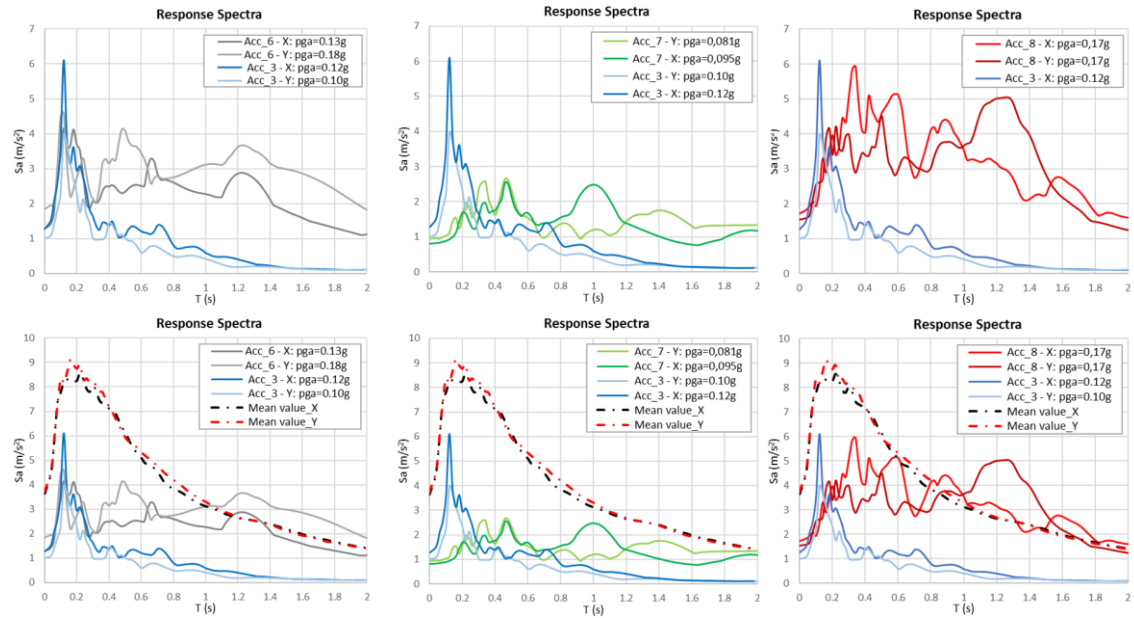
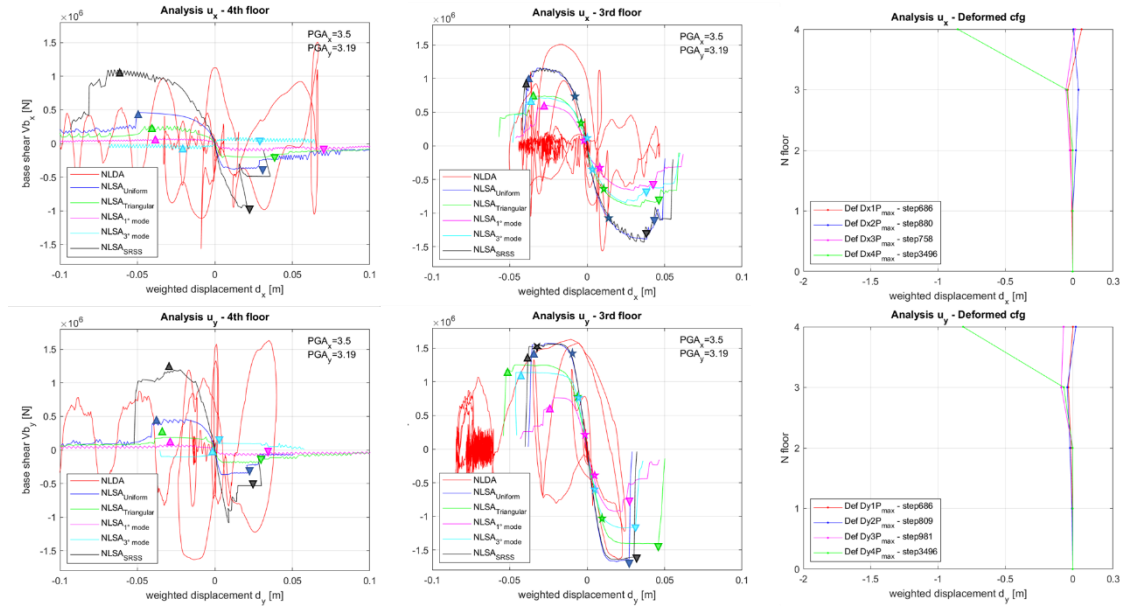
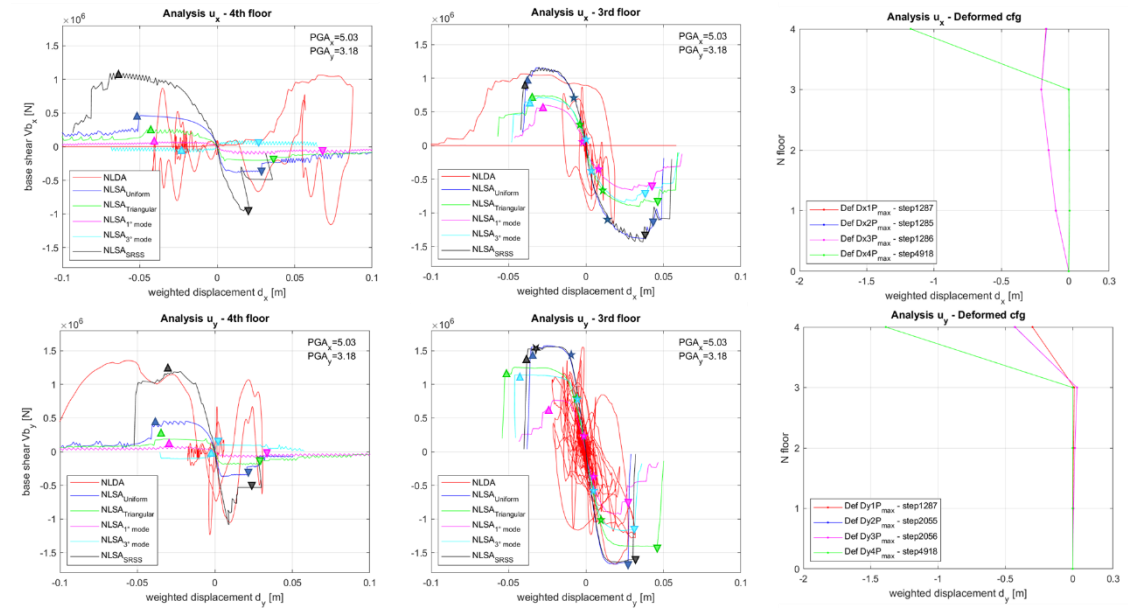


Figure 8.2 - Acc_6; Acc_7; A Acc_8

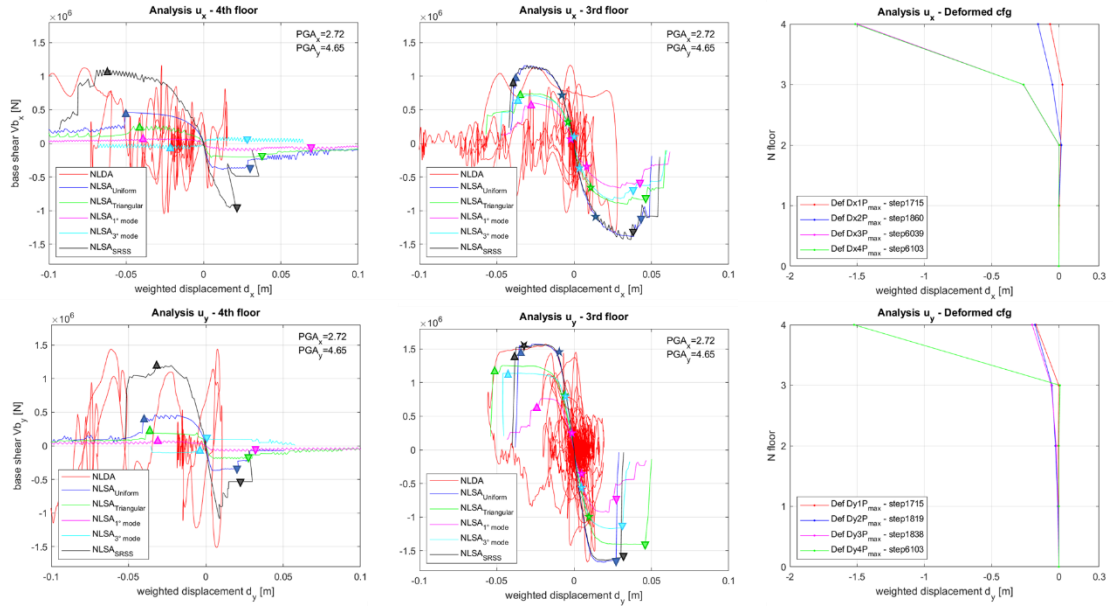
Acc_9:



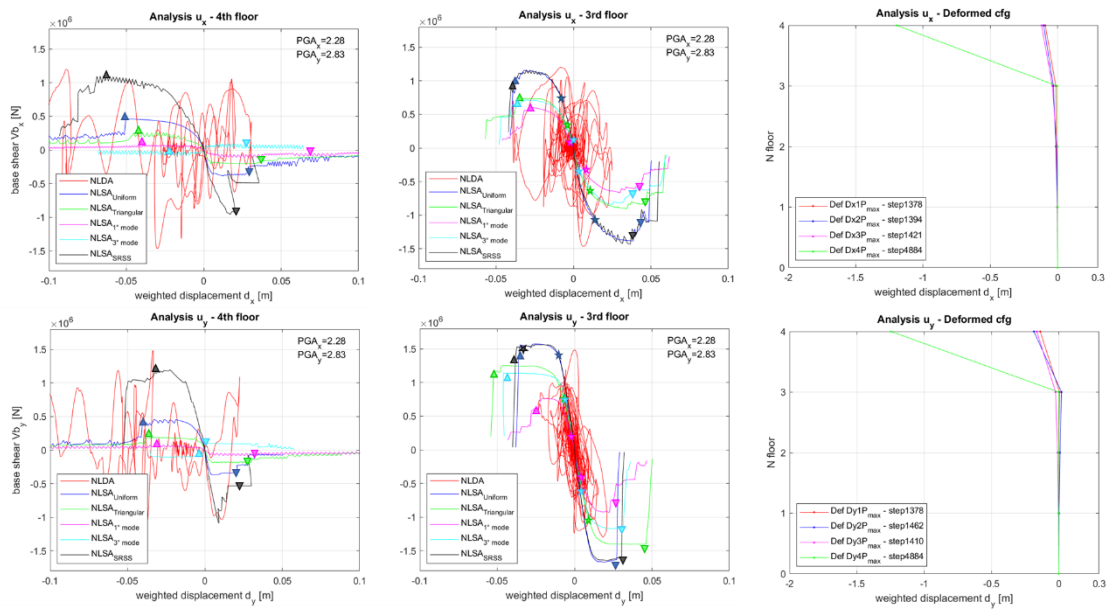
Acc_10:



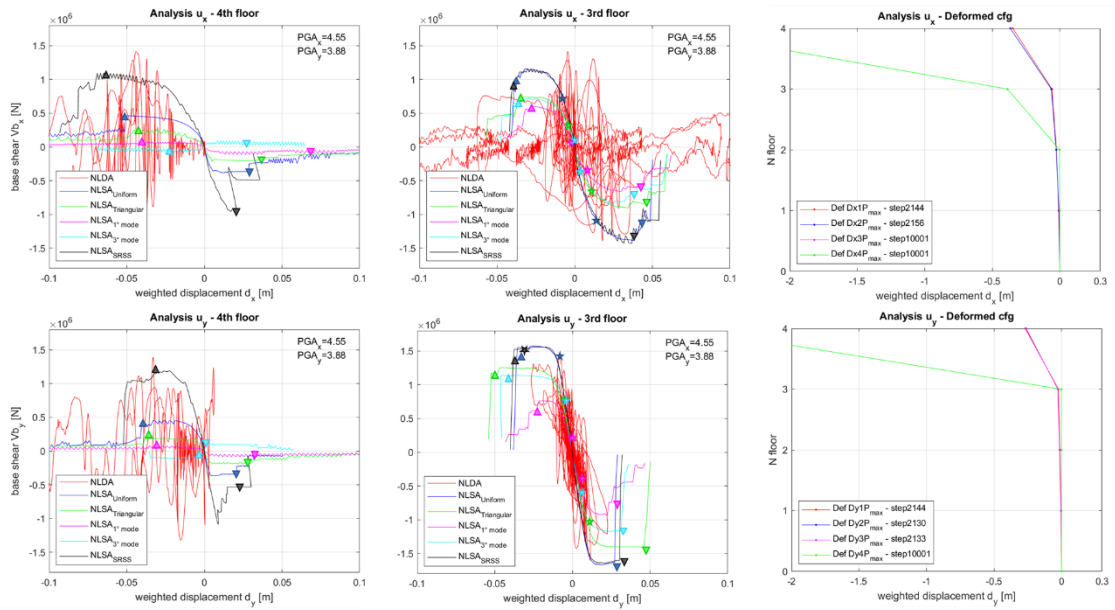
Acc_11:



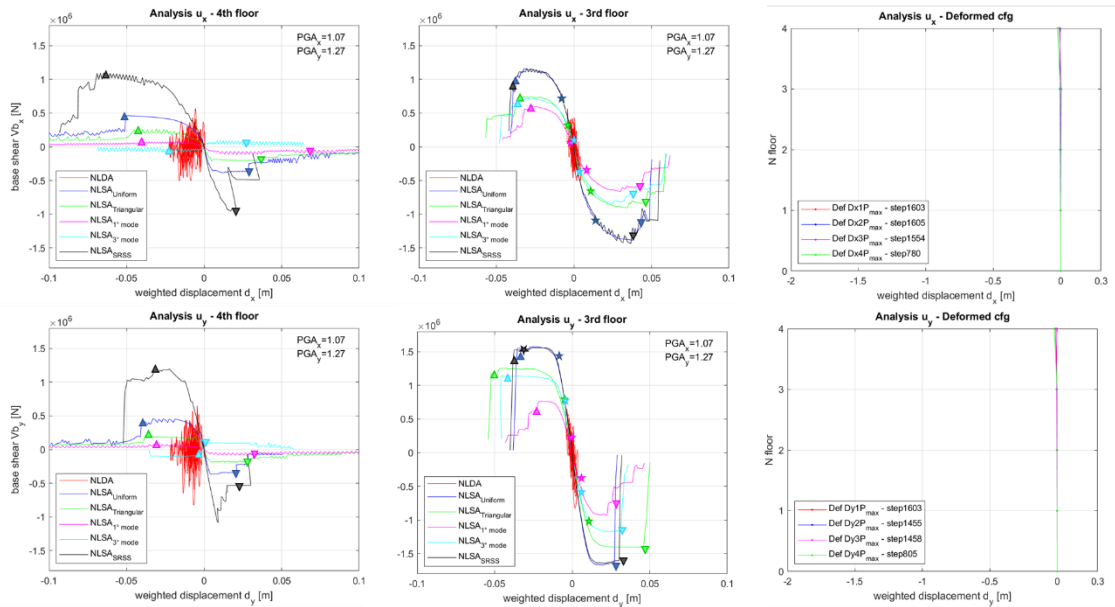
Acc_12:



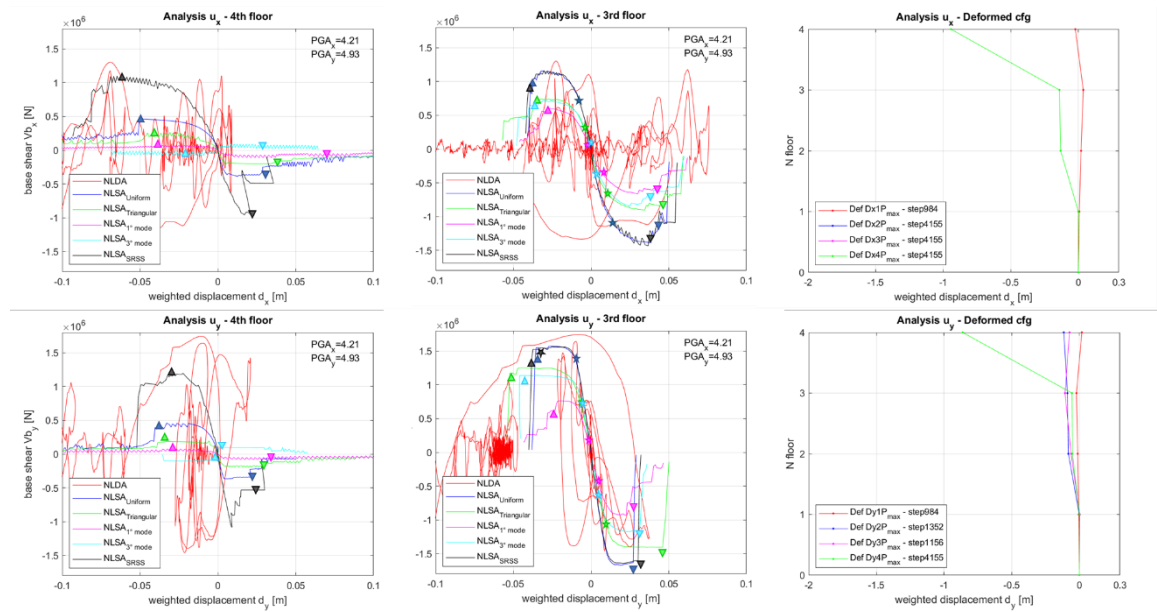
Acc_13:



Acc_14:



Acc_15:



Acc_16:

